

12-2016

Development of a Tissue-Mimicking Brain Phantom for Neurosurgical Pre-Operative Planning and Training

Miriam Navarro Lozoya
Clemson University

Follow this and additional works at: https://tigerprints.clemson.edu/all_theses

Recommended Citation

Lozoya, Miriam Navarro, "Development of a Tissue-Mimicking Brain Phantom for Neurosurgical Pre-Operative Planning and Training" (2016). *All Theses*. 2550.
https://tigerprints.clemson.edu/all_theses/2550

This Thesis is brought to you for free and open access by the Theses at TigerPrints. It has been accepted for inclusion in All Theses by an authorized administrator of TigerPrints. For more information, please contact kokeefe@clemson.edu.

**DEVELOPMENT OF A TISSUE-MIMICKING BRAIN PHANTOM FOR
NEUROSURGICAL PRE-OPERATIVE PLANNING AND TRAINING**

A Thesis
Presented to
the Graduate School of
Clemson University

In Partial Fulfillment
of the Requirements for the Degree
Master of Science
Bioengineering

by
Miriam Navarro Lozoya
December 2016

Accepted by:
Dr. Delphine Dean, Committee Chair
Dr. Bruce Gao
Dr. Jiro Nagatomi

ABSTRACT

Direct physical intervention in the treatment of patients in the area of neurosurgery represents a high risk which can be minimized with the employment of 3D physical models. These models provide a thorough physical display in 3D with detailed information related to the morphology of internal structures and their spatial location with surrounding structures. The aim of this study was to develop a brain substitute material based on gelatin that simulates the mechanical properties of brain tissue. Tissue mimicking materials were developed by matching the mechanical properties of porcine brain tissue under compressive loading at strain rates typical of surgical procedures. A brain phantom was fabricated using the tissue mimicking material, the brain (cortex and internal structures) and skull were created in a 3-step process where molds were fabricated with a 3D modeling software, printed in Polylactic Acid (PLA) and finally cast with brain tissue-mimicking material. To further test the quality of the developed material, a haptic test was conducted at Clemson University. A total of 22 bioengineering students assessed the haptic sense of two different tissue-mimicking material brain phantoms comparing them with real brain tissue. It was possible to fabricate two brain substitute materials that resembled the mechanical properties of brain tissue which were used to recreate patient-specific brain replicas in the form of tissue mimicking phantoms. These brain phantoms provide a realistic haptic sense similar to brain tissue which realism

has potential as an educational tool and preoperative planning device for neurosurgery procedures.

DEDICATION

To my dear parents Mr. Mario A. Navarro Leon and Mrs. Alma R. Lezoya

Amaro.

This work is a sign of my love to you!

And

To my husband Gustavo Moran.

Your support, patience, understanding and most of all love, made this achievement possible.

ACKNOWLEDGEMENTS

I would like to thank my advisor Dr. Delphine Dean for her sharing of her research insight as well as her guidance through this project. I would also like to thank my committee members Dr. Bruce Gao and Dr. Jiro Nagatomi for their direction. It is difficult to overstate my appreciation to Dr. Jorge Rodriguez who got my interest in brain modeling as well as his support, advice and direction in this project and the assistance to execute the mechanical testing. I would like to express my gratitude to Dr. Jane E. Joseph, Professor of the Department of Neurosciences and Director of the Neuroimaging Division at the Medical University of South Carolina (MUSC) who provided the MRI data for the 3D modeling. I appreciate the direction of Dr. Marian Kennedy regarding mechanical characterization. Additional thanks to my lab members for their support as well as Britney Cotton for her assistance in preparing and testing sample materials. I wish to thank everybody who made this experience possible, first my husband who decided to start this adventure with me and continuously kept encouraging me to go on despite the adversities, always staying positive and looking forward, my mother in law and all those who played their part to make my studies possible, my parents who gave me the wings to fly and pursue my dreams, who always supported me and inspired me to do my best in all matters in life. My sister, my sisters in law my friends and all those who have been present during this journey special thanks for all the support, advice and love.

Finally, I would like to thank the National Council of Science and Technology (CONACYT) for their funding which gave me the opportunity to study in USA.

This work was partially performed on the facilities supported by a grant from NIGMS of the National Institutes of Health under the award number 5P20GM103444.

TABLE OF CONTENTS

	Page
TITLE PAGE	i
ABSTRACT.....	ii
DEDICATION	iv
AKNOWLEDGEMENTS.....	v
LIST OF TABLES.....	xii
LIST OF FIGURES.....	xiv
CHAPTER 1: MOTIVATION AND BACKGROUND	1
1.1 - Introduction	1
1.2 - Current approaches	4
CHAPTER 2: RESEARCH AIMS.....	7
2.1 - Specific Aims	7
CHAPTER 3: TISSUE-MIMICKING MATERIAL- Development and Mechanical Characterization.....	9
3.1 - Brain Tissue.....	9
3.1.1 - Introduction.....	9
3.1.1.1 - White and gray matter.....	10
3.1.1.2 - Vivo vs in situ vs in vitro.....	12
3.1.1.3 - Friction.....	12
3.1.1.4 - Preconditioning	12
3.1.2 - Material and Methods.....	14
3.1.2.1 - Specimen preparation.....	14
3.1.2.2 - Experimental set up.....	17
3.1.2.3 - Experimental protocol.....	18
3.1.3 - Results	20
3.1.3.1 - Effect of anatomical location and origin	23

Table of Contents (Continued)

	Page
3.1.3.2 - Post mortem time.....	24
3.1.3.3 - Strain Rate dependency.....	26
3.2 - Hydrogel.....	27
3.2.1 - Introduction.....	27
3.2.2 - Material and methods.....	29
3.2.2.1 - Gelatin-Agarose Hydrogels preparation	29
3.2.2.2 - Experimental set up	30
3.2.2.3 - Experimental protocol	31
3.2.3 - Results	32
3.2.3.1 - 3% Gelatin- 1% Agarose.....	40
3.2.3.2 - Strain Rate dependency.....	41
3.3 - Emulsion	42
3.3.1 - Introduction.....	42
3.3.2 - Materials and methods	44
3.3.2.1 - Emulsion preparation	44
3.3.2.2 - Experimental set up.....	45
3.3.2.3 - Experimental protocol	46
3.3.3 - Results	47
3.3.3.1 - Strain Rate dependency.....	49
3.4 - Temperature	50
3.5 - Relaxation test	54
3.6 - Degradation Test	61
3.6.1 - Macroscopic findings.....	62
3.6.2 - Mechanical test	66
3.6.3 - Weight loss	68
3.7 - Discussion	69
3.7.1 - Brain Tissue.....	70
3.7.2 - Brain substitute materials	72
CHAPTER 4: SEGMENTATION AND 3D PRINTING	75
4.1 - Introduction	75

Table of Contents (Continued)

	Page
4.2 - Materials and methods	76
4.2.1 - 3D Printing.....	77
4.2.2 - Mold Making	81
4.2.3 - Brain Phantom.....	82
4.3 - Results.....	83
4.4 - Discussion	85
CHAPTER 5: HAPTIC TEST- TISSUE-MIMICKING BRAIN PHANTOMS.....	89
5.1 - Introduction	89
5.2 - Materials and Methods	89
5.3 - Results.....	91
5.4 - Discussion	97
CHAPTER 6: CONCLUSIONS AND FUTURE WORK	99
6.1 - Conclusions	99
6.1.1 - Tissue-mimicking material mechanical characterization	99
6.1.2 - 3D modeling	99
6.1.3 - Haptic Test.....	100
6.1.4 - Summary.....	100
6.2 - Limitations of the present study and future work	101
6.2.1 - Limitations	101
6.2.2 - Future work	103
REFERENCES	106
APPENDICES	113
APPENDIX A	114
A.1 - Gelatin (G) with Chromium (Cr) Mechanical Characterization	114

Table of Contents (Continued)

	Page
A.2 - 4% Gelatin - 0.6% Agarose Mechanical characterization	116
APPENDIX B	117
B.1 - Anatomical location affect. Anterior vs Mid vs Posterior regions of the brain. (95% Confidence interval)	117
B.2 - Post-mortem time effect affect. 24hrs vs 6hrs post-mortem thresholds times. (95% Confidence interval)	120
B.2.5 - Elastic Moduli 50% Strain	124
B.3 - Brain tissue and brain substitute materials comparison	125
B.3.1 - Peak stress of Brain vs Emulsion.	125
B.3.2 - Peak stress of Brain vs Hydrogel. (95% Confidence interval)	128
B.3.3 - Elastic moduli of Brain vs Emulsion. (95% Confidence interval).....	131
B.3.4 - Elastic moduli of Brain vs Hydrogel. (95% Confidence interval).....	134
B.4 - Relaxation test	137
B.5 - Degradation Test (Mechanical characterization)	147
B.5.1 - Frozen Emulsion	147
B.5.2 - Non-Frozen Emulsion	154
B.5.3 - Frozen Hydrogel.....	160
B.5.4 - Non-Frozen Hydrogel.....	166
B.6 - Degradation Test – Emulsion Weight loss	172
APPENDIX C	173
C.1 - Internal Structures Axial Plane Measurements A, B, C, D and E	173
C.2 - Internal Structures Sagittal Plane Measurements F and G.	174
C.3 - Internal Structures Coronal Plane Measurements H and I.....	175
C.4 - Brain Cortex Axial Plane Measurements J and K.	176

Table of Contents (Continued)

	Page
C.5 - Brain Cortex Sagittal Plane Measurements L and M.	177
C.6 - Brain Cortex Coronal Plane Measurements N.....	178
C.7 - Skull Axial Plane Measurements O, P and Q.....	179
C.8 - Skull Sagittal Plane Measurements R.	180
C.9 - Skull Coronal Plane Measurements S and T.	181
APPENDIX D.....	182

LIST OF TABLES

Table	Page
Table 3.1: Loading rate, post mortem time, and anatomical location.	20
Table 3.2: Apparent Elastic Moduli of Brain Tissue. Measurements performed in this study were found to be similar to previous studies [18], [20]. (ANOVA, P-value > 0.05).....	22
Table 3.3: Apparent elastic moduli of the three identified regions on the Brain. (P-Value < 0.01 (Mean \pm SD).....	24
Table 3.4: Averaged apparent Elastic Moduli of brain tissue measured at 24hrs. and 6hrs post-mortem.	25
Table 3.5: Averaged apparent elastic moduli of brain tissue at 30% strain at 1, 0.1, 0.01 1/s strain rates (Mean \pm SD).....	27
Table 3.6: Number of samples and loading rate applied in mechanical tests under compression for hydrogels.	32
Table 3.7: Apparent Elastic moduli at different strain rates for 3% Gelatin- 1% Agarose material.	42
Table 3.8: Concentration of Lipids in Gray matter, White matter and Myelin of Human Brain established by O’ Brien et al. [50]. Values are expressed as a percentage of dry weight except water.....	43
Table 3.9: Number of samples and loading rates for mechanical testing of Emulsions	47
Table 3.10: Apparent elastic moduli of Emulsion B at different strain rates.	50
Table 3.11: Relaxation test parameters for brain tissue and brain substitute materials.	54
Table 3.12: Force percentage decreased after 1 sec of reaching a peak stress during relaxation experiments.....	58
Table 3.13: Compressive force values of brain tissue and brain substitute materials for the first time constant τ_1	60

List of Tables (Continued)

Table	Page
Table 3.14: Parameter values (mean \pm SD) for brain tissue and substitute materials' relaxation functions of the form $Gt = G1e(-t/\tau1) + G2e(-t/\tau2) + G3e(-t/\tau3) + G4e(-t/\tau4) + G5$	60
Table 3.15: Number of samples tested per material every week over the course of a month.....	61
Table 3.16: Macroscopic findings of oil and hydrogel based materials after 1, 8, 15, 22 and 29 days frozen and non-frozen.....	63
Table 3.17: Percentage of weight loss of tissue mimicking materials tested at day 1, 8, 15, 22 and 29. (Mean \pm SD)	68
Table 4.1: Dimension measurements performed in cast, 3D printed and Virtual models of brain structures (Appendix C defines each measurement performed).....	84

LIST OF FIGURES

Figure	Page
Figure 3.1: Coronal Slice with gray and white mater. Photograph by John A. Beal, distributed under a CC-BY 2.5 license.[78]	11
Figure 3.2: Identified Regions of the cerebral cortex	14
Figure 3.3: Sampling areas of the brain for unconfined compression mechanical test.	15
Figure 3.4: Porcine Brain Tissue sample for unconfined compression mechanical test.	16
Figure 3.5: Unconfined Compression Mechanical Test of porcine brain tissue at 40% Strain.	17
Figure 3.6: Definition of apparent elastic modulus used in this study. This method of measurement was chosen to be consistent with prior measurements reported in literature from Tamura et al.[20]	18
Figure 3.7: Typical response of Brain Tissue in compression test obtained at strain rate of 1/s.....	21
Figure 3.8: Stress-Strain Relationships comparison in unconfined compression. Averaged tissue response measured in compression on 14mm high specimen to 50% strain at 1/s strain rate [20] and first load response on 9mm high specimen to 50% strain at 1/s strain rate[18].	22
Figure 3.9: Averaged Regional Stress-Strain Relationships of Pig brain tissue at a strain rate 1/s. Posterior (n=16). Mid (n=6), Anterior (n=16). No significant differences in peak stress among samples with different anatomical origin measured up to 30% strain. (P-value>.05).....	23
Figure 3.10: Averaged Stress-Strain response of brain tissue at two different thresholds of post-mortem time.	25
Figure 3.11: Averaged stress-strain relationships in unconfined compression test for 1/s, 0.1/s and 0.01/s strain rates.	26
Figure 3.12: A) Emulsion allowed to set in the petri dish. B) Hydrogel samples cut for measurement of mechanical properties.	29

List of Figures (Continued)

Figure	Page
Figure 3.13: Unconfined compression mechanical Test of 3% Gelatin-1% Agarose at 40% strain and 1/s strain rate.....	31
Figure 3.14: Stress-Strain Relationships of Hydrogel based materials and silicones tested under compressive loads at 35% strain and strain rate of 1/s.	33
Figure 3.15: Stiffest materials from figure 3.14. Stress-Strain Relationships of Hydrogel based materials and silicones tested under compressive loads at 35% strain and strain rate of 1/s. These materials resulted too stiff to be suitable for mimicking brain tissue, thus discarded for further analysis.....	34
Figure 3.16: Stress-Strain Relationships of Hydrogel based materials and silicones tested under compressive loads at 35% strain and strain rate of 1/s.	35
Figure 3.17: Stress-strain mechanical response of silicones at a strain rate of 1/s compressed 30% and compared to mechanical behavior of brain tissue tested under same conditions.....	36
Figure 3.18: Stress-strain mechanical response of gelatin-agarose mixtures at a strain rate of 1/s compressed 30% and compared to mechanical behavior of brain tissue tested under same conditions.....	38
Figure 3.19: Stress-strain mechanical response of brain substitute materials and brain tissue at a strain rate of 1/s and strain of 30%.....	39
Figure 3.20: Typical Stress-Strain response of hydrogel samples at a strain rate of 1/s and 30% strain.	40
Figure 3.21: Averaged Stress- Strain curves of 3% Gelatin- 1% Agarose material at different strain rates.	41
Figure 3.22: Unconfined Compression Mechanical Test of Emulsion B at 35% Strain.....	46
Figure 3.23: Stress-Strain curve of emulsions A and B compared to brain tissue mechanical response at a strain rate of 1/s and 30% strain	47

List of Figures (Continued)

Figure	Page
Figure 3.24: Typical response of emulsion B at a strain rate of 1/s up to a 30% strain level.	48
Figure 3.25: Averaged stress-strain relationships of Emulsion B mechanical response at different strain rates.	49
Figure 3.26: Emulsion peak stress response over time after removal from refrigerator. Mechanical properties were relatively stable 0 - 60 min emulsion samples.	51
Figure 3.27: Hydrogel peak stress response over time after removal from refrigerator. Mechanical properties were relatively stable 0 - 60 min emulsion samples.	52
Figure 3.28: Averaged Normalized peak stresses of Oil Based material (Green), Hydrogel Based material (Red) and Brain Tissue (Black) tested at 1/s strain rate.	53
Figure 3.29: Averaged relaxation response of brain substitute materials and brain tissue.	55
Figure 3.30: Averaged Relaxation curves of emulsion at two different compressive strain levels at a Strain Rate of 10mm/s	57
Figure 3.31: Time course of the averaged normalized relaxation responses of brain tissue and tissue-mimicking materials against a logarithmic time scale.	59
Figure 3.32: Normal Hydrogel Sample (A) vs frozen hydrogel sample (B).	63
Figure 3.33: Frozen hydrogel sample in petri dish. Cuts caused but ice crystals' expansion during freezing. A) 15 days frozen, B) 8 days frozen. Shrinkage of materials after one month of storage.	64
Figure 3.34: Shrinkage of materials after one month of storage. A) Non-Frozen emulsion sample (29 days), B) Frozen Hydrogel sample (29 days). A) Non-Frozen emulsion sample (29 days), B) Frozen Hydrogel sample (29 days).	64

List of Figures (Continued)

Figure	Page
Figure 3.35: A) Non-frozen hydrogel sample (22 days) B) Frozen Hydrogel sample (22 days) C) Frozen hydrogel sample (29 days).....	65
Figure 3.36: Oil based Brain Phantom. A) Fresh B) 29 days stored. No macroscopic differences could be found but a slight darker color.	66
Figure 3.37: Peak stresses at 30% strain of Frozen and Non-Frozen hydrogel and emulsion. Lines depict a trending line for each material, non-frozen materials tended to stiffen while frozen materials wouldn't, specifically frozen emulsion.....	67
Figure 3.38: Percentage of weight loss of tissue mimicking materials tested at days: 1, 8, 15, 22 and 29.	69
Figure 4.1: 3D printed anatomical structures. A) Core brain, B) Brain cortex and C) Skull.....	79
Figure 4.2: Sagittal view of brain internal structures. Each color represents a mask which in turn defines a single structure. 1) Corpus Callosum, 2) Ventricles, 3) Caudate Nucleus, 4) Thalamus, 5) Internal Capsule, 6) Brainstem, 7) Cerebellum.....	80
Figure 4.3: Mimics Research 17.0 Work area. A) Coronal plane, B) Axial Plane, C) Sagittal Plane, D) 3D Calculated 3D from Mask. All structures but the ventricles were united in a single structure.	80
Figure 4.4: Brain cortex Negative Mold with 3D printed core brain positioned into place.....	82
Figure 4.5: Cast brain phantoms. A) Oil based material, B) Hydrogel Based Material.....	83
Figure 5.1: Similarity rating for hydrogel and oil based brain phantoms compared to brain tissue. Tool: Finger.	92
Figure 5.2: Similarity rating for hydrogel and oil based brain phantoms compared to brain tissue. Tool: Mall Probe.	93
Figure 5.3: Similarity rating for hydrogel and oil based brain phantoms compared to brain tissue. Tool: Scalpel.	93

List of Figures (Continued)

Figure	Page
Figure 5.4: Similarity rating for hydrogel and oil based brain phantoms compared to brain tissue. Tool: Forceps.	94
Figure 5.5: Similarity rating for hydrogel and oil based brain phantoms compared to brain tissue. Tool: Scissors.....	94
Figure 5.6: Overall similarity between hydrogel phantom and Brain Tissue.	96
Figure 5.7: Overall similarity between emulsion phantom and Brain Tissue.	96
Figure 5.8: Final vote of participants regarding the question which brain phantom resembles better the feel of brain tissue.	97
Figure A.1: Stress-Strain response for Gelatin- Chromium samples tested at 1/s strain rate and 45% strain.....	114
Figure A.2: Stress-Strain response for Gelatin- Chromium samples tested at 1/s strain rate and 45% strain.....	115
Figure A.3: Stress-Strain response for Gelatin- Agarose samples tested at 1/s strain rate and 45% strain.	116

CHAPTER 1

MOTIVATION AND BACKGROUND

1.1 - Introduction

Computed Tomography (CT) scans and Magnetic Resonance Imaging (MRI) have been used to image brain structures. Although CT and MRI are precise and sensitive modalities, 2D sectioned imaging has its drawbacks, including that 3D images are observed through 2D screens, thus, generating limitations related to image interpretation. On the other hand, neurosurgery requires experience and training surgical skills which are acquired through practice before getting ready for the operating room experience. Typical methods for learning include cadavers which are costly, need special facilities and usually are meant for single use. Live anesthetized animals do not represent true human anatomy. While alternative techniques developed using Virtual Reality (VR) simulation tools show some promise, they can be very expensive and have distinct limitations on their ability to mimic tissues and generate force and tactile feedback to the user[1].

The progress and expansion of rapid prototyping techniques allowed its introduction to the health care area. This has boosted the development of suitable human organ models for a wide range of training, education, and research purposes. Models are routinely used for the purpose of training surgeons, medical residents, and students. In

addition, patient specific models can aid in the diagnostic quality and understanding of the underlying anomalies, in the planning a complex surgery, and in the explanation of a surgical procedure to patients and their relatives. Rapid prototyping technology is becoming more affordable and accepted as 3D models improve their precision and material quality.

Rapid prototyping is a technology that uses 3-dimensional CAD data sets to fabricate 3D physical models. Stereolithography and 3D printing are the two rapid prototyping methodologies most used in the area of medicine to recreate anatomical structures used in preoperative planning or as reference tools during a surgical intervention. Stereolithography is a subtractive manufacturing technique that uses polymers that are cured by UV laser. By contrast, 3-D printers typically use additive manufacturing and are fuse deposition machines that extrude heated thermoplastic materials layer by layer [2].

Neurosurgery requires some of the most complex surgeries in medicine due to the sensitivity of brain tissue and the inaccessibility that represents some anatomical areas of the skull. This makes surgeries technically challenging for the surgeon and of high risk for the patient. Recent technologies have been developed to assist surgeons in diagnosis and planning. These include the advent of more realistic and detailed 3D images and the development of better hardware and software platforms for support. However, these still have limitations in the lack of haptic and tactile realism. In addition, the financial impact

of traditional surgical training is considerable [3]. However, newer technologies requiring VR environments for neurosurgical planning and training have significant costs which can be difficult for hospitals to absorb. This suggests the need for alternative methods of neurosurgery training and surgical planning. In neurosurgery, the utilization of anatomical models as simulators has become of great importance. The development of 3D printers has allowed the manufacture of patient-specific neurosurgical models of more realistic natures with multiple materials and varying consistencies adding reality to the models. However, these materials do not resemble the physical properties of brain tissue. This represents a severe limitation of these models for training of neurosurgeons. Giving a resident simulation tools that provide realistic feel as they perform a surgery task and manipulate the tissue is of great importance. In addition, studies have shown that not having suitable tactile feedback can have negative consequences. If the model doesn't have appropriate mechanical properties the trainees may apply more force than needed when they go into real surgery, significantly increasing the risk of causing traumatic injury.

Based on these limitations in current neurosurgery training and surgical planning, we aim to develop a brain substitute material that mimics the mechanical properties of brain tissue and to fabricate a brain tissue-mimicking material phantom that can have the following medical applications:

- Medical Education

The brain phantom would allow to explain and show to the neurosurgery residents how to perform the required steps in a neurosurgical procedure as well as allowing the trainees to practice and go through the steps of an entire procedure as many times as needed allowing room for mistakes with a zero-risk environment, repetitive practice and multiple case studies i.e. craniotomy or simple tumor excisions.

- Surgical Planning

It is important to establish high quality preoperative data in order to establish an accurate diagnosis based on a 3D appreciation instead of 2D CT or MR images for optimal surgical planning to minimize time, morbidity, and even mortality.

- Communication

3D models can facilitate communication with colleagues before and during surgery as well as the explanation of procedures to patients and relative.

1.2 - Current approaches

Conventional surgical training programs make use of techniques including animals, cadaver sections as well as real patients in an operating room. Simulation, a relatively new area currently in development, provides excellent tools to acquire surgical competence during high risk procedures. Simulation tends to increase safety, provide a

non-threatening controlled environment for practice, and allows immediate feedback. In neurosurgery, simulation based training ranges from play dough [4], to single or multiple material printed head models [5]–[8], and even to sophisticated VR surgical simulators [9].

Kentaro et al. fabricated stereolithographic models of skull base tumors which helped for preoperative planning, in patient education, and as a reference tool in the operating room [5]. Waran et al. used the new-generation 3D printers to create more realistic models for training neurosurgeons and planning surgical procedures [10]. This printed model consisted in a skull which included skin, bone, Dura mater, cerebrum as well as a tumor. Waran was able to create different types of consistency and density to mimic the different parts conforming his model, looking for characteristics like pliability of the skin, the cutting and suturing consistency of the same one, texture of the bone and handling of Dura mater and tumor [10]. Wurm et al. developed a simulation based training technique for cerebrovascular interventions based on 3-dimensional biomodels of cerebral vessels and a solid skull fabricated by means of rapid prototyping technologies (stereolithography and 3D printing) [11].

In recent years, work has been done in the development of virtual reality (VR) techniques. Researchers aim to find appropriate mathematical models of the brain mechanical properties for computer simulation of neurosurgical procedures. Applications of computer simulation of neurosurgery include virtual reality training, operation planning systems, and calibration of robotic devices to perform minimally invasive brain

surgery. However, VR simulators lack force and tactile feedback to the user; in other words, operators cannot feel the weight, texture, or compliance of the surface or object with which they are working. At present, sophisticated 3D models have been created for professional software which provides not only a visual 3-dimensional overview of neurologic anatomical structures but also applies haptic feedback through specific devices which are based on CT or MRI scans. Oishi et al. recently developed a surgical simulation technique which employs patient specific imaging data to perform surgical simulation for a skull base or deep tumor surgery using CAD software and manipulation of a haptic device which consisted in a 3D color printed model made out of plaster [12]. Although there have been efforts to overcome the deficiencies in haptic feedback of VR simulators by adding handy robotic devices; plaster, silicones or resins do not mimic the “feel” of real brain tissue which is of great importance. If the model does not have suitable mechanical properties, which will provide the trainees with proper feel as they manipulate the simulated tissue, negative consequences could arise in the transition from training on models to operation on live patients. Surgeons on these simulators and models learn to apply improper forces, which leads to increasing risks of traumatic injury in patients.

CHAPTER 2

RESEARCH AIMS

The need of biomimic materials to create brain models with a realistic haptic sense has motivated us to develop a patient-specific 3D brain phantom that resembles the mechanical properties of human brain tissue. The long-term aim of this project is that this material will aid surgeons in preoperative planning, clinician-patient communication, and the training of neurosurgery residents.

2.1 - Specific Aims

Aim 1: Development of a Brain tissue-mimicking material.

Unconfined compression tests will be carried out in hydrogel and oil based materials as well as brain tissue to characterize their mechanical properties and determine potentially brain substitute materials to use in the fabrication of tissue-mimicking brain phantoms.

Aim 2: Fabrication of a brain phantom from MRI data.

The objective is to develop a customized life-like, tissue-mimicking brain phantom using 3-dimensional printing and casting to make a replica of anatomic structures of the brain from MRI data and using brain substitute materials that simulate the feel of real brain tissue.

Aim 3: Realistic haptic sense testing of tissue mimicking brain model.

The feel of the brain substitute materials will be tested by Clemson University students. A series of tasks using surgical instrumentation will be performed which will allow the participants to compare between brain tissue-mimicking phantoms and real brain tissue in order to rate their level of similarity regarding the haptic sense or “feel” when manipulating the real and fake brains.

CHAPTER 3

TISSUE - MIMICKING MATERIAL

Development and Mechanical Characterization.

3.1 - Brain Tissue

3.1.1 - Introduction

The interest in the mechanical properties of soft tissue like brain, kidney, liver and prostate has been motivated both by the basic science importance of tissue mechanical properties to biological processes (e.g., mechanotransduction) as well as, more recently, the development of computer-integrated tools and robot-aided surgery and virtual reality techniques. Much of the work on characterizing the mechanical properties of brain tissue has focused on the development of mathematical models applicable to in silico (performed via computer simulation) brain models used for surgery and injury simulation. However, this study aims to develop brain simulant materials with mechanical properties comparable to those of brain tissue in order to develop brain phantoms that can aid in medical teaching and surgical planning.

Brain tissue has been extensively characterized in vitro under the modes of shear [13]–[16], compression [17]–[22] and tension [19], [23]–[25] [26], [27] as well as in situ

and in vivo under the modes of magnetic resonance elastography (MRE) [28]–[33], surface suction [34] and indentation [27], [35]–[38].

In this section, we will present the experimental measures of two potential brain substitute materials and porcine brain tissue tested in-vitro, under unconfined compression loads at three different strain rates.

3.1.1.1 - White and gray matter

The human brain is formed by gray matter which constitutes the brain cortex. White matter is composed of the myelinated nerve cell projections (axons) that connect the gray matter areas of the brain to each other. After years of research about the mechanical properties in brain tissue, some disagreement regarding differences in mechanical properties of white and gray matter tissues still remains.

Gray matter is constituted by cell bodies. It has been suggested that gray matter does not have significant mechanical anisotropy (i.e. large differences in directional properties). In contrast, white matter tissue is composed of oriented nerve fibers and is stiffer than gray matter [39][40][26]. In general, white matter is considered to be anisotropic while gray matter is nearly isotropic [40]. Therefore, a more consistent response can be found for gray matter than for white matter, that is, less variability in the mechanical characterization[26].

According with Kaster et al. [41] the difference in elastic modulus between white and gray matter is statistically significant ($P < 0.01$) that seems to validate the assumption

made in MRE studies [33] which conclude white matter is stiffer than gray matter. However, in our study of the mechanical properties of the cerebrum, separating gray matter from white matter would mean working with very small samples. The human cerebral cortex (gray matter), which is also a folded sheet, has a depth ranging from 1 to 4.5mm [42] (Fig.3.1). This small thickness, complex folding geometry, and extremely soft and delicate properties of brain tissue, make it difficult to perform tests of the mechanical properties of gray matter separately from white matter under unconfined compression tests in vitro. Therefore, in order to ensure the integrity and stability (the sample must be able to maintain a shape while performing the test) brain samples tests were conducted on samples with mixed white and gray matter.

Figure 3.1: Coronal Slice with gray and white mater.
Photograph by John A. Beal, distributed under a CC-BY 2.5 license.[78]



3.1.1.2 - Vivo vs in situ vs in vitro

The hypothesis that pressurized vasculature plays a role in the mechanical properties of brain tissue has been tested by many researchers. Prevost et al.[27] observed in situ and in vitro response measurements to be significantly stiffer than in vivo. However, the difference, although significant, remained relatively small. Miller et al. [36] found that in vivo and in vitro mechanical response remained in the same order of magnitude. Geffen et al. (Gefen and Margulies 2004) reported that the lack of blood pressure does not affect the stiffness of brain tissue.

3.1.1.3 - Friction

According to Karol Miller [43], for brain tissue mechanical properties characterized in unconfined compression tests, even low values of friction have a significant effect in producing shear stresses, which leads to increases in measured reaction forces. Thus, there is a possibility that test results in this study might be affected by friction and we may be overestimating the measured tissue stiffness. However, care was taken to minimize friction during our experimental tests to minimize this source of error.

3.1.1.4 - Preconditioning

Precondition means that the response of the first loading (virgin or unconditioned response) is measured to be significantly stiffer than those observed for the immediate

subsequent loadings. This may be due to interstitial diffusion within the tissue [18]. The lower the rate of deformation the effects appear to be attenuated [27].

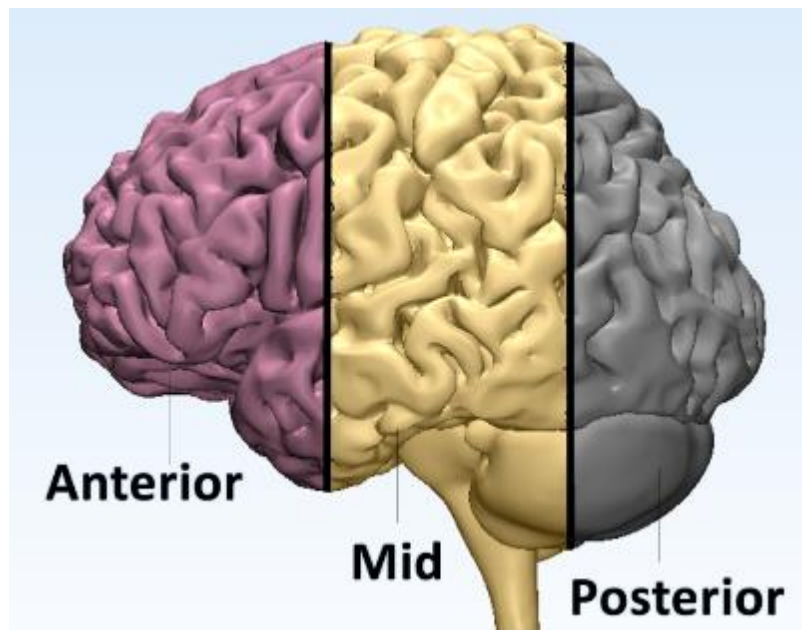
Although some authors have considered to employ precondition in order to get a standardized initial condition, Prevost et al. [27] observed that preconditioning in the tissue or altering the rate of load-unload sequence in vivo, in situ, and in vitro does not significantly impact measurements. These observations corroborate previously reported results in vitro tested uniaxial compression tests [18]. On the other hand, Kaster et al.[41] considered the second loading cycle as the most appropriate for analysis because the first cycle was “less smooth” than the following cycles. Given these prior results, we chose not to perform preconditioning in this study. The first loading cycle can sometimes induce non-reversible tissue damage at higher strains due to the tissues delicacy and adhesiveness. In addition, brain tissue does not experience cyclic loading inside the cranium during the surgical procedures we aim to mimic with the brain phantom because surgeons try to minimize repeated motion and handling of the tissue during surgery.

3.1.2 - Material and Methods

3.1.2.1 - Specimen preparation

A total of 19 brains from six-months old swines were collected from Godley Snell Research Center, Clemson University. Pig heads were obtained as a by-product of other terminal procedures performed at the facility. Heads were collected from the Research Center immediately after death, placed in ice and transported to the lab where the brains were harvested within 1 hr. post-mortem. Porcine brain tissue was selected as a substitute for human brain tissue due to the accessibility to reduce the post-mortem time testing. In addition, porcine brains have been found to have mechanical properties similar to human brains by other researchers[44]. To prevent dehydration and slow down degradation of the tissue, the brains were placed in physiological saline solution (PBS)

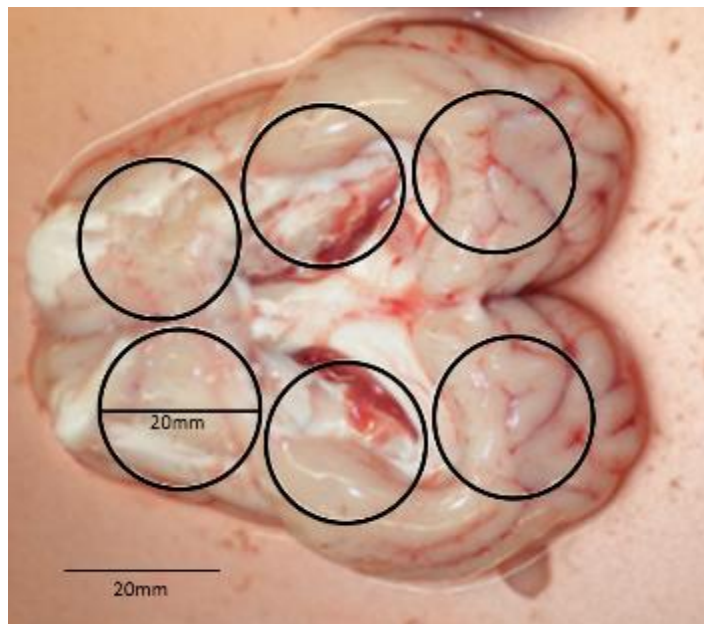
Figure 3.2: Identified Regions of the cerebral cortex



at 4 °C immediately after harvesting and refrigerated at 4 °C until the experiment, where they were warmed to room temperature (~23 °C) for specimen preparation. Brain weight average was 90.918 ± 5.16 g. (Mean \pm SD). The Dura-mater, midbrain and thalamus were removed during sample preparation. Three different regions of the cerebral cortex were identified as illustrated in Figure 3.2. In most cases, one sample was taken from the anterior, medial and posterior portions of each hemisphere for each porcine brain.

Six cylindrical specimens with 20mm of diameter and 10mm of thickness were cored out from each brain in the inferior-superior direction by utilizing a 20mm inner diameter steel pipe with sharp edges. By doing so, the Pia mater and arachnoid membrane could be cut by the edge of the steel pipe with slight distortion. Subsequently, specimens were cut with a surgical scalpel to make them about 10 mm thick as well as

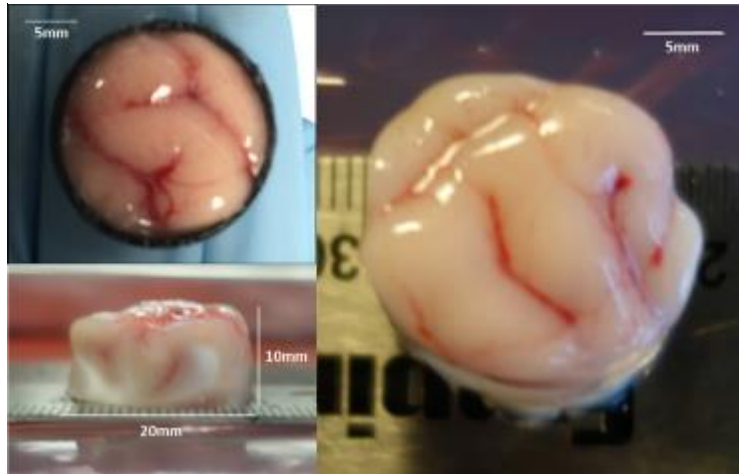
Figure 3.3: Sampling areas of the brain for unconfined compression mechanical test.



both faces of each sample were smoothed. For each brain, sample preparation was performed before testing to prevent dehydration. Two samples were taken from each identified region of the brain (left and right hemisphere) as depicted in figure 3.3. Samples of mixed white and gray matter were obtained. The arachnoid and Pia membranes as well as the gyri remained part of the sample. This will avoid the spread of the cortex foldings while performing the compression test.

Thickness and diameter measurements were conducted at all samples. For the diameter dimensions the upper and bottom faces were measured and the average was used as the input diameter. The actual diameter and height of the unloaded specimens were 19.00 ± 0.79 mm and 9.82 ± 0.80 mm (mean \pm SD, n=97), respectively.

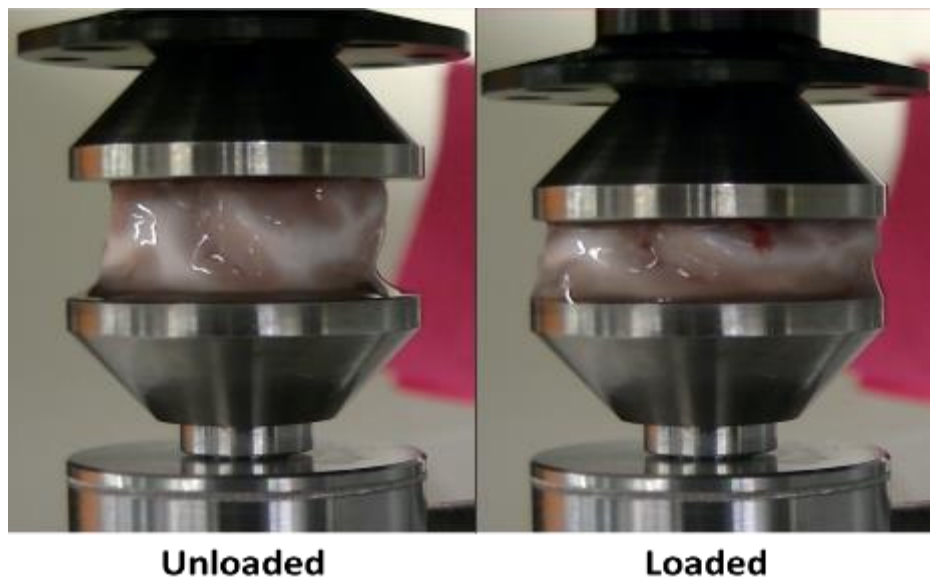
Figure 3.4: Porcine Brain Tissue sample for unconfined compression mechanical test.



3.1.2.2 - Experimental set up

Uniaxial unconfined compression test was conducted on pig brain tissue as shown in figure 3.5. Cylindrical specimens were placed between two platens and compressed in its axial direction. A load cell with measurement range of -17.5N to +22.0 N was attached under the bottom platen. The experiment was recorded with a camcorder JVC Everio GZ-E200BU and the recorded images were used to measure the initial diameter and thickness for all specimens, the radial displacement to ensure that each sample was compressed uniformly between the upper and lower platens. The initial diameter was used to obtain the initial cross-section area of each sample.

Figure 3.5: Unconfined Compression Mechanical Test of porcine brain tissue at 40% Strain.

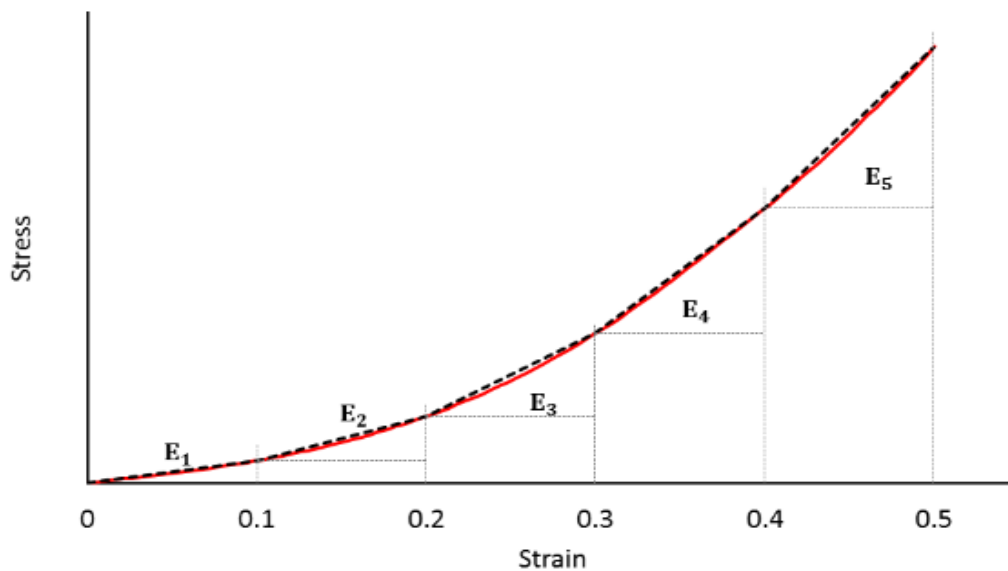


3.1.2.3 - Experimental protocol

Samples were axially compressed between two impermeable platens. One loading cycle was executed on each sample and all procedures were performed at room temperature. For loading, the specimen was placed in the bottom platen and the upper platen was manually positioned such that the platen's face was in contact with the specimen and to ensure full contact the tissue sample was preloaded with a force of 0.01N.

While conducting the experiment, care was taken to minimize friction between the sample and the platens since, as previously mentioned, friction significantly affects measured mechanical properties for brain tissue. Friction can be assumed to be zero when the sample expands uniformly during the compression test [43]. Platens and tissue

Figure 3.6: Definition of apparent elastic modulus used in this study. This method of measurement was chosen to be consistent with prior measurements reported in literature from Tamura et al.[20]



were hydrated with PBS to ensure pure slip boundary between the face of each platen and the upper and bottom surfaces of the tissue sample as well as to maintain the specimen wet to limit tissue degradation. Pure slip boundary was confirmed by visual inspection of recorded images.

Preloading was applied at .01N at the beginning of each test. Thus, the underformed height of the specimen was determined by the gap between the upper and lower platens after preloading was applied, and used as the initial dimension of the specimen to calculate the nominal strain. Nominal stress was calculated based on the axial force and initial cross-section area of each specimen. Apparent elastic moduli E_1, E_2, E_3, E_4 and E_5 was also obtained as the slope of the stress-strain curve in the strain ranges of (0-.1, .1-.2, .2-.3, .3-.4 and .4-.5, respectively (Fig. 3.6).

The displacement and force applied were acquired with a BOSE-ElectroForce test instrument (Model 3230, System 11-231). A series of compression test were carried out at three different loading rates. The velocity of the upper platen was set at 10mm/s, 1mm/s and 0.1mm/s which correspond to strain rates of 1/s, 0.1/s and 0.01/s, respectively. Strain rate sensitivity of brain tissue was examined as a reference point for development of brain tissue-mimicking materials. Anatomical location and post-mortem time effects were considered for this study, as well.

First, specimens in the inferior-superior direction were obtained from three different anatomical locations, to check regional heterogeneity of the cerebral cortex, stress-strain responses at a strain rate of 1/s were compared between specimens excised

from: anterior (n=16), mid (n=6), and posterior (n=16) regions. Second, to check post-mortem time effects: samples tested 24 hrs. post-mortem at a strain rate of 1/s were compared with specimens tested within 6 hrs. post-mortem. The mechanical response of brain tissue at different strain rates (1/s, 0.1/s and 0.01/s) was also examined. The stress-strain relationships obtained in the regional heterogeneity experiment will be used as a baseline for brain tissue-mimicking materials' development. Table 3.1 summarizes the number of specimens used for all experiments. Appendix B summarizes the statistical analysis performed for each mechanical parameter tested in this study.

Table 3.1: Loading rate, post mortem time, and anatomical location.

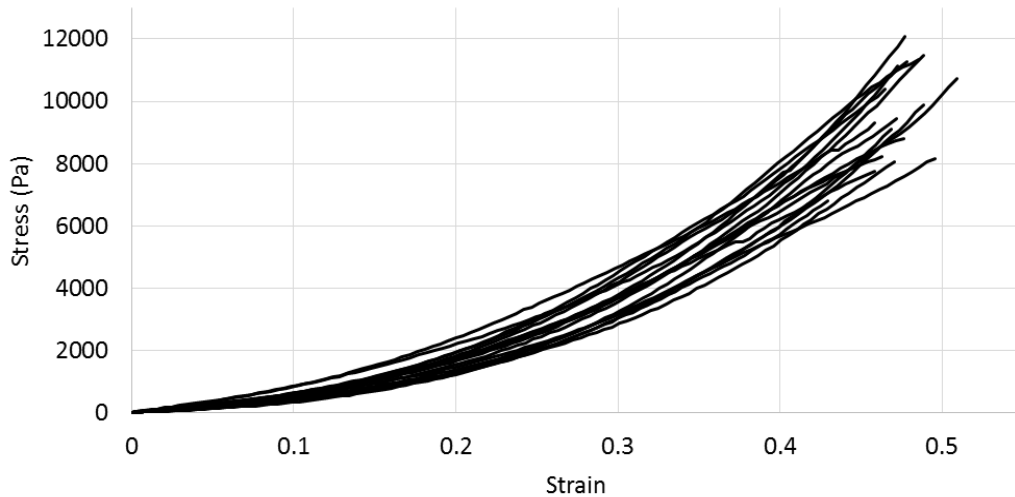
Velocity (mm/s)	Strain Rate (1/s)	Number of brains (N)	Number of samples(n)	A	M	P	Post-mortem time (hr.)
10	1	8	38	16	6	16	24
10	1	2	11	4	3	4	6
1	0.1	3	15	5	5	5	24
0.1	0.01	3	17	5	6	6	24
		19	98	36	25	38	

* A=Anterior Region, M- Mid Region, P- Posterior Region, N- number of brains, n- number of samples

3.1.3 - Results

The main objective in this section was to investigate the behavior of brain tissue under compressive loadings at rates comparable to surgery conditions. Force and

Figure 3.7: Typical response of Brain Tissue in compression test obtained at strain rate of $1s^{-1}$.



displacement were obtained at three different strain rates. The force (N) was divided by the cross-sectional area to determine the compressive nominal stress. The stress strain curves resulted concave upward for all compression loading velocities showing a non-linear behavior of brain tissue. Figure 3.7 depicts typical responses of brain tissue under compression loadings at $1s^{-1}$. One loading cycle was performed on each specimen which results were averaged into a single value for every strain rate. A total of 19 swine brains were tested, the results are affected by variation inherent for biological material and variation on the cross-sectional area due to deviation from cylindrical shape (up to 8%). However, brain tissue response was similar to those measured in previous studies by Tamura et al and Prevost et al. [18], [20]. There were no significant differences in elastic moduli E_1, E_2, E_3, E_4 and E_5 between both authors and our collected data (One way

Analysis of variance, P -value > 0.05 , Fig. 3.8). Measured Elastic Moduli are summarized in table 3.2.

Figure 3.8: Stress-Strain Relationships comparison in unconfined compression. Averaged tissue response measured in compression on 14mm high specimen to 50% strain at 1 s^{-1} strain rate [20] and first load response on 9mm high specimen to 50% strain at 1 s^{-1} strain rate[18].

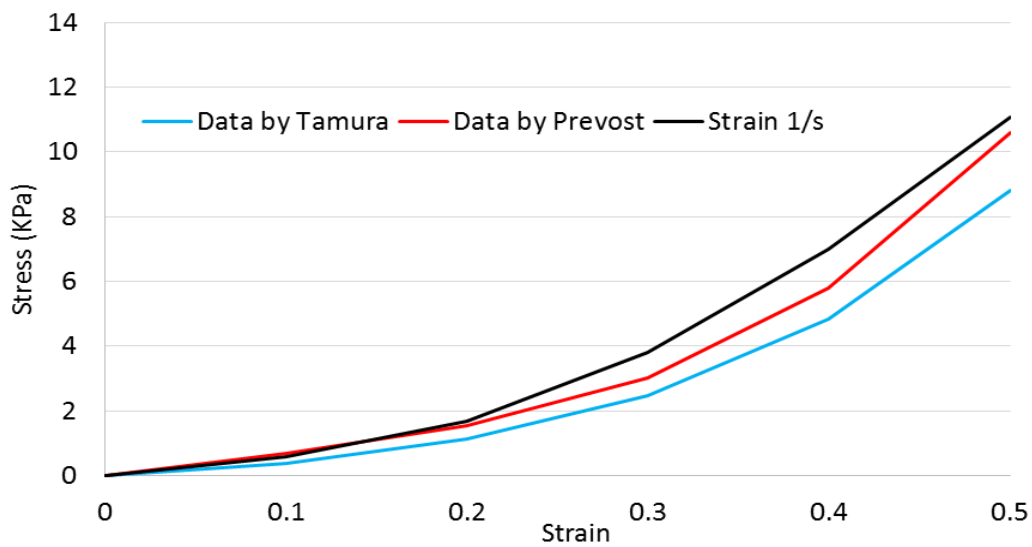


Table 3.2: Apparent Elastic Moduli of Brain Tissue. Measurements performed in this study were found to be similar to previous studies [18], [20]. (ANOVA, P -value > 0.05).

	E_1	E_2	E_3	E_4	E_5
Strain rate 1/s	5.70	11.26	21.16	31.76	41.00
Prevost et al. measurements	7.02	8.42	14.74	27.72	48.16
Tamura et al. measurements	3.62	7.25	14.27	24.11	41.78

3.1.3.1 - Effect of anatomical location and origin

Measurements performed in brain tissue were compared quantitatively across sample regions in terms of peak force level reached and elastic modulus. Mechanical properties of samples with different anatomical origin were found to be similar (Fig. 3.9). There were no significant differences between regions in the brain cortex up to 30% strain. One way analysis of variance was conducted and elastic moduli E_1 , E_2 and E_3 , and peak stresses were not found to be statistically different (P-Value > 0.05). Although E_4 and E_5 resulted statically different for the mid region, the difference in the measurements remained small. Data obtained from different regions of the brain were considered homogeneous up to 30% strain, thus, combined together for further analysis. Table 3.3 summarizes elastic moduli for the three regions of the brain.

Figure 3.9: Averaged Regional Stress-Strain Relationships of Pig brain tissue at a strain rate $1s^{-1}$. Posterior ($n=16$). Mid ($n=6$), Anterior ($n=16$). No significant differences in peak stress among samples with different anatomical origin measured up to 30% strain. ($P\text{-value}>.05$).

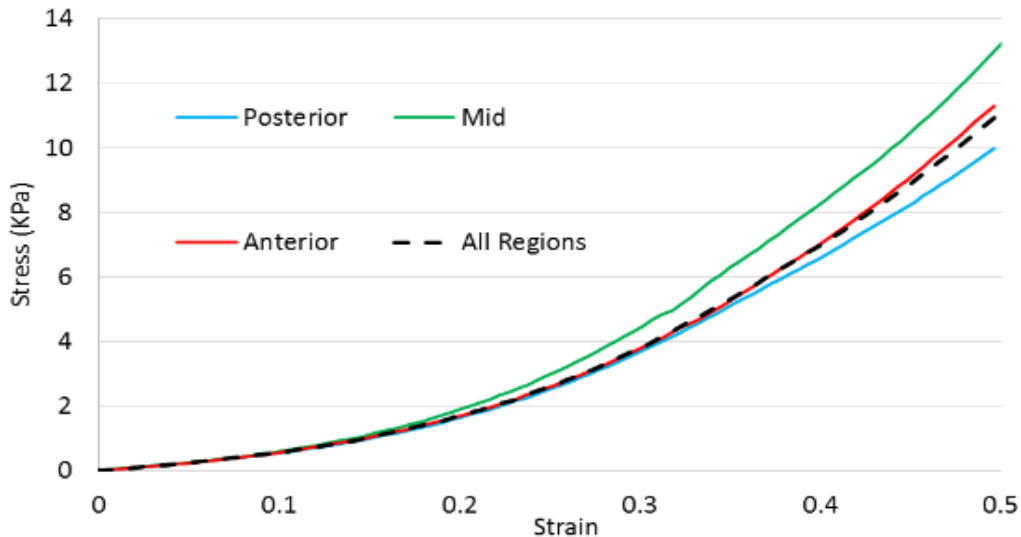


Table 3.3: Apparent elastic moduli of the three identified regions on the Brain. (P-Value < 0.01 (Mean \pm SD)

Region	E_1 KPa	E_2 KPa	E_3 KPa	E_4 KPa	E_5 KPa
Posterior	5.33 \pm 1.52	10.34 \pm 2.6	19.04 \pm 2.88	29.27 \pm 4.36	33.27 \pm 10.11
Mid	5.76 \pm .63	12.19 \pm 1.5	24.72 \pm 2.62	39.77 \pm 5.28	45.02 \pm 14.85
Anterior	5.30 \pm 1.52	10.41 \pm 2.49	19.19 \pm 4.01	30.85 \pm 6.31	39.11 \pm 6.14

3.1.3.2 - Post mortem time

The effects of post-mortem time response was investigated. Fig. 3.10 depicts the averaged stress-strain relationship of samples measured within 6hrs post-mortem versus samples with 24hrs post-mortem. A decrease of approximately 4.45 KPa was found for averaged peak stresses at a strain of 50% and 1/s strain rate for samples tested 24hrs post-mortem. Unpaired Student's t-test was conducted and Elastic Moduli E_1 , E_2 and E_3 were not statistically different just as their peak stresses (P-Value > 0.05) while E_4 and E_5 resulted significantly different between post-mortem threshold times (Table 3.4).

Figure 3.10: Averaged Stress-Strain response of brain tissue at two different thresholds of post-mortem time.

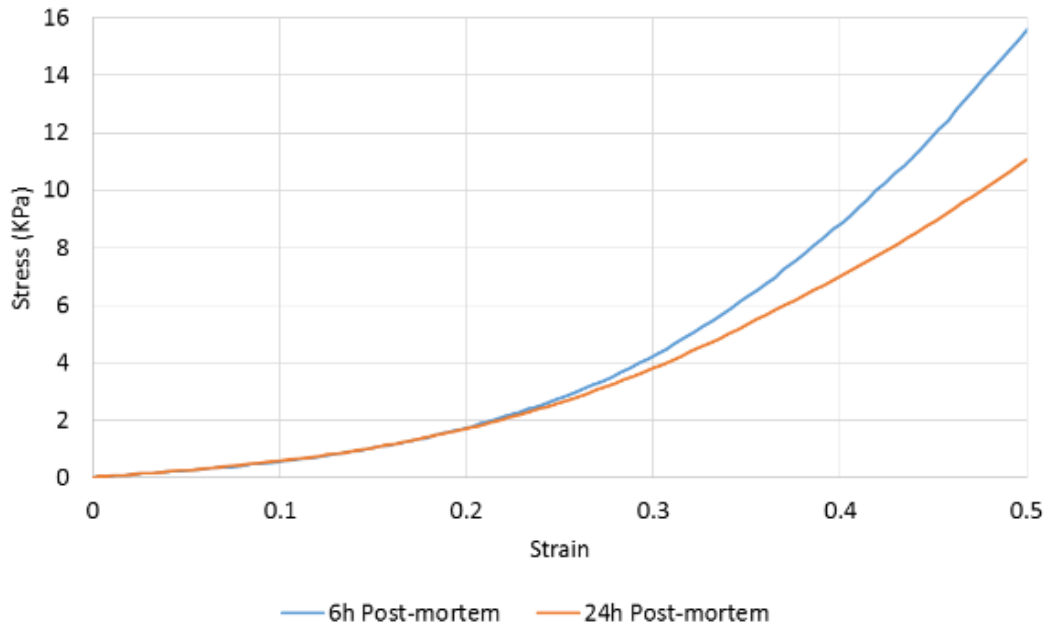


Table 3.4: Averaged apparent Elastic Moduli of brain tissue measured at 24hrs. and 6hrs post-mortem.

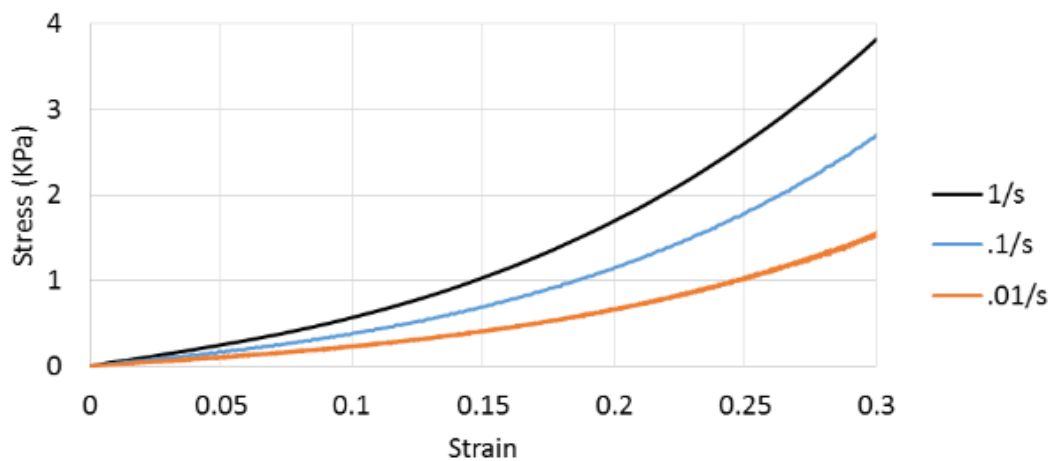
Post-Mortem time	E_1 KPa	E_2 KPa	E_3 KPa	E_4 KPa	E_5 KPa
6h	5.36 ± 1.31	11.77 ± 2.98	25.24 ± 5.59	46.92 ± 8.42	58.37 ± 7.85
24h	5.52 ± 1.4	10.94 ± 2.44	20.53 ± 3.82	32.43 ± 6.39	39.66 ± 10.72

Since it could not be demonstrated that brain tissue mechanical response was independent of anatomical location and post-mortem time at strain levels greater than 30%, further mechanical analysis of brain tissue and development of tissue mimicking materials would be carried out at strain levels up to 30% of strain. It should be noted that

high strains are not expected to be applied during neurosurgery procedures, since previous studies suggest that Traumatic Brain Injury (TBI) occurs at strains greater than ~20% and strain rates greater than $10s^{-1}$ [20]. In our search for brain substitute materials, strain levels up to 30% would be tested to compensate the low strain rates applied in this study.

3.1.3.3 - Strain Rate dependency

Figure 3.11: Averaged stress-strain relationships in unconfined compression test for $1s^{-1}$, $0.1s^{-1}$ and $0.01s^{-1}$ strain rates.



The stress-strain relationship for the three strain rates tested in this study indicated the stress response to be nonlinear with a toe region. Averaged stress-strain relationships were summarized in Fig 3.11. Tissue response was found to be highly rate dependent where tissue dramatically stiffens at greater strain rates. The increase in the stress response was 70% and 40% from 0.01 to 0.1/s and 0.1 to 1/s respectively at 30%

strain. One way ANOVA test shows there is significant difference between the apparent elastic moduli at each strain rate (P-value > 0.05). Elastic moduli E_1 , E_2 and E_3 are summarized in Table 3.5.

Table 3.5: Averaged apparent elastic moduli of brain tissue at 30% strain at 1, 0.1, 0.01 s^{-1} strain rates (Mean \pm SD).

Strain Rate s^{-1}	E_1 KPa	E_2 KPa	E_3 KPa
1	5.53 \pm 1.12	10.95 \pm 0.34	20.54 \pm 1.02
0.1	3.88 \pm 0.09	7.71 \pm 0.23	14.32 \pm 0.41
0.01	2.31 \pm 0.35	4.32 \pm 0.16	8.34 \pm 0.71

3.2 - Hydrogel

3.2.1 - Introduction

Hydrogels or hydrophilic gels are polymer networks which have the ability to swell retaining significant amounts of water. The large water content provides the material a degree of flexibility similar to that of natural tissue [45], [46]. Gelatin and Agarose are hydrogels often used in biomedical engineering for tissue culture as well as phantom materials to mimic mechanical properties of soft tissue. Gelatin is a product derived from collagen which is the principal component of skin, connective tissue, cartilage and bone. Agarose is a polymer generally extracted from seaweed and is frequently used in molecular biology for electrophoresis [45], [47]–[49].

The creation of a phantom to mimic brain tissue aims to reproduce its physical and mechanical properties, but some requirements need to be met for the design of a suitable phantom material which makes possible the development and manufacture of a brain model that will serve as a tool for training neurosurgery residents or planning a brain surgery.

1. Material stiffness measured under compressive loads needs to match that of brain cortex stiffness measured by the same protocol.
2. The material needs to be structurally stable at room temperature.
3. The material needs to be structurally stable while having a very low stiffness, so it would maintain its structure at the time of casting, handling and in future terms, sufficiently stable to be 3D printed.

Focus was put on matching the brain cortex composition of the brain with synthetic or natural materials. Different materials (in different combinations of ingredients as well as varying concentrations) were made to attempt to develop a suitable material that matched the mechanical properties of brain tissue under compression loading. These materials included silicones of different hardness, gelatin with and without chromium, agarose and emulsions. Emphasis was put in two materials, one hydrogel based material (3% Gelatin- 1% Agarose) and an emulsion which had similar mechanical properties to brain tissue. In this chapter some of the materials tested that helped in the development of the brain substitute material will be addressed. The two materials with

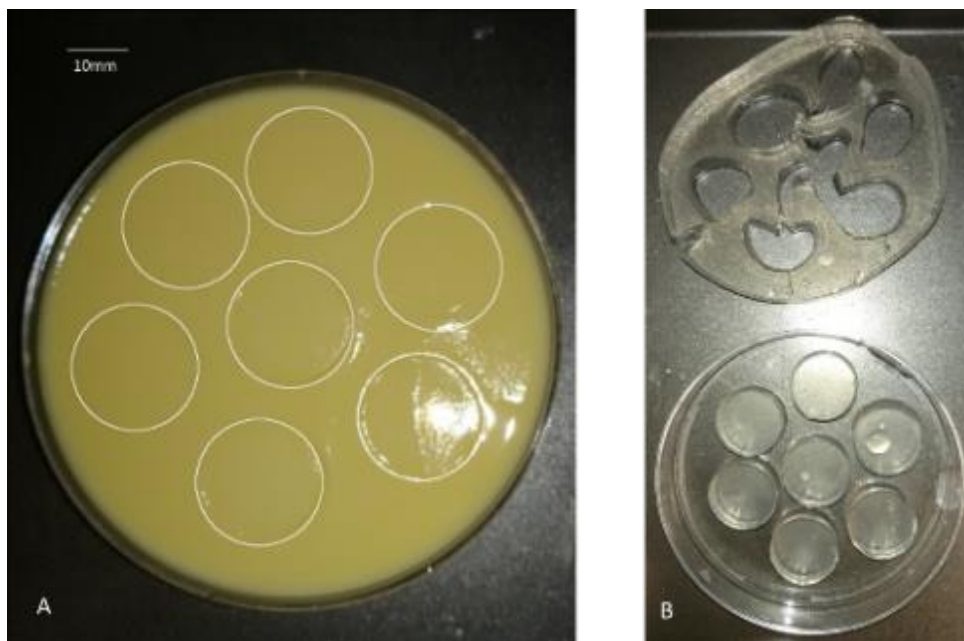
the closest mechanical behavior to that of brain tissue will be addressed with more detail. For more information about other materials used in the development of a brain tissue-mimicking material see Appendix A.

3.2.2 - Material and methods

3.2.2.1 - Gelatin-Agarose Hydrogels preparation

The Hydrogel was prepared mixing Agarose and Gelatin. Granulated gelatin was acquired from Carolina Biological Supply Company and Agarose Type I, Low electroendosmosis (EEO) was purchased from Sigma Aldrich. The aqueous solution was prepared adding 4g of Gelatin and 0.4g of Agarose ratio 3 to 1 respectively, (3% Gelatin-

Figure 3.12: A) Emulsion allowed to set in the petri dish. B) Hydrogel samples cut for measurement of mechanical properties.



1% Agarose), to 100ml of distilled water with a temperature of 80 °C. Then 100 x 15mm petri dishes were filled with the obtained aqueous solution up to 10mm. to match the sample thickness needed for the mechanical testing. After pouring the mixture into the petri dishes, the samples were allowed to set at room temperature. Ready samples were covered and stored for 12 hrs. at 4 °C to prevent dehydration and degradation until the experiment.

Approximately seven cylindrical specimens of diameter 20mm and 10mm of thickness were cored out from each petri dish by using a 20mm inner diameter steel pipe with sharp edges. (Fig. 3.12) Sample cutting was performed before testing to prevent deformation of original shape.

Thickness and diameter measurements were conducted at all samples. For the diameter measurements the upper and bottom faces were measured and the average was used as the input diameter. The actual diameter and height of the unloaded specimens were 20.44 ± 0.49 mm and 9.5 ± 0.13 mm (mean \pm SD, n=10), respectively.

3.2.2.2 - Experimental set up

Uniaxial unconfined compression test was conducted on Hydrogels as shown in figure 3.13. To test hydrogels under compressive loads, the same experimental set up used to test brain tissue was applied (Section 3.1.2.2).

3.2.2.3 - Experimental protocol

Figure 3.13: Unconfined compression mechanical Test of 3% Gelatin-1% Agarose at 40% strain and 1/s strain rate.



Protocol from section 3.1.2.3 was used to test hydrogels for mechanical properties under compression. In section 3.1.2 only measurements obtained under deformations up to 30% during compression were taken into account, although the strain applied was, for most of the different kinds of mixtures, 35%; due to significance in the difference between identified regions of the brain 3.1.3.1 and post-mortem time 3.1.3.2. In addition, some hydrogel mixtures, especially those with high concentrations of agarose were no able to withstand strain levels greater than 35% of their initial thickness without reaching failure point. Thus, the strain applied was reduced to 30% and apparent elastic moduli E_1 , E_2 and E_3 were obtained as the slope of the stress-strain curve in the strain ranges of (0-.1, .1-.2 and .2-.3.

Compression tests were carried out at three different loading rates. The velocity of the upper platen was set at 10mm/s, 1mm/s and .1mm/s. which corresponds to strain rates of 1/s, .1/s and .01/s, respectively.

The mechanical response of hydrogels at different strain rates was examined and the stress-strain relationships were obtained and compared with measurements obtained from brain tissue. Table 3.6 summarizes the number of samples used for the hydrogel experiments.

Table 3.6: Number of samples and loading rate applied in mechanical tests under compression for hydrogels.

Mechanical testing under compressive loadings			
Velocity (mm/s)	Strain Rate (1/s)	number of samples (n)	Strain (%)
10	1	25	30
1	0.1	11	30
0.1	0.01	10	30

3.2.3 - Results

The aim in this section was to find a material with similar mechanical properties as brain tissue under compressive loadings at rates comparable to surgery conditions. Materials like gelatin and agarose mainly, in different concentrations and mixed at different ratios as well as silicones with different hardness were tested to attempt to create a suitable stiffness material similar to brain tissue.

Figure 3.14: Stress-Strain Relationships of Hydrogel based materials and silicones tested under compressive loads at 35% strain and strain rate of 1/s.

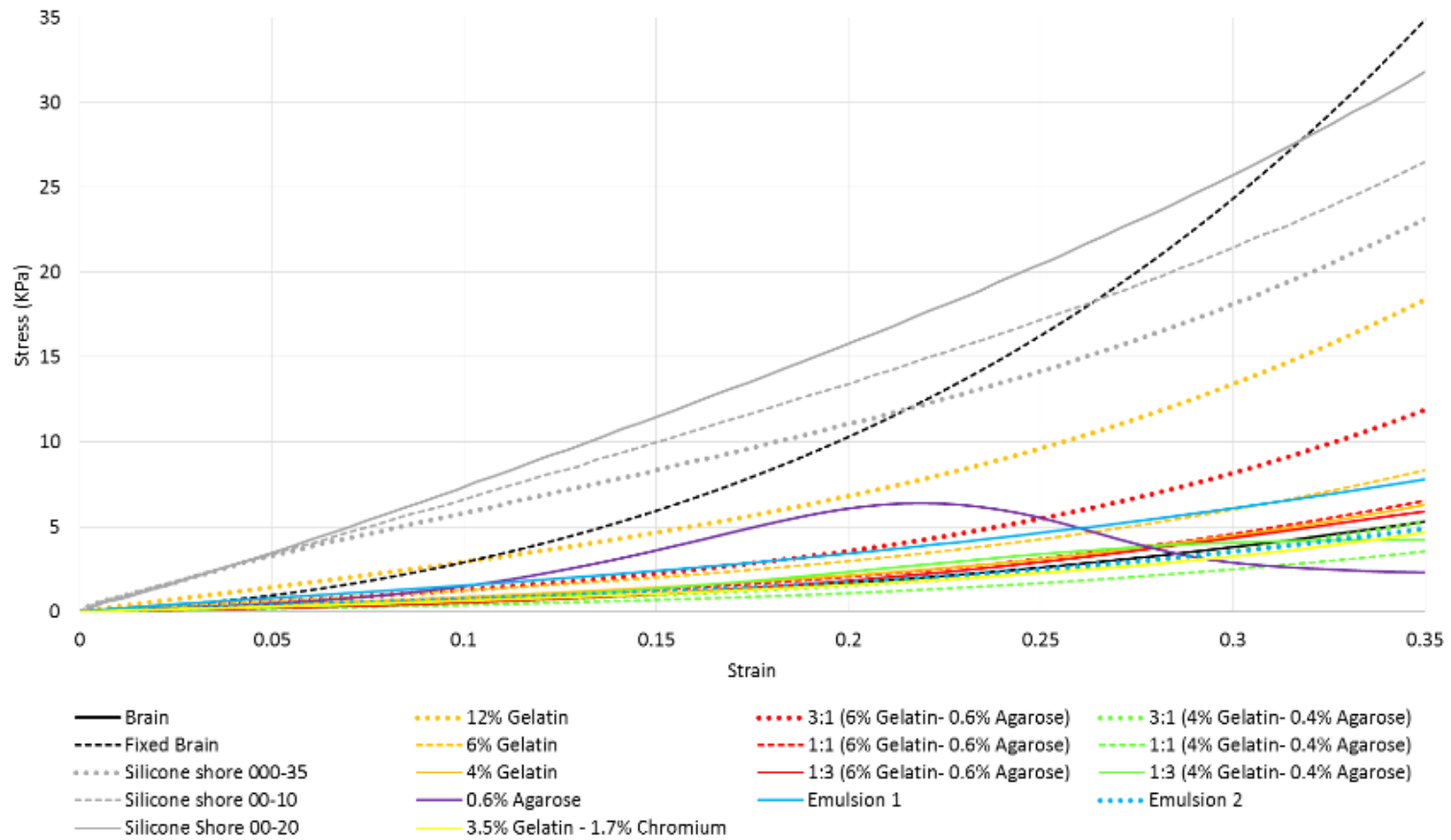


Figure 3.15: Stiffest materials from figure 3.14. Stress-Strain Relationships of Hydrogel based materials and silicones tested under compressive loads at 35% strain and strain rate of 1/s. These materials resulted too stiff to be suitable for mimicking brain tissue, thus discarded for further analysis.

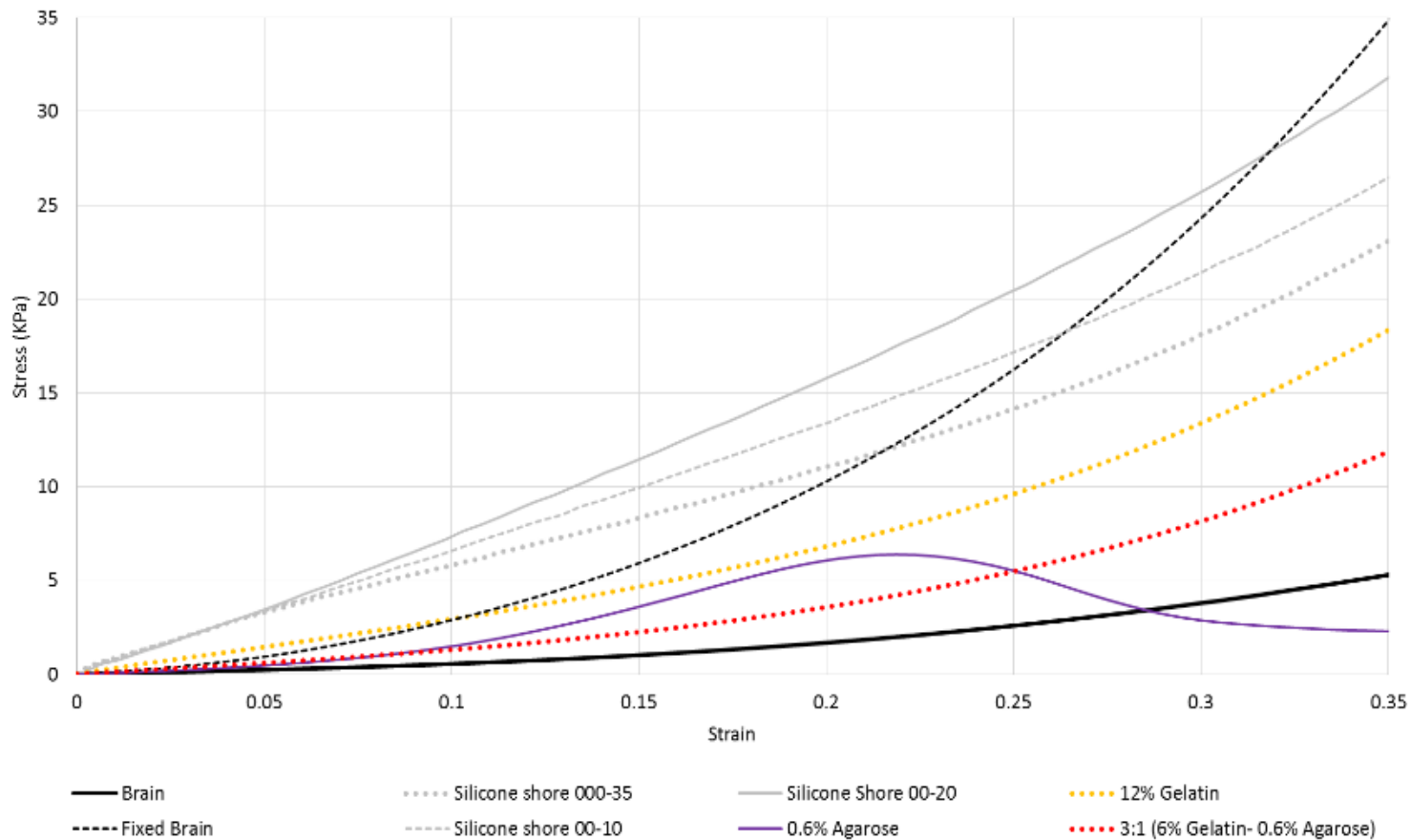


Figure 3.16: Stress-Strain Relationships of Hydrogel based materials and silicones tested under compressive loads at 35% strain and strain rate of 1/s.

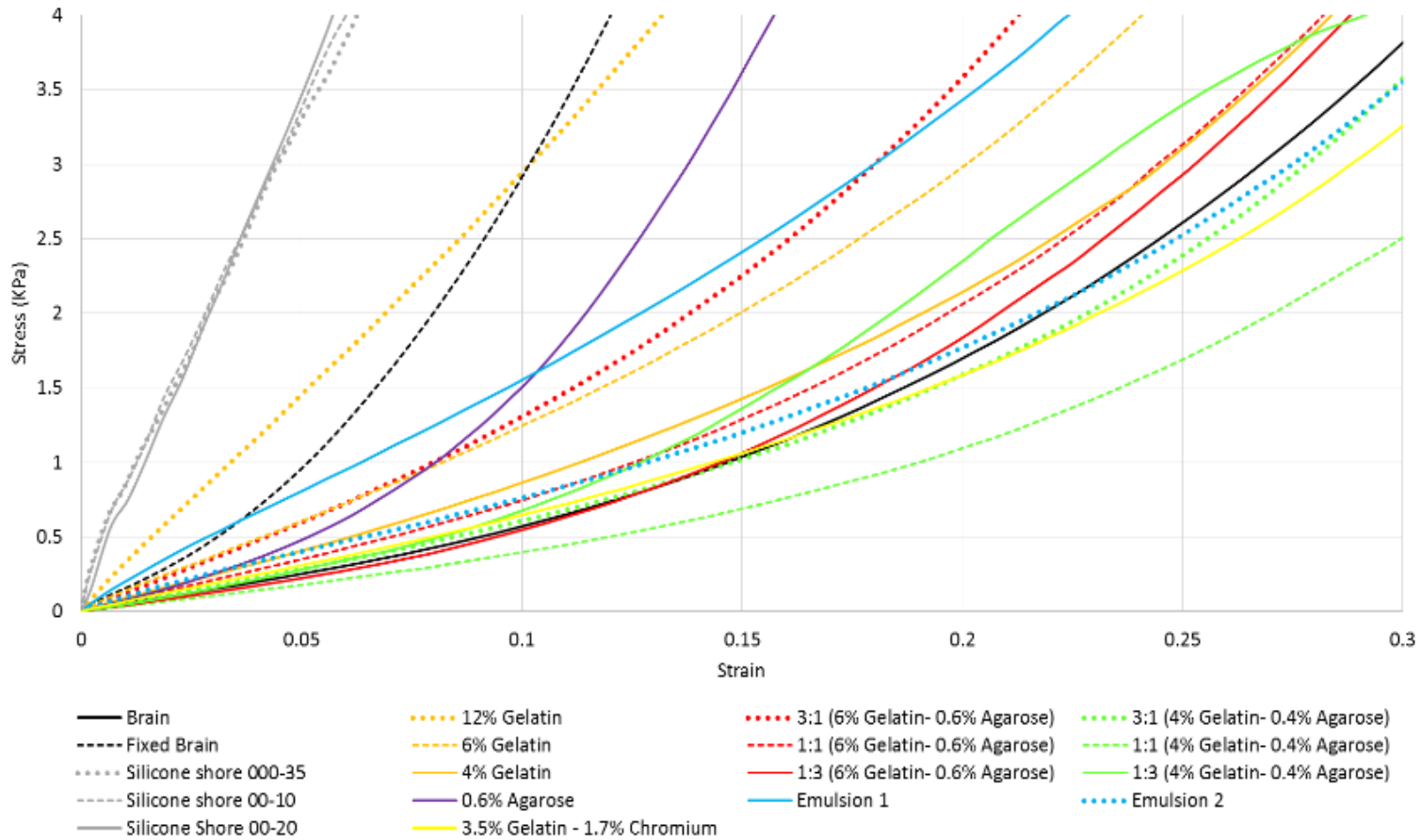
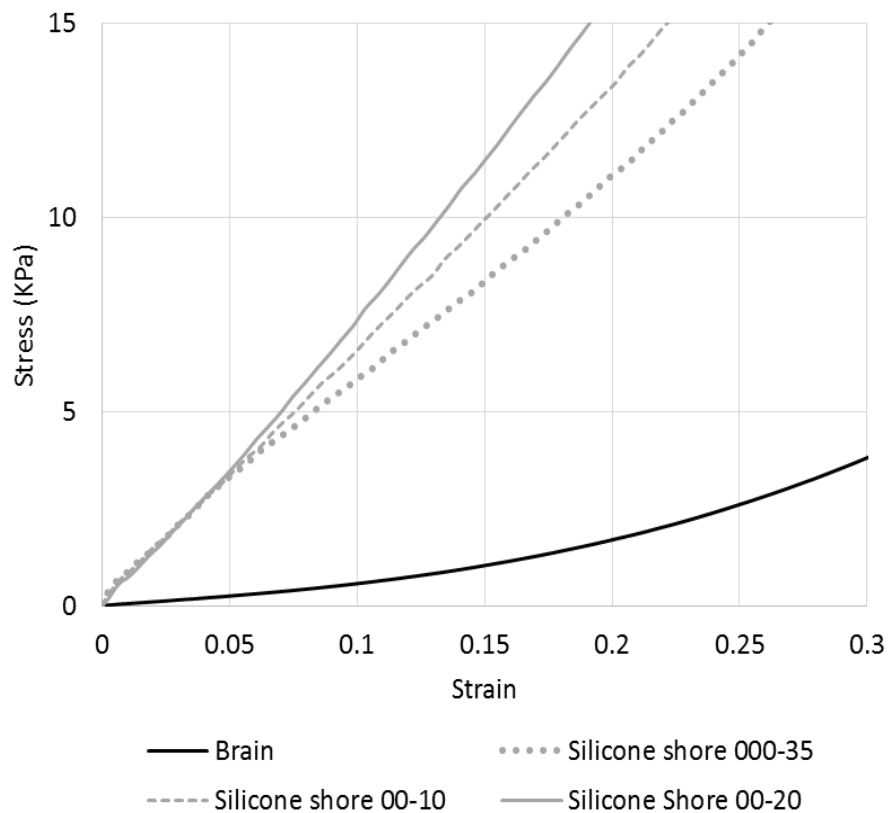


Fig. 3.14, 3.15 and 3.16 display the averaged stress-strain relationship of some hydrogels and silicones tested at 30% strain during the evolution of our tissue-mimicking material development compared against the brain tissue mechanical behavior. Fixed brain tissue was also tested to have an overall picture how stiff brain tissue becomes acquiring different mechanical properties when preserved for teaching purposes (black dashed line). As can be seen in the graph, gelatin 12% and 6%, is considerably stiffer than brain tissue (black solid line), 4% gelatin had closer behavior but testing very low concentrations of gelatin resulted hard due to the nearly nonexistent entanglements

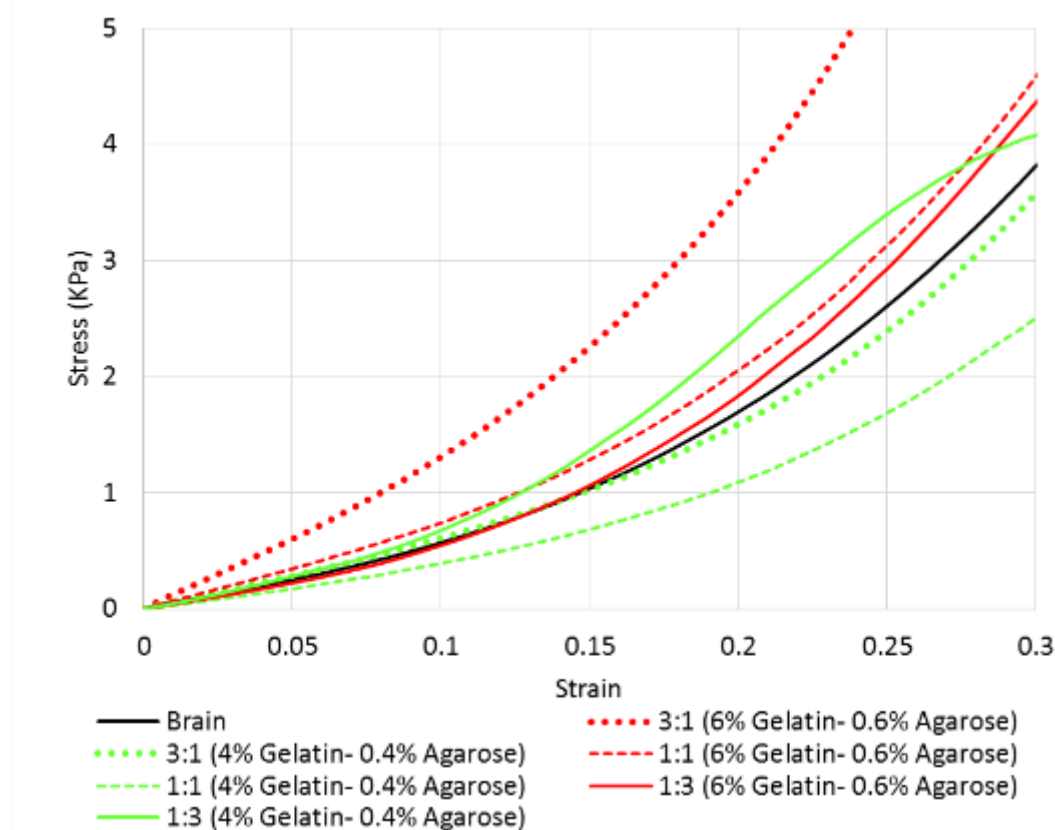
Figure 3.17: Stress-strain mechanical response of silicones at a strain rate of 1-s compressed 30% and compared to mechanical behavior of brain tissue tested under same conditions.



which provides a hydrogel with strength and stability, hence, giving the material high damage sensitivity and poor handleability. Agarose alone is also stiffer than brain tissue in addition to have a reduced failure point (less than 25% strain). Shore 000-35 silicone was the softest silicon tested, showing a much stiffer mechanical response compared to brain tissue, 00-20, 00-10 and 000-35 silicones' (Ecoflex-series, Smooth-On Inc. Macungie, PA) peak stress at 30% strain were much higher than brain (6.7, 5.6 and 4.7 times higher, respectively) and their stress-strain responses were linear instead of concave upwards as brain response revealed to be (Fig. 3.17).

Mixed gelatin (6% and 4%) and agarose (0.6% and 0.4%) at different ratios exhibited a mechanical behavior similar in shape to that of brain tissue. (Fig 3.18). Gelatin 4%- Agarose 0.4%, 3:1 ratio (3% Gelatin- 1% Agarose, green solid line) resulted the best approximation to stress-strain relationship of brain.

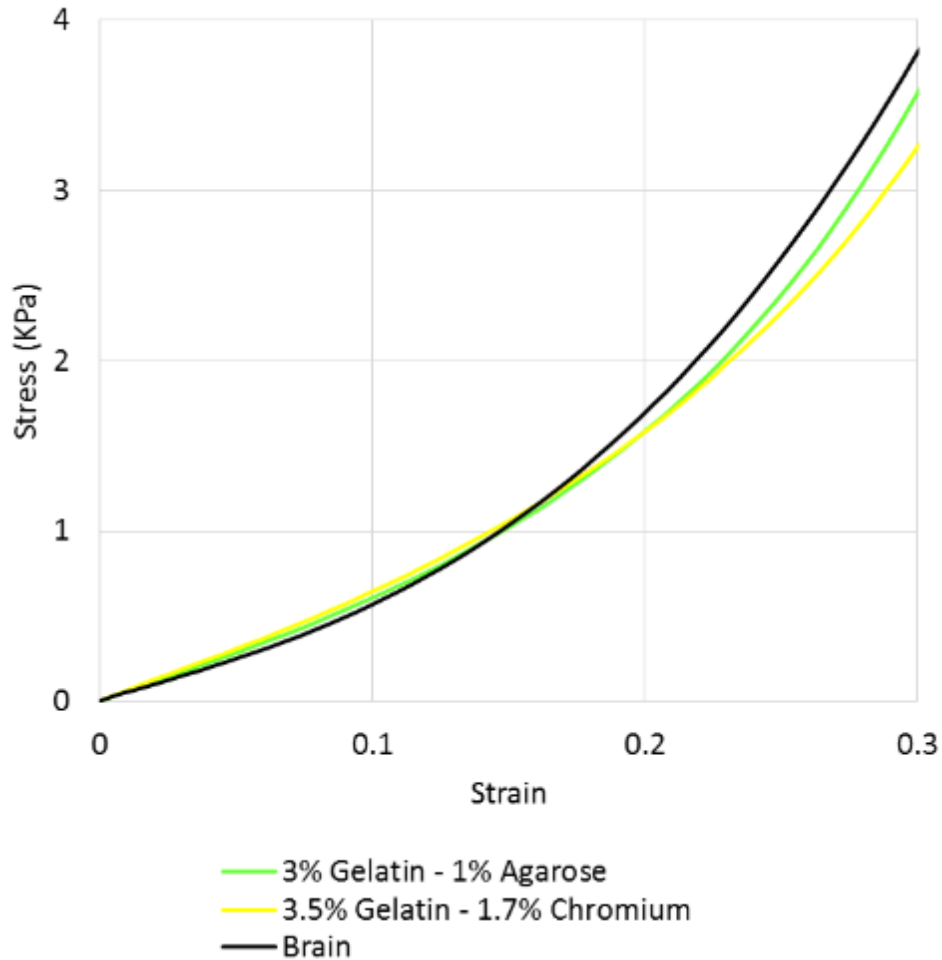
Figure 3.18: Stress-strain mechanical response of gelatin-agarose mixtures at a strain rate of 1-s compressed 30% and compared to mechanical behavior of brain tissue tested under same conditions.



The strength in a hydrogel is derived from the cross-links in the system, since gelatin showed to be weak and not handleable at low concentrations, it was strengthened with chromium. Chromium acts as a cross-linker agent for gelatin, increasing the number of bonds within the polymer network, hence improving its mechanical strength. Tests of gelatin mixed with different concentrations of chromium were carried out and results showed improvement of the polymer mechanical response and reduction of brittleness allowing 4% gelatin concentrations withstand strain levels greater than 50%. Adding 1.7%

of chromium to a 4% gelatin solution exhibited a similar behavior as brain tissue. Fig. 3.19 depicts the mechanical behavior of the two substitute materials that had the closest mechanical response to that of brain tissue. However, Gelatin-Chromium mechanical behavior at greater strains than 30% were much different than brain tissue (Appendix A.1), thus, only gelatin-agarose will be further analyzed.

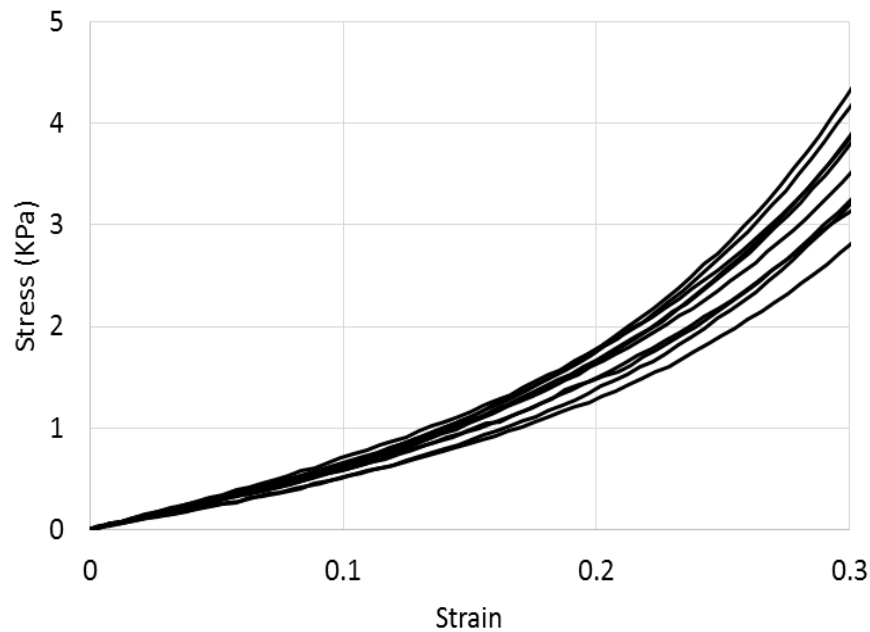
Figure 3.19: Stress-strain mechanical response of brain substitute materials and brain tissue at a strain rate of 1-s and strain of 30%.



3.2.3.1 - 3% Gelatin- 1% Agarose

Force and displacement were obtained at three different strain rates. The force (N) was divided by the cross-sectional area to determine the compressive nominal stress. The stress strain curves resulted concave upward for all compression loading velocities. Fig 3.20 depicts typical responses of hydrogels under compression loadings. A total of 25 samples were tested at 10mm/s up to 30% strain. One loading cycle was performed in each specimen which results were averaged into a single value for every strain rate.

Figure 3.20: Typical Stress-Strain response of hydrogel samples at a strain rate of 1/s and 30% strain.



3.2.3.2 - Strain Rate dependency

The stress response was found to be nonlinear. Mechanical behavior was found to be highly rate dependent where tissue dramatically stiffened with increasing strain rate. Stress strain relationships are summarized in Fig 3.21. The increase in the stress response was found to be ~20% and ~50% from 0.01 to 0.1/s and 0.1 to 1/s respectively at 30% strain. One way ANOVA test determined there is significant difference between the apparent elastic moduli at each strain rate (P-value < 0.05) as shown in Table 3.7.

Figure 3.21: Averaged Stress- Strain curves of 3% Gelatin- 1% Agarose material at different strain rates.

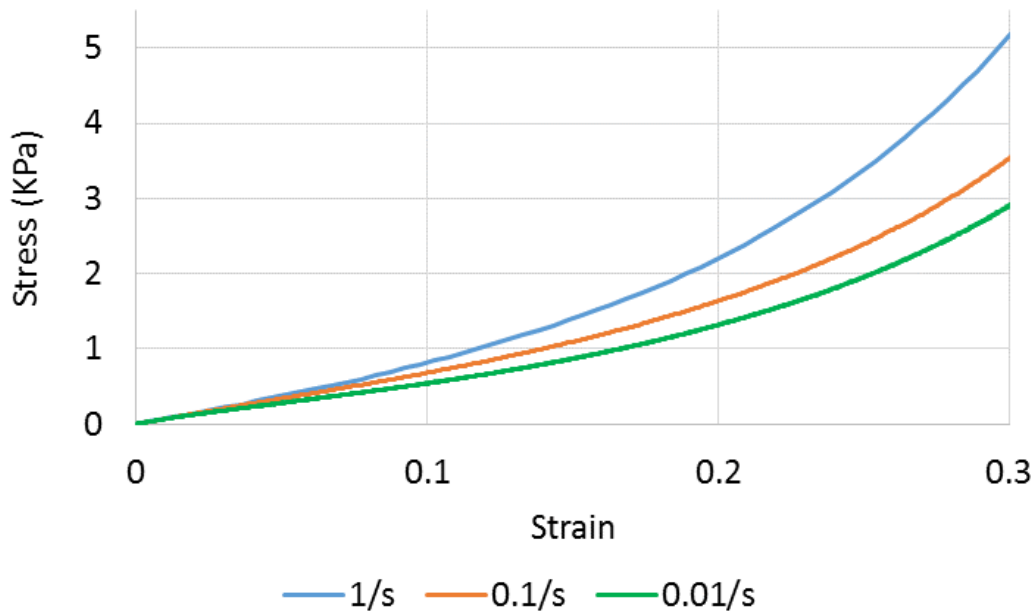


Table 3.7: Apparent Elastic moduli at different strain rates for 3% Gelatin- 1% Agarose material.

Strain Rate s^{-1}	E_1 KPa	E_2 KPa	E_3 KPa
1	7.93 ± 0.52	13.47 ± 0.79	28.57 ± 2.33
0.1	6.84 ± 0.93	9.65 ± 1.50	18.83 ± 1.84
0.01	5.24 ± 0.55	7.41 ± 1.03	14.92 ± 2.61

3.3 - Emulsion

3.3.1 - Introduction

The normal human brain of an adult is mainly composed of water, comprising 78.8 wt%, lipids conform 11.5 wt% and Non-lipid-residuals make up 9.7 wt%. A brain substitute material was based on these values to reproduce the high lipid content of human brain tissue in order to close the gap between the mechanical properties of the hydrogel developed in last section (gelatin-agarose) and brain tissue. Table 3.8 presents the concentration of lipids in gray matter, white matter and myelin of human brain for a child and an adult respectively.

Table 3.8: Concentration of Lipids in Gray matter, White matter and Myelin of Human Brain established by O’ Brien et al. [50]. Values are expressed as a percentage of dry weight except water.

	9-yr old			55-yr old		
	Gray matter	White matter	Myelin	Gray matter	White matter	Myelin
Water	85.8	77.4	-	82.3	75.2	-
Total lipid	37.6	66.3	78	39.6	64.6	78
Nonlipid residue	62.4	33.7	22	60.4	35.4	22
Total Glycero-phosphatides	21.2	25.9	31.9	21.1	21.5	24.8
Total sphingolipids	5.6	19.9	25	5.5	21.5	24.5
Unidentified	3.5	7.3	2.5	5.8	6.5	9
Cholesterol	7.2	13.2	18.6	7.2	15.1	19.7

In the previous section a series of hydrogel based materials were tested in order to find a brain substitute hydrogel that had a similar stress-strain behavior to brain tissue. Due to the high content of lipid constituting the brain oils were added to the hydrogel which had the best approximation to brain tissue mechanical response with the purpose of getting a mechanical response closer to that of brain tissue and increase the failure point, as hydrogels couldn’t stand deformations greater than 40%, thus, reducing the brittleness of the brain tissue -mimicking material making it more suitable for training or planning surgery brain models. Adding oils to hydrogels forming an emulsion, would also prevent syneresis by strengthening and increasing the number of bonds that form the polymer structure. Syneresis is the expulsion of water from a gel structure especially when frozen, which will close-pack the tridimensional network pushing out water

molecules. In this section the mechanical properties of two different emulsions will be discussed.

3.3.2 - Materials and methods

3.3.2.1 - Emulsion preparation

Two different emulsions were prepared: emulsion A and emulsion B. Both consisted of two phases: lipid phase and water phase. For emulsion A, the lipid phase included organic, pure and unrefined Flax oil, soybean lecithin and stearic acid, Flax oil contains many of the polyunsaturated lipids as the brain. For emulsion B, the stearic acid was not included. Stearic acid is a saturated fatty acid used in candle making as a hardener, in addition to its hardening properties, stearic acid would replace the content of cholesterol in the brain. The water phase included distilled water, gelatin and borax. Gelatin would work as a substitute for the non-lipid contentment of the brain. The soybean lecithin and borax were used as emulsifiers.

The lipid and water phases were prepared separately. Soybean lecithin, flax oil and stearic acid (only for emulsion B), were mixed at 50 °C. The water phase was prepared adding gelatin to distilled water at 50 °C, once the solution becomes clear, borax is added. Once both phases are ready, the lipid phase is added to the water phase for emulsification mixing vigorously with an electric blender during 2 min. The resulting mixture was poured into 100 x 15mm petri dishes filled up to 10mm in order to match the sample thickness

needed for the mechanical testing. After pouring the mixture into the petri dishes, the samples were allowed to set at room temperature. Ready samples were covered and stored for 12 hrs. at 4 °C to prevent dehydration and degradation until the experiment.

Seven cylindrical specimens of diameter 20mm and 10mm of thickness were cored out from each petri dish by using a 20mm inner diameter steel pipe with sharp edges. Sample cutting was performed before testing to prevent deformation of cylindrical shape.

Thickness and diameter measurements were conducted at all samples. For the diameter dimensions the upper and bottom faces were measured and the average was used as the input diameter. The actual diameter and height of the unloaded specimens were $20.76 \pm 0.25\text{mm}$ and $9.8 \pm 0.81\text{mm}$ (mean \pm SD, n=10) for emulsion A and $20.66 \pm 0.33\text{mm}$ and $9.5 \pm 0.30\text{mm}$ (mean \pm SD, n=10) for emulsion B.

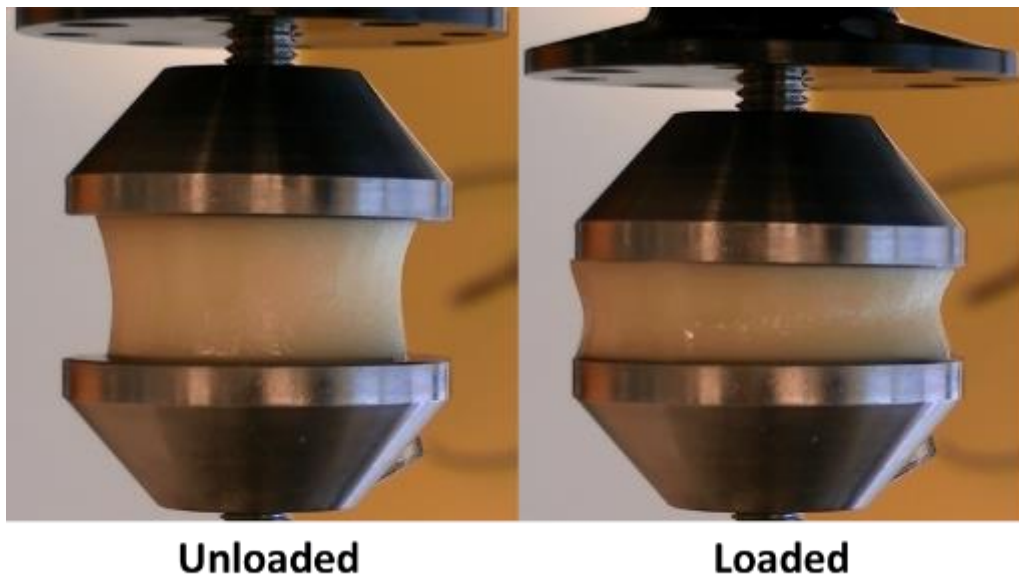
3.3.2.2 - Experimental set up

Sample preparation was performed following the protocol used for brain tissue (see section 3.1.2.2).

3.3.2.3 - Experimental protocol

Hydrogels experimental protocol was applied for the mechanical testing of emulsions. (Section 3.2.2.1). Briefly, a series of compression tests were carried out at three different loading rates, the velocity of the upper platen was set at 10mm/s, 1mm/s and 0.1mm/s. which correspond to strain rates of 1/s, 0.1/s and 0.01/s, respectively.

Figure 3.22: Unconfined Compression Mechanical Test of Emulsion B at 35% Strain.



The mechanical response of the emulsion at different strain rates was examined and the stress-strain relationships were obtained and compared with responses obtained from brain tissue and hydrogel samples. Table 3.9 summarizes the number of specimens used for the emulsion experiments.

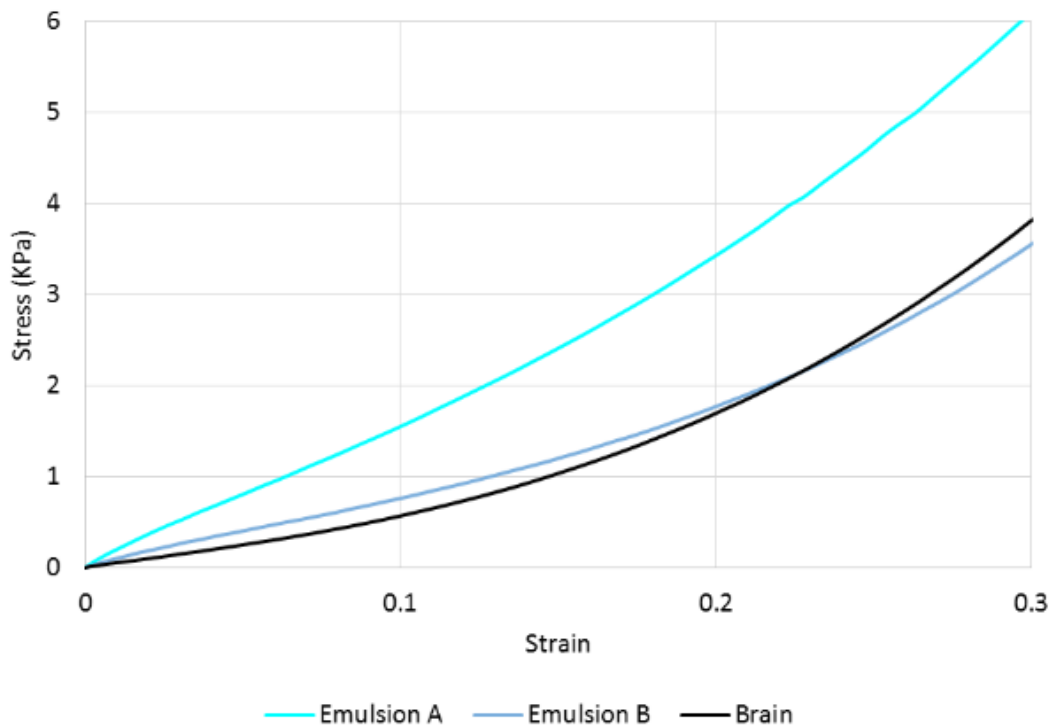
Table 3.9: Number of samples and loading rates for mechanical testing of Emulsions

Type of Emulsion	Velocity (mm/s)	Strain Rate (1/s)	Number of samples (n)	Strain (%)
B	10	1	30	30
B	1	0.1	10	30
B	0.1	0.01	10	30
A	10	1	10	30

3.3.3 - Results

Fig. 3.23 depicts the averaged stress-strain relationship of emulsions A and B compared to brain tissue mechanical response. As shown in the graph, emulsion A is too stiff compared with brain tissue stress-strain curve. This is due to stearic acid which acts

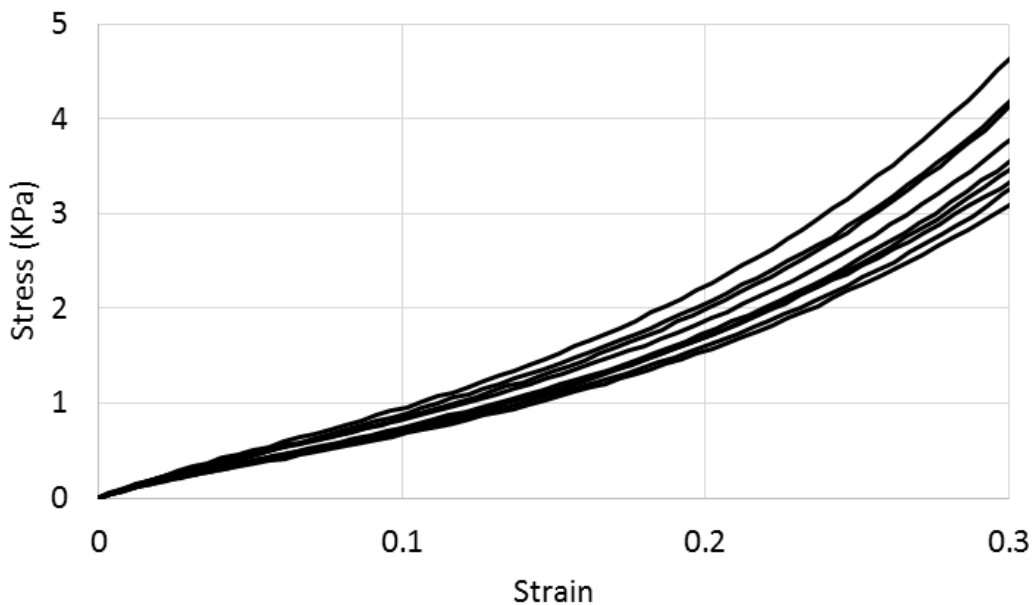
Figure 3.23: Stress-Strain curve of emulsions A and B compared to brain tissue mechanical response at a strain rate of 1/s and 30% strain.



as a hardener, even low concentrations made a big difference in the mechanical response of the emulsion. In the other hand emulsion B has a good approximation to brain tissue response. Thus, further analysis was made for emulsion B only.

Force and displacement were obtained at three different strain rates. The stress strain curves resulted concave upward for all velocities, the same behavior shown by brain tissue and the hydrogel material. Fig. 3.24 depicts typical responses of emulsion B under compression loadings. A total of 30 samples were tested. One loading cycle was performed in each specimen which results were averaged into a single value for every strain rate.

Figure 3.24: Typical response of emulsion B at a strain rate of $1s^{-1}$ up to a 30% strain level.



3.3.3.1 - Strain Rate dependency

Mechanical behavior was found to be highly rate dependent where tissue stiffens at greater strain rates. Stress strain relationships are summarized in Fig 3.25. The increase in the stress response is ~ 22% and ~ 40% from 0.01 to 0.1/s and 0.1 to 1/s respectively at 30% strain. One way ANOVA test showed there is significant difference between the apparent elastic moduli at each strain rate (P-value < 0.05). Table 3.10 summarizes the apparent elastic moduli for each stress rate.

Figure 3.25: Averaged stress-strain relationships of Emulsion B mechanical response at different strain rates.

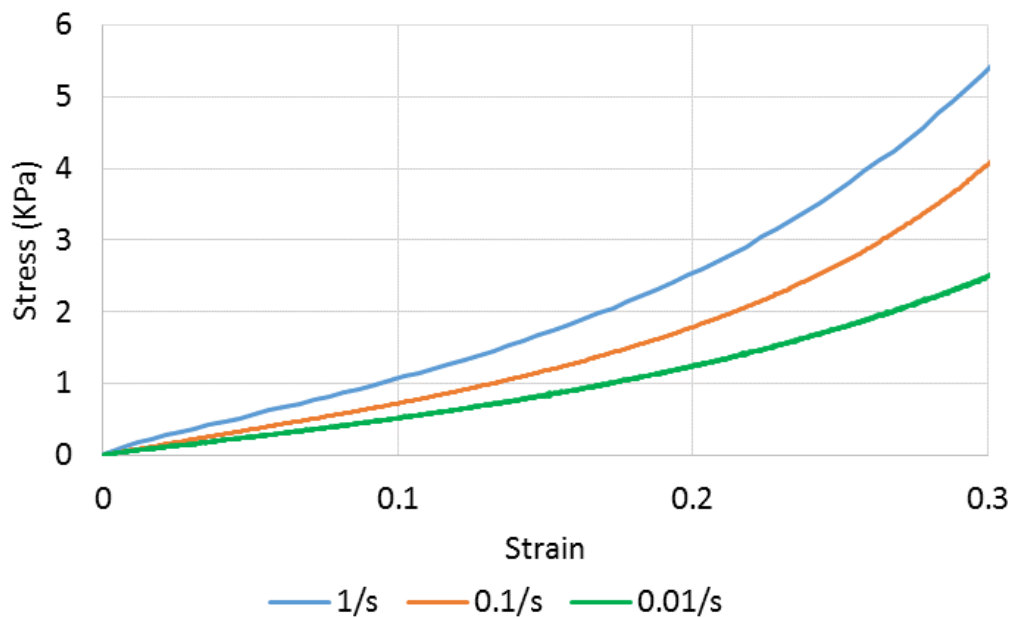


Table 3.10: Apparent elastic moduli of Emulsion B at different strain rates.

Strain Rate s^{-1}	E_1 KPa	E_2 KPa	E_3 KPa
1	10.35 ± 0.45	13.92 ± 0.78	26.59 ± 1.92
0.1	7.89 ± 0.51	10.64 ± 0.75	19.10 ± 1.63
0.01	6.65 ± 0.66	8.99 ± 0.76	15.61 ± 1.38

3.4 - Temperature

A well know problem when trying to characterize the mechanical properties of materials is the disparity in protocols which will lead to variation of results in the literature, specially, when working with living tissues. Specifically, one aspect that will yield to differences in measurements is the temperature at which tests are carried out. Although, many would claim that our studies should address mechanical testing of brain tissue and mimicking materials due to the alleged difference between in vivo and in vitro mechanical properties of brain tissue, since one of our purposes is to train new neurosurgeons, a brain phantom made out of our mimicking materials, would be utilized at room temperature, furthermore, the materials used to fabricate these phantoms are prone to biodegradation and dehydration if not preserved at low temperatures.

A series of mechanical test were conducted on hydrogel and emulsion materials at a strain rate of 1/s and up to 30% strain, with the purpose to determine the effect of temperature on the mechanical properties of these materials. Samples were maintained

at 4 °C, then 5 samples of each material were tested at minutes 0, 10, 20, 30, 40, 50, 60, 70, 240(4hrs) and 400 (8hrs) after being removed from the fridge and placed at room

temperature. Fig. 3.26 and Fig. 3.27 display the peak stresses of emulsion B and Hydrogel respectively.

Stress was found to change as a function of temperature. For both materials, it is visible that mechanical behavior softens with increasing temperature (0min = 4 °C, 400 min = 23 °C). During the testing the peak stresses continued decreasing gradually within an hour. The peak stresses decreased ~45% in 60 min. after samples were removed from the refrigerator. Emulsion seemed to stabilize within an hour while gelatin continued warming up. After 4hr, both materials have reached a 23 °C temperature.

Figure 3.26: Emulsion peak stress response over time after removal from refrigerator. Mechanical properties were relatively stable 0 - 60 min emulsion samples.

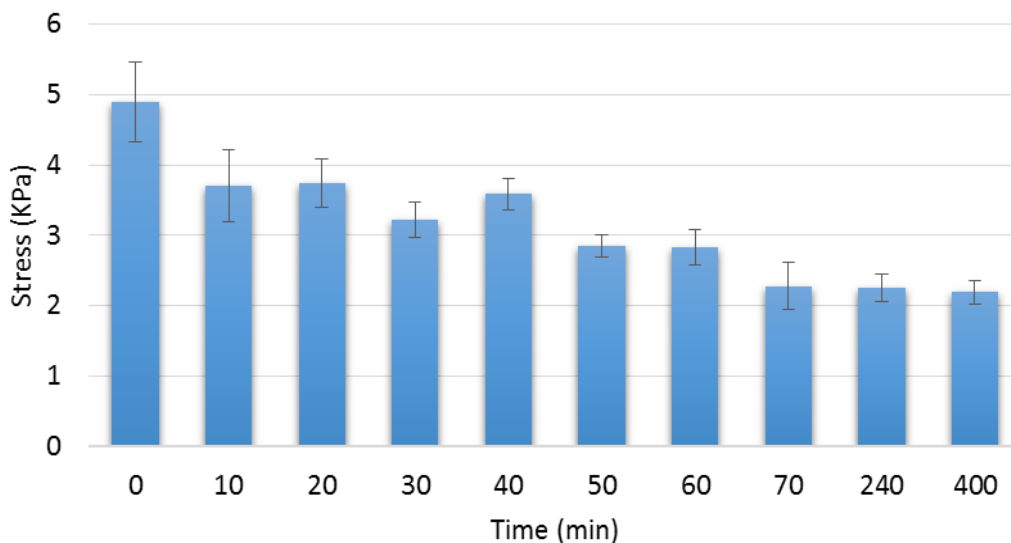
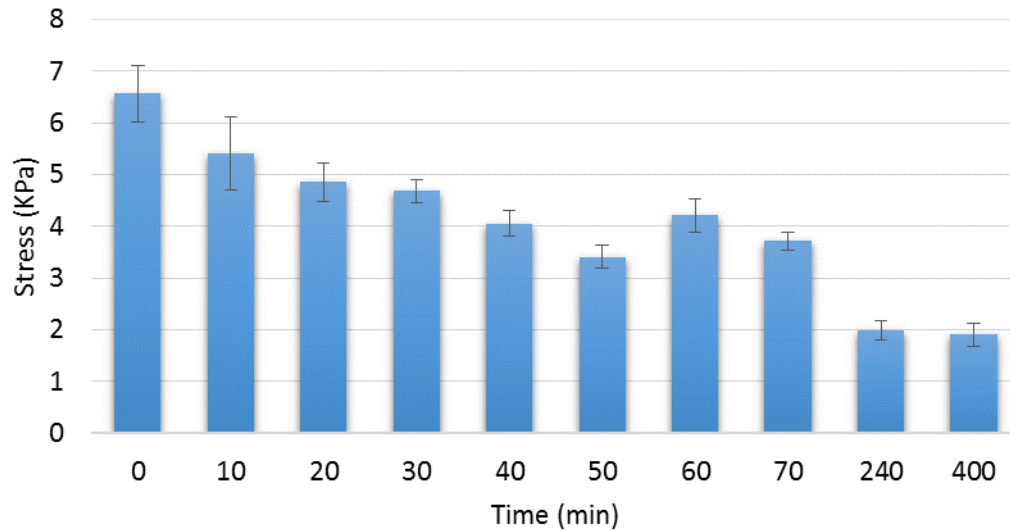
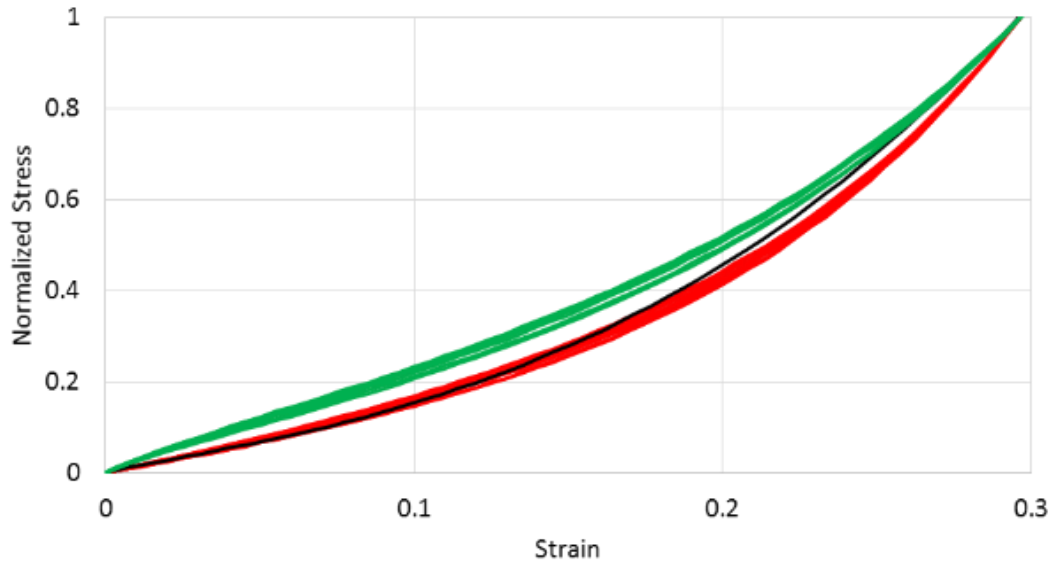


Figure 3.27: Hydrogel peak stress response over time after removal from refrigerator. Mechanical properties were relatively stable 0 - 60 min emulsion samples.



Stress was found to change as a function of temperature. By normalizing the stress-strain responses with its peak force in each case, mechanical response of both materials could be compared with each other as well with brain tissue mechanical response. Analysis of variance was used to determine that Elastic moduli E_1 , E_2 and E_3 of Oil based material, hydrogel based material and brain tissue are temperature dependent (p -value < 0.05). Figure 3.28 represents the averaged normalized peak stresses measured at minutes 0, 10, 20, 30, 40, 50, 60, 70, 240, and 400 for each material, as well as the normalized stress-strain curve of brain tissue measured at room temperature.

Figure 3.28: Averaged Normalized peak stresses of Oil Based material (Green), Hydrogel Based material (Red) and Brain Tissue (Black) tested at 1/s strain rate.



It is worth mentioning that same experimental protocol was followed to measure mechanical properties of all materials. Specimens were kept at 4 °C and 10-20 minutes before testing, samples were placed at room temperature while previous sample set was being tested. From Fig. 3.26 and 3.27, it is apparent that while the materials have not completely equilibrated during the first 10-20min, they do not vary significantly in the hour following the initial 10-20min warm up time.

3.5 - Relaxation test

Relaxation experiments were performed following compression tests. A series of ramp and hold tests were conducted on brain tissue and brain substitute materials, Specimens were compressed at 1/s to two different strain levels and held for 600s. Table 3.11 summarizes the number of samples and specifications for each experiment. Force vs time data was recorded in all cases.

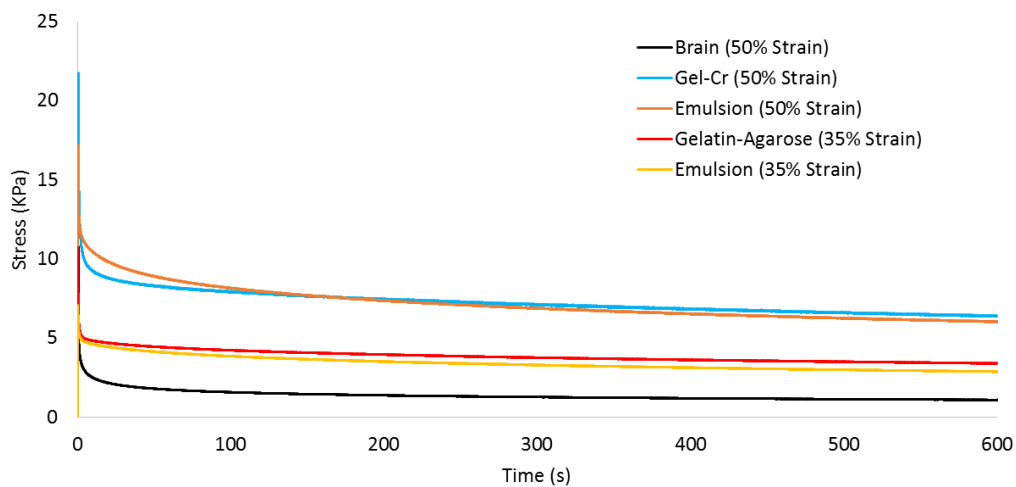
Table 3.11: Relaxation test parameters for brain tissue and brain substitute materials.

Material	Number of Samples (n)	Strain Rate	Time Held (s)	Strain Level (%)
Brain Tissue	34	1	18	50
Cr-Gelatin	5	1	10	50
Emulsion	10	1	10	50
Emulsion	10	1	15	35
Gelatin-Agarose	15	1	15	35

The mechanical response of a material consists of a viscoelastic part and an elastic part. The plateau values of the relaxation curve are determined by the elastic part but the elastic and viscoelastic together affect the height of the peak response when loads are applied. [16]. In Fig. 3.29 it can be observed that there are differences in the elastic and viscoelastic contributions of the materials tested for relaxation response. Comparing between same strain levels, gelatin with chromium, the emulsion and brain tissue do not

match on either the elastic or viscoelastic part. Gelatin-Cr and emulsion (50% strain) have similar plateau values but their averaged peak stress (21.75 KPa, 17.2 KPa, 10.76 gelatin-Cr, emulsion and brain tissue respectively) differ for $\sim 20\%$ while brain differs in both contributions. Same case with emulsion 35% and gelatin-agarose material. Gelatin-Agarose had an averaged peak stress of 10.7 KPa, and emulsion (35% strain) 7.1 KPa peak stress.

Figure 3.29: Averaged relaxation response of brain substitute materials and brain tissue.



Gelatin-Agarose material was no able to withstand compressive strains over 35% without reaching failure point. As the other materials were tested at 50% strain, in order to be able to compare the relaxation curves among all materials and to investigate the effect of the applied strain levels, some relaxation experiments were conducted using emulsion samples. Data was obtained at two different magnitudes (50% and 35%) of compressive strains at a strain rate of $1s^{-1}$. The time-dependent stress response was

obtained by normalizing the relaxation measurements by the maximum peak stress in each case (Eq. 1) and approximated by a sum of exponentials to compare the time course of brain tissue and brain substitute materials (Eq.2).

$$G(t) = \frac{\sigma(t)}{\sigma(0)} \quad (\text{Eq. 1})$$

where $\sigma(0)$ is the peak stress or instantaneous load.

$$G(t) = G_1 e^{-t/\tau_1} + G_2 e^{-t/\tau_2} + G_3 e^{-t/\tau_3} + G_4 e^{-t/\tau_4} + G_5 \quad (\text{Eq. 2})$$

where τ_1, τ_2, τ_3 and τ_4 are the time constants. The coefficients G_1, G_2, G_3, G_4 and G_5 satisfy below condition (Eq. 3), because instantaneous modulus $G(0)$ is unity.

$$G(0) = G_1 + G_2 + G_3 + G_4 + G_5 = 1 \quad (\text{Eq. 3})$$

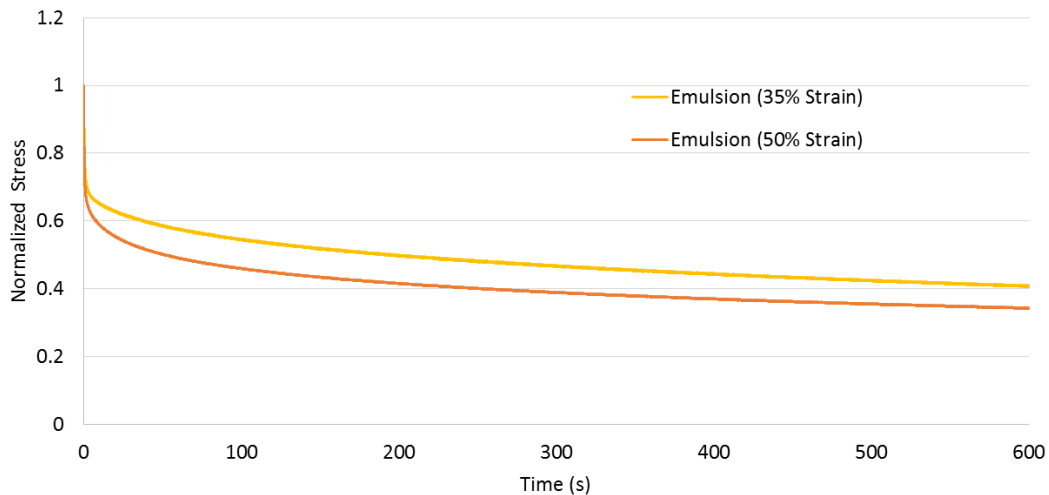
and

$$G_5 = 1 - (G_1 + G_2 + G_3 + G_4) \quad (\text{Eq. 4})$$

The time constants (Tau) represent the elapsed time required for the material response to relax to zero if the relaxation response had continued to decay at the initial rate, however, because of the progressive change in the rate of relaxation, the material relaxation response will have actually decreased in value to $1/e$ or 36.79 per cent of the

initial value for a given step decrease. The curve fitting procedure using four exponentials provided a good fit, both statistically ($R^2 \sim 99.9$) and visually.

Figure 3.30: Averaged Relaxation curves of emulsion at two different compressive strain levels at a Strain Rate of 10mm/s



During relaxation, the force appeared to change as a function of applied strain (Fig. 3.29). Nevertheless, once the relaxation curves of the emulsion at strain levels of 35% and 50% were normalized with its peak force (Fig 3.30) Emulsion relaxation response was found to be independent of the strain applied representing a time-strain separable material, in other words, the relaxation response is in function of time but does not depend on the level of strain applied.

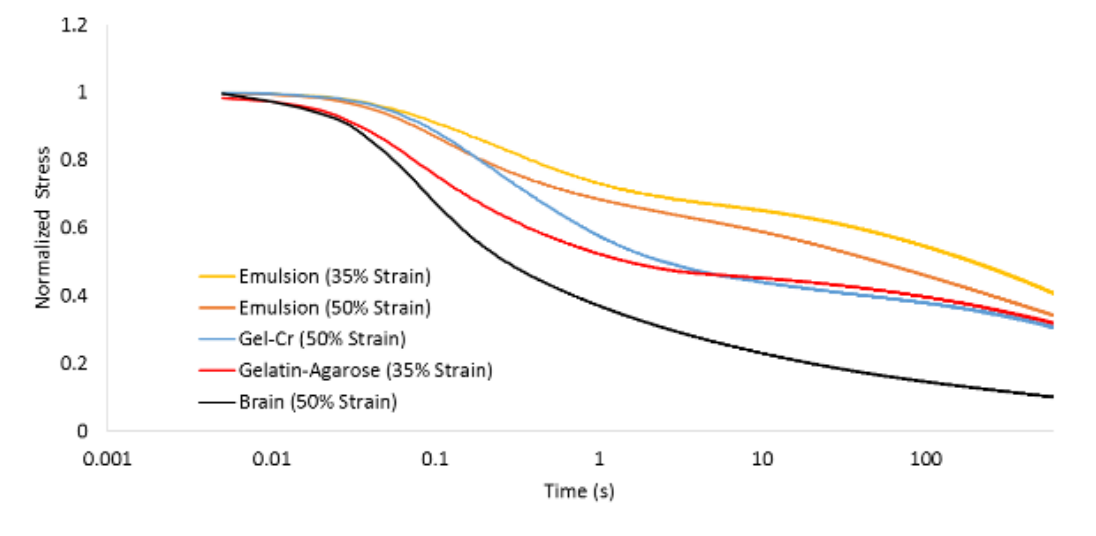
During the stress relaxation test, the compressive force decreased very rapidly within 0.5 s and continued decreasing gradually during the time range allowed, any

material reached a plateau. Table 3.12 summarizes the decrease of the compressive force (%) in 1s after reaching a peak stress. Notice that the force of the emulsion at 50% and 35% strain levels dropped about 30% and 28% respectively after 1.5s after load was applied which demonstrates a strain independency. Based on these results Gelatin-Agarose relaxation response will be assumed independent of applied strain level, thus, it can be compared with brain tissue and Gelatin-Cr material relaxation curves tested at 50% strain. Figure 3.31 depicts the normalized stress response of brain tissue and brain substitute materials.

Table 3.12: Force percentage decreased after 1 sec of reaching a peak stress during relaxation experiments.

Material	% Decrease in force
Brain	63%
Gelatin-Agarose	49%
Gelatin-Cr	43%
Emulsion 50% strain	30%
Emulsion 35% strain	28%

Figure 3.31: Time course of the averaged normalized relaxation responses of brain tissue and tissue-mimicking materials against a logarithmic time scale.



The coefficients $G_1, G_2, G_3, G_4, G_5, \tau_1, \tau_2, \tau_3$ and τ_4 were determined for each individual test for all materials in order to study the differences in time courses of the relaxation response $G(t)$ of brain tissue and three brain substitute materials. Tukey-Kramer test was performed for each coefficient. All coefficients revealed differences across materials. However, these differences remained in the same order. Furthermore, it was found that compressive forces decreased very rapidly within the first time constant (τ_1), $\sim 1s$ after the load was applied, which in terms of haptic sensation - topic that is addressed in Chapter 4 - it is improbable that humans would be able to perceive such small differences in terms of compressive force (Table 3.13), happening at such a small time lapse.

Table 3.13: Compressive force values of brain tissue and brain substitute materials for the first time constant (τ_1).

Material	Force (KPa)
Brain	1.188048
Emulsion (50%)	2.593428
Gelatin-Cr	1.733397
Emulsion (30%)	1.399845
3% Gelatin-1% Agarose	0.492281

The long term time constant τ_2 and τ_4 were found to be not statistically different between brain substitute materials but all were significantly different to brain tissue. Brain tissue time constant τ_1 resulted significantly different to emulsion and gelatin with chromium as well as time constant τ_3 was found to be similar only to Gelatin-Cr material. Table 3.14 summarizes the parameter values for brain tissue and brain substitute materials.

Table 3.14: Parameter values (mean \pm SD) for brain tissue and substitute materials' relaxation functions of the form $G(t) = G_1e^{-t/\tau_1} + G_2e^{-t/\tau_2} + G_3e^{-t/\tau_3} + G_4e^{-t/\tau_4} + G_5$.

Material	Brain	Emulsion	Gelatin-Cr	Emulsion	3%Gelatin-1%Agarose
Strain	50	50	50	30	30
G1	0.53 \pm 0.02	0.31 \pm 0.03	0.37 \pm 0.03	0.25 \pm 0.01	0.36 \pm 0.02
T1 (s)	0.60 \pm 0.01	1.17 \pm 0.01	1.23 \pm 0.03	1.40 \pm 0.02	0.55 \pm 0.01
G2	0.18 \pm 0.01	0.08 \pm 0.01	0.16 \pm 0.04	0.08 \pm 0.01	0.16 \pm 0.01
T2 (s)	2.03 \pm 0.21	4.07 \pm 1.02	2.44 \pm 0.92	2.87 \pm 1.12	1.02 \pm 0.13
G3	0.09 \pm 0.01	0.10 \pm 0.01	0.05 \pm 0.01	0.08 \pm 0.01	0.04 \pm 0.01
T3 (s)	21.57 \pm 0.75	37.53 \pm 2.55	25.29 \pm 6.26	43.98 \pm 3.20	34.35 \pm 4.43
G4	0.08 \pm 0.01	0.17 \pm 0.01	0.13 \pm 0.01	0.23 \pm 0.01	0.13 \pm 0.01
T4(s)	240.35 \pm 11.18	330.41 \pm 23.78	507.01 \pm 70.93	433.73 \pm 36.97	425.66 \pm 47.39
G5	0.10 \pm 0.01	0.31 \pm 0.04	0.26 \pm 0.02	0.34 \pm 0.02	0.28 \pm 0.01

3.6 - Degradation Test

Between fabrication of the brain phantom and utilization of the same one by a neurosurgeon, there will be a space of time where the phantom will need to be stored, preserved and even transported. As polymers used in this study are biodegradable, meaning that are prone to disintegration by bacteria, fungi or other biological means, changes in mechanical properties should be expected due to biodegradation, therefore, storage conditions should be studied to investigate the ratio of mechanical change in order to determine shelf life of the tissue mimicking materials.

A series of mechanical tests were carried out on hydrogel and oil based materials non-frozen (kept at 4 °C) and frozen during 1, 8, 15, 22, 29 days, sample preparation and experimental protocol used were the same as in sections 3.2 and 3.3. Table 3.15 summarizes the number of samples tested for each group.

Table 3.15: *Number of samples tested per material every week over the course of a month.*

Material	Storage Method	Days Stored				
		1	8	15	22	29
Hydrogel	Frozen	5	6	8	7	4
Hydrogel	Non-Frozen	10	10	10	10	10
Emulsion	Frozen	10	10	11	10	10
Emulsion	Non-Frozen	9	10	11	11	11

To address the weight loss of these materials, another set of samples were prepared in petri dishes (30 x 10mm) and weights of each sample without the container were measured before and after storage.

Samples to be tested the same day would be tightly packed together but separated by material type. For example, frozen emulsion samples to be tested on day 8 would be packed in one bag and frozen hydrogel samples to be tested on the same day would be packed in another bag.

3.6.1 - Macroscopic findings

Table 3.16 describes the characteristics observed on brain substitute materials after their respective time stored and registered before mechanical testing.

Table 3.16: Macroscopic findings of oil and hydrogel based materials after 1, 8, 15, 22 and 29 days frozen and non- frozen.

Material	Storage Method	Observations
Hydrogel	Frozen	Hydrogel structure affected (Fig 3.32). Starting at week 1, cuts were found within the sample structure (Fig. 3.33), the expansion of ice crystals compromised the polymer structure. Syneresis observed. Week 3, volume reduction was remarkable (Fig 3.34) and surface of sample was clearly uneven (Fig. 3.35).
Hydrogel	Non-Frozen	Clear changes appeared at week three, stiffening and dehydration were remarkable, and at week 4 bumps could be observed over the surface and shrinkage of the whole structure.
Emulsion	Frozen	Major change observed was a thin oily layer over the sample surface and a light change of color. No shrinkage.
Emulsion	Non-Frozen	At week three samples felt stiffer. Shrinkage observed at week four (Fig 3.35).

Figure 3.32: Normal Hydrogel Sample (A) vs frozen hydrogel sample (B).

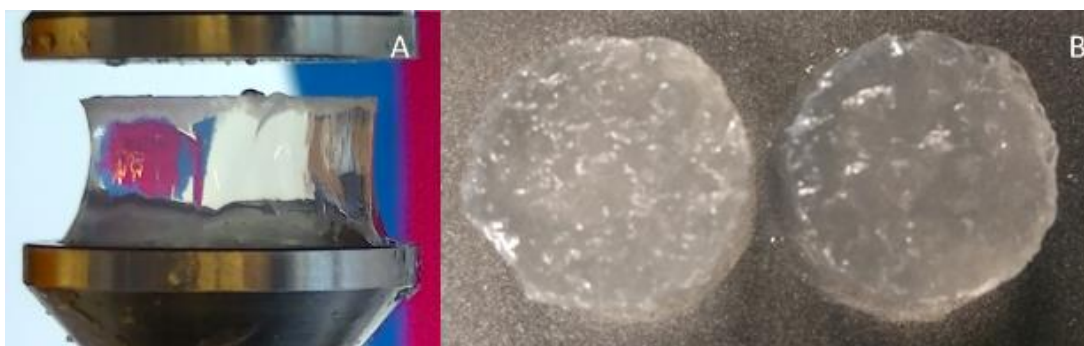


Figure 3.33: Frozen hydrogel sample in petri dish. Cuts caused but ice crystals' expansion during freezing. A) 15 days frozen, B) 8 days frozen. Shrinkage of materials

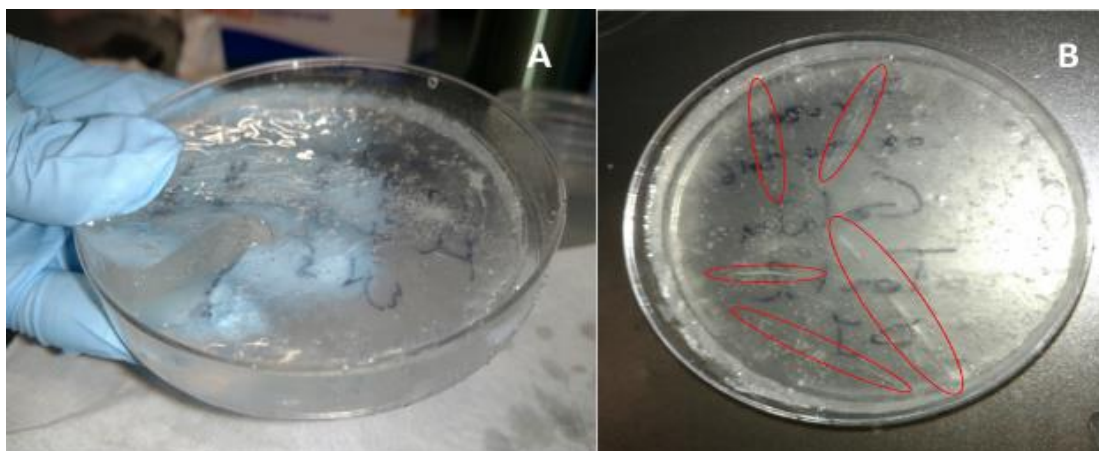


Figure 3.34: Shrinkage of materials after one month of storage. A) Non-Frozen emulsion sample (29 days), B) Frozen Hydrogel sample (29days). A) Non-Frozen emulsion sample (29 days), B) Frozen Hydrogel sample (29days).

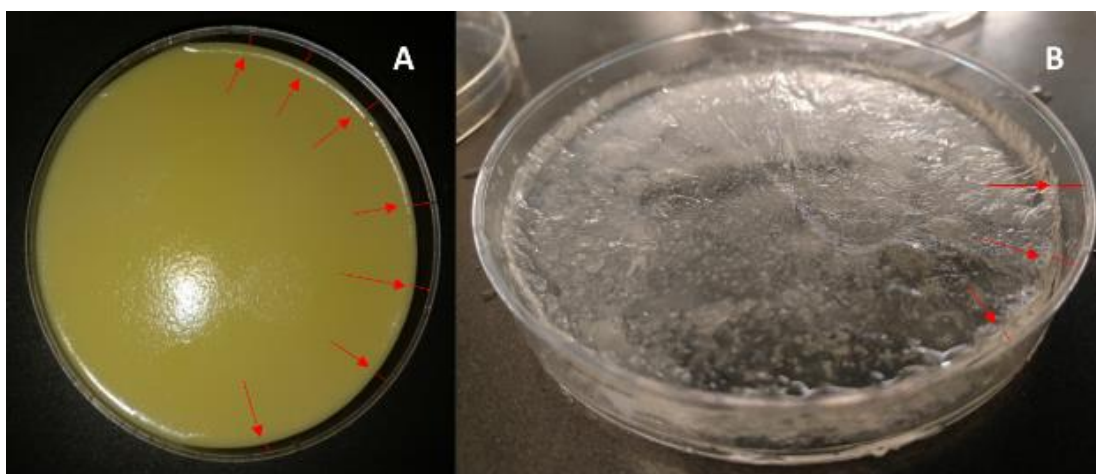
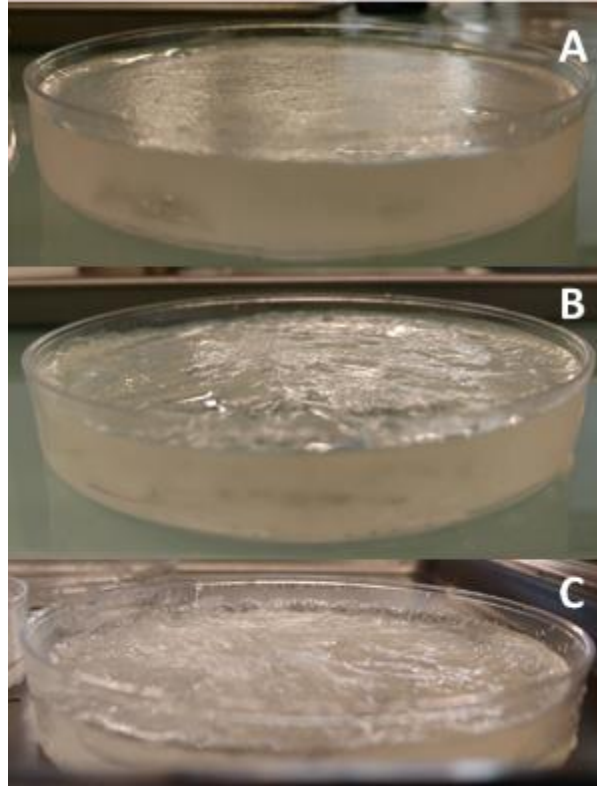
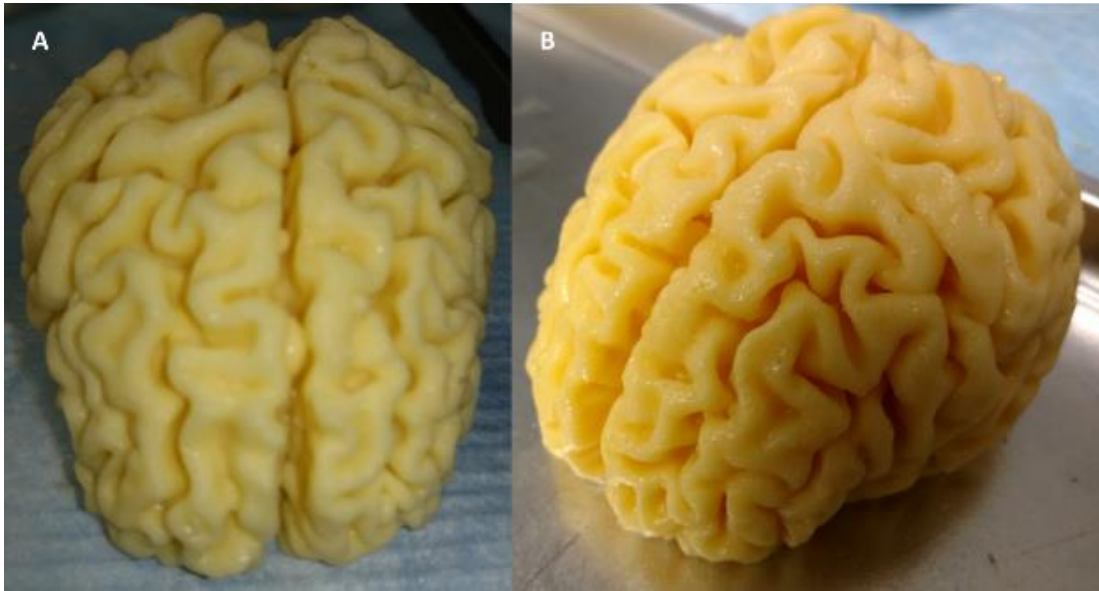


Figure 3.35: A) Non-frozen hydrogel sample (22 days) B) Frozen Hydrogel sample (22 days) C) Frozen hydrogel sample (29 days)



Two brain phantoms, one made out of hydrogel and one made out of the emulsion were vacuumed sealed and stored during 1 month in order to see the effects that the tight packing would make to their shape. Vacuum sealing could not avoid syneresis in the hydrogel based phantom which structure was evidently damaged, nevertheless, the emulsion phantom was intact with no detectable changes in its shape (Fig. 3.36) suggesting vacuum sealing neither affects the physical characteristics of the emulsion brain phantom.

Figure 3.36: Oil based Brain Phantom. A) Fresh B) 29 days stored. No macroscopic differences could be found but a slight darker color.

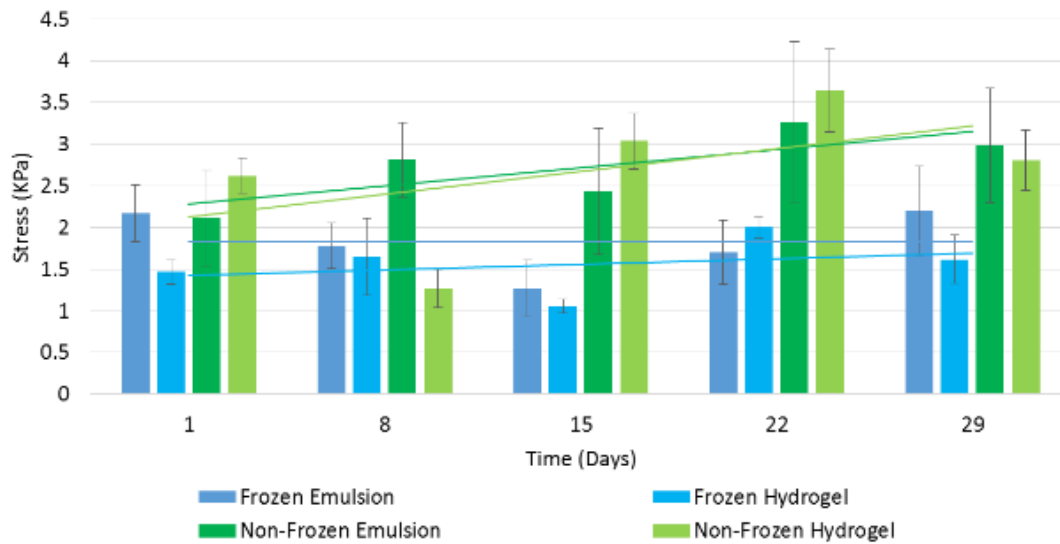


3.6.2 - Mechanical test

Fig. 3.37 represents the peak stresses measured at a 30% strain level. In general, non-frozen materials tended to stiffen through time as trending lines (green and light green) confirm. In the other hand, frozen materials did not showed important changes in peak stresses over a one-month period of storage, similar behavior was found in Elastin Moduli measurements. One way ANOVA and Fisher's Least Significant Difference (LSD) statistical methods were used to compare E_1 , E_2 and E_3 and the peak stress measured at 10%, 20% and 30% strain levels. All materials except frozen emulsion, were significantly different at least in one measured parameter for all five tests. Frozen emulsion was the

only one found to be not statistically different over the 29 days that lasted the experiment. However samples from day 15 showed to be statistically different to days 1, 8, 22 and 29, packing damage would be the probable cause for these outcome in samples measured at week 2. Frozen hydrogel samples broke during the mechanical experiments (reached failure point) and only few samples could be tested due to the cuttings caused by ice crystals, this could explain the significant difference yielded by the statistical analysis.

Figure 3.37: Peak stresses at 30% strain of Frozen and Non-Frozen hydrogel and emulsion. Lines depict a trending line for each material, non-frozen materials tended to stiffen while frozen materials wouldn't, specifically frozen emulsion.



3.6.3 - Weight loss

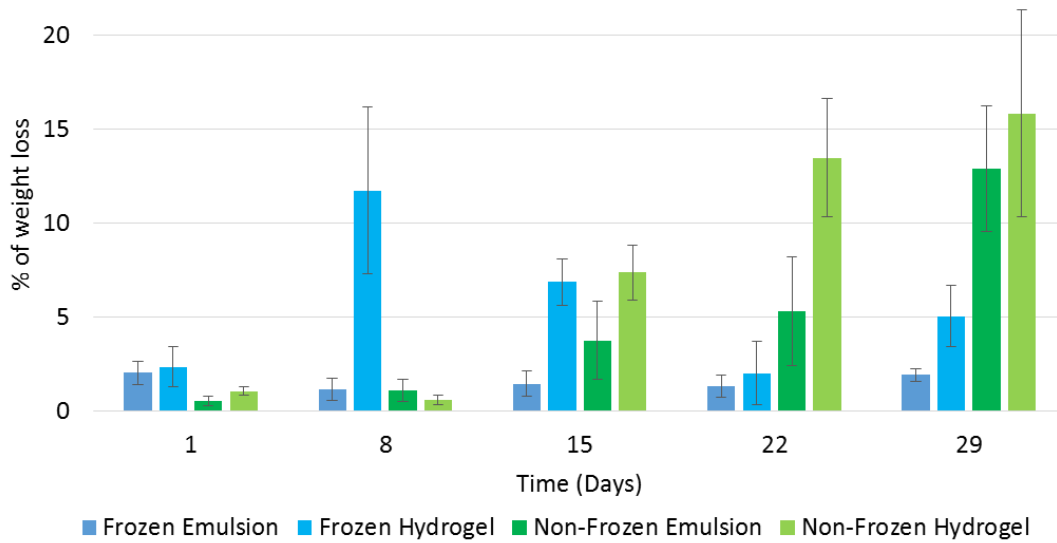
Fig. 3.38 displays the percentage of weight loss for each material measured every week during 1 month. One way ANOVA was used to determine that non-frozen materials experienced a significant loss of weight at week 2 and thereafter. Frozen hydrogel also had a significant loss of weight especially in week 1, a reason for this might be a bad sealing of the bag when samples were packed or some kind of rupture allowing air filtering. In the other hand, frozen emulsion did not show a significant change in weight during the four weeks. Table 3.17 summarizes the averaged values of weight loss for each material.

Table 3.17: Percentage of weight loss of tissue mimicking materials tested at day 1, 8, 15, 22 and 29. (Mean \pm SD)

	Day 1	Week 1 (Day 8)	Week 2 (Day 15)	Week 3 (Day 22)	Week 4 (Day 29)
Frozen Emulsion	2.04 \pm 0.61*	1.17 \pm 0.60*	1.45 \pm 0.66	1.32 \pm 0.57*	1.92 \pm 0.33*
Frozen Hydrogel	2.35 \pm 1.06	11.74 \pm 4.44	6.88 \pm 1.24	2.02 \pm 1.71	5.05 \pm 1.63
Non-Frozen Emulsion	0.529 \pm 0.23	1.120 \pm 0.59	3.755 \pm 2.08	5.319 \pm 2.88	12.885 \pm 3.35
Non-Frozen Hydrogel	1.06 \pm 0.21	0.58 \pm 0.25	7.37 \pm 1.44	13.50 \pm 3.13	15.85 \pm 5.50

*P-value > 0.05

Figure 3.38: Percentage of weight loss of tissue mimicking materials tested at days: 1, 8, 15, 22 and 29.



3.7 - Discussion

Brain phantoms can be used as model simulators for preoperative planning and training. An important component of such models is the material that mimics the physical properties of brain tissue.

In this study, unconfined compression mechanical tests were carried out on brain tissue and potential brain substitute materials which were subjected to compressive loads at various strain rates up to 50% strain. Brain tissue contained no linear portion as well as gelatin based materials. In contrast silicon materials behaved linearly, consequently were discarded for further analysis.

3.7.1 - Brain Tissue

The experiments conducted in this study were designed to give an insight into the brain tissue mechanical behavior in order to develop two brain substitute materials with brain tissue mimicking qualities at low compressive strain rates typical for surgical procedures considered from 0.01 to 1/s [36].

Despite of more than fifty years of research on brain mechanics, it is still difficult to determine the mechanical properties of brain tissue due to the large inconsistency in results reported in literature. The reason for variation in the reported viscoelastic properties by different authors is still unclear, but might be attributed to several reasons such anisotropy, regional differences, white matter and grey matter heterogeneity and differences between species as well as specimen shape, specimen size, post-mortem time, in vivo in situ or in vitro experiments, definition of zero strain point, sample preparation and experimental methodology (tension, compression or indentation).

Based on these difficulties brain tissue mechanical characterization was performed in order to define a protocol which results would serve as a baseline in the development of brain tissue substitute materials.

Brain specimens were tested under compression loadings and consisted of pig brain mixed white and gray matter which were tested 6 and 24 hrs. post-mortem at different strain rates. Porcine brain tissue was selected as a substitute for human brain tissue due to the accessibility and possibility to reduce the post-mortem time testing.

According to Nicolle et al. there is no significant difference between human brain and porcine brain tissue response. [44]

Although, Prange and Margulies showed that there is significant difference between white matter and grey matter attributed to anisotropy [40], their sample size was 1mm. of thickness, at small dimension scales directional properties will be identified but working with large enough samples, soft tissue does not exhibit directional structure [17], [20], [23], [36], [43], [51]–[55]. Measurements made at numerous samples, with different concentrations of gray matter and white matter did not appear to have an influence in the mechanical response of brain tissue under compressive loadings which is consistent with the studies made by Kaster et al. [41], besides, separation of grey matter and white matter would compromise the integrity of the tissue.

Stress-Strain behavior of samples with different anatomical location was conducted in order to investigate whether there is a regional effect in the mechanical properties of brain tissue at 50% strain. Results showed there is no statistical difference among samples up to 30% strain, nevertheless, the mid region was found to be different than the anterior and posterior regions at strain levels greater than 30% which can be attributed to the high content of white matter located in the region. Donnelly et al. [56] also reported that stress-strain relationship was independent on the sample location, in which samples of fresh human brain 17mm diameter and 12mm thickness were employed. Therefore, brain tissue samples of 20mm diameter and 10mm height tested in this study were assumed to behave isotropic with no significant regional effects.

The tissue was noticeably rate sensitive and the averaged stress-strain relationships obtained in this study showed to be similar compared to previous results obtained under moderate loadings [18], [20]. This is consistent with other authors who tested brain tissue in vivo, in situ[27] and in vitro[17], [20], [26], [27] where tissue was found to dramatically stiffen at greater strain rates.

Post-mortem time test was also carried out in which tissue response resulted statistically different between 6hrs and 24 hrs. post-mortem with a decrease of ~20% and ~30% of stress at 40% and 50% strain levels, respectively. In several studies tissue mechanical property variations related to post-mortem degradation and dehydration were found to be negligible up to 15hrs. [16], [18]–[25], [27]–[33], [36]–[38], [57]. There have been studies that reported tissue stiffening with increasing post-mortem time [44], [58], however, many authors have reported otherwise, which is consistent with this study at high strain levels, suggesting degradation takes place with increasing post-mortem time due to autolytic process, rigor mortis or osmotic swelling [35], [39], [40], [59], [60].

3.7.2 - Brain substitute materials

This experimental study comprehensively examines the mechanical properties of hydrogel and oil based materials comparable with brain tissue mechanical behavior. Two tissue-mimicking materials with similar mechanical properties to brain tissue were formulated. Both materials exhibited similar peak stresses and apparent elastic moduli at different strain levels up to 30%. It also presents experiments to quantify the effect of

temperature on brain substitute materials. It was found that measured results were clearly temperature dependent, for both materials (emulsion and hydrogel) were stiffness decreased with increasing temperature. Studies about temperature effects on brain tissue response have also reported a temperature dependency on brain tissue mechanical properties [61]–[63].

Preconditioning was not performed in the current study because brain tissue is not supposed to experiment cyclic loading in normal conditions. However preconditioning in substitute materials may have a significant effect on the mechanical properties, hence, affect the haptic sense of the material since handling of the brain phantoms during surgical planning or training can be associated with preconditioning of the tissue-mimicking material. However, the tissue response obtained in this study can be considered consistent without preconditioning.

This study also assessed the relaxation response of brain tissue and tissue mimicking materials, although, relaxation response was found to be different between materials, differences were not of different magnitudes. However, when measuring the relaxation response of brain substitute materials, hydrogel presented a mechanical failure constraining factor. This material is not able to withstand strains higher than 35% without breaking up, although, relaxation response showed to be strain independent, the hydrogel mechanical failure at low strains makes it less suitable as a model material for brain tissue phantoms. Additionally, the degradation test carried out to assess the effects of storage conditions on tissue mimicking materials showed hydrogel to be more sensitive

to aging than the emulsion material. Hydrogel presented significant physical (weight loss) and mechanical changes in frozen and non-frozen storage modes since the first week, while the frozen emulsion appeared to experience no changes during the time range tested here.

CHAPTER 4

SEGMENTATION AND 3D PRINTING

4.1 - Introduction

2D images like CT and MRI scans are difficult to interpret, especially in cases of complex anatomy and pathology in the area of neurosurgery [64]. Radiological advances in CT and MRI scanning has provided benefits like 3-dimensional imaging which has the ability to demonstrate the tridimensional relationship between bones, vasculature and internal structures of the head compared with regular imaging modalities. Rendering the volume of a head or other anatomical structures enables the evaluation of special locations and extension of malignancies like a tumor in relation to the surrounding structures which is essential in surgical interventions. However, 3D images are examined through a 2D screen which can lead to misinterpretation in addition to the lack of haptic feedback.

3-dimensional anatomic models have been extensively used in neurosurgery, facial surgery and other complex interventions to aid in the comprehension and subsequent surgical procedures of bone reconstruction, organ malignancies or vascular issues. [10], [11], [65]–[68].

3D printing is the process of making a 3D object from a digital model using a 3D printer that instead of placing a single layer of ink on paper, it places successive layers, one on top of other, of material to form a 3D replica of the virtual one. 3D printing allows the fabrication of solid replicas using 3D-imaging of anatomical structures which will help to improve the surgeon's perception of the initial procedure overview, enhancing both the certainty and safety of the neurosurgical intervention compared to the use of standard visualization modalities for preoperative planning and intra-operative anatomical reference.

An optimal simulator of neurosurgery should represent accurately the anatomic structures and have realistic haptic tissue characteristics. By using rapid prototyping and casting was possible the fabrication of a brain phantom with similar mechanical properties to those of brain tissue to be used as a surgical planning and reference tool as well as a teaching aid for neurosurgery training.

4.2 - Materials and methods

Working in collaboration with Dr. Jane E. Joseph, Professor of the Department of Neurosciences and Director of the Neuroimaging Division at the Medical University of South Carolina (MUSC), three brain MRI (T1 weighted scans) were obtained from two healthy different patients. Patient A: matrix 512 x 512 pixels, slice thickness 1mm, voxel size 1mm³. From patient B, two MRI's were obtained at different resolutions 1) matrix:

384 x 384 pixels , slice thickness 0.5mm, voxel size .350mm³, 2) matrix 512 x 512 pixels, slice thickness 1mm, voxel size 1mm³ in order to create physical 3D brain models of the cortex as well as some internal structures of the brain.

4.2.1 - 3D Printing

The 3D model was designed as a set of three pieces. The skull, the cortex, and internal structures (core brain) including the brainstem, basal ganglia, thalamus, corpus callosum and ventricles, cerebellum was added to this third piece. The skull will serve as a base for the brain phantom (Fig. 4.1). The cortex will represent the whole brain including cerebellum and brain stem, the cortex and the core brain will be used as models for making a silicon matrix. All structures were processed using Mimics Research 17.0 (Materialise. USA). The default image threshold for segmentation of hard tissue (skull) and soft tissue (all other structures) was initially used to create an initial mask, afterwards, each MRI slice was edited manually segmenting to a particular threshold each desired structure and removing unwanted areas (Fig 4.2 and 4.3). Subsequently a 3D object is generated from the resulted mask and smoothed to fix empty voxels or bad edges (Fig 4.2 D). Later, a second mask is created from the 3D smoothed object to make sure the smoothing process did not deviated the volume from the original structure. This process was repeated until the 3D object didn't need further editing. Next, the object is rendered in 3-Matic Research 9.0 (Materialise.USA) for minimal edition to be prepared for printing.

In this step the core brain structures that were segmented separately were united as a single 3D object. Finally the DICOM files were exported as STL format.

A Fuse Deposition Machine (FDM) was used to fabricate the core brain, brain cortex and skull (Fig xx). Polylactic Acid (PLA) and Acrylonitrile butadiene styrene (ABS) were used for 3D printing the segmented brain structures, both are thermoplastics that become soft and moldable when heated and return to a solid form when cooled. The resulting printed models were cleaned and polished with sandpaper. ABS objects can be smoothed with acetone vapor to remove the tiny ridges covering all the surface inherent in the printing process with a typical filament based printer which builds the object layer by layer.

Figure 4.1: 3D printed anatomical structures. A) Core brain, B) Brain cortex and C)

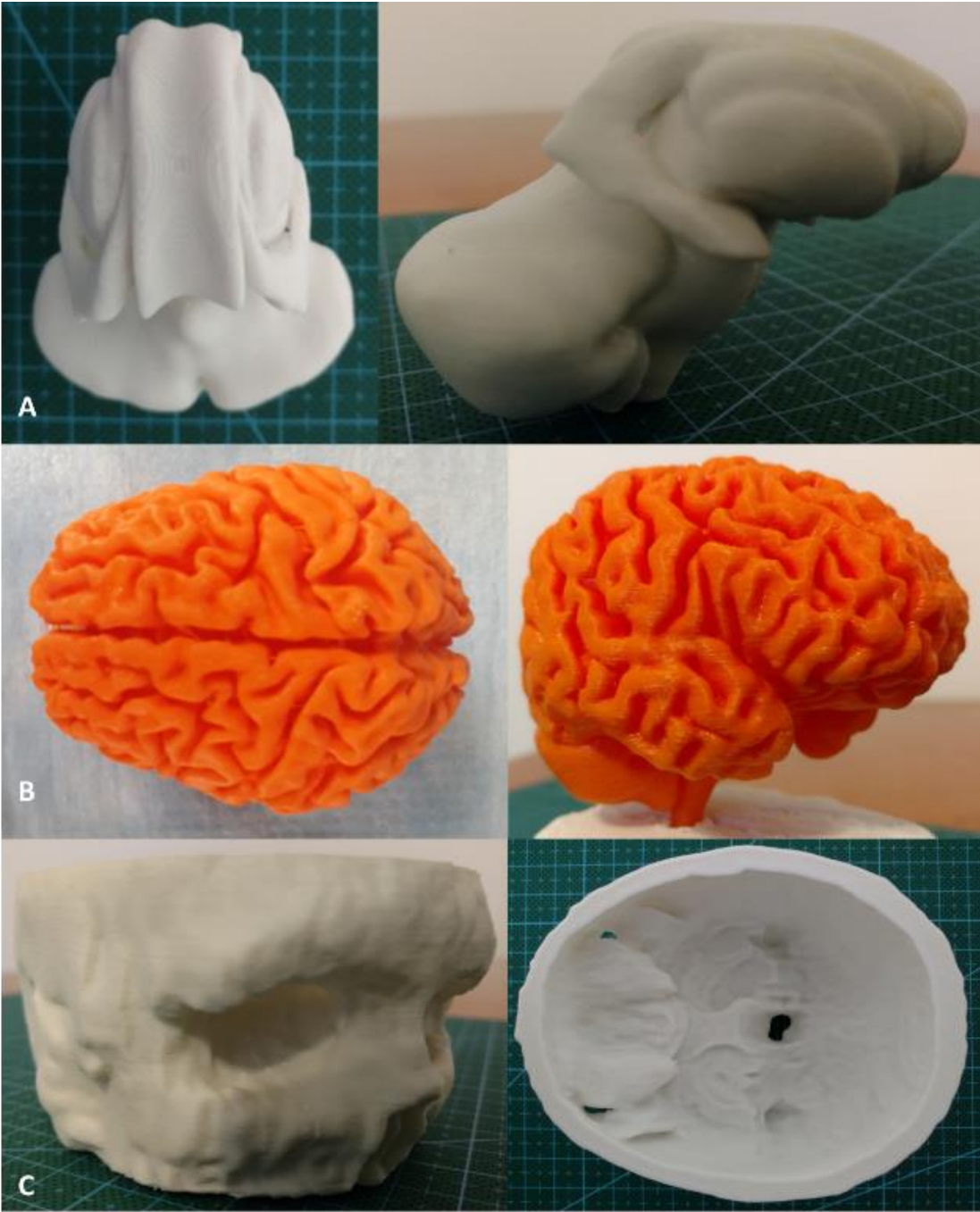


Figure 4.3: Mimics Research 17.0 Work area. A) Coronal plane, B) Axial Plane, C) Sagittal Plane, D) 3D Calculated 3D from Mask. All structures but the ventricles were united in a single structure.

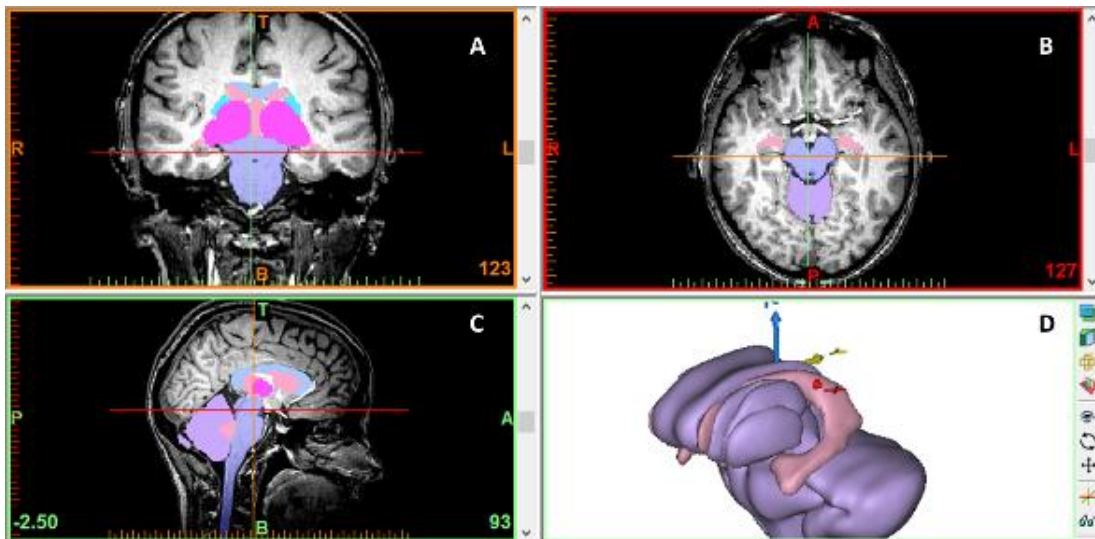
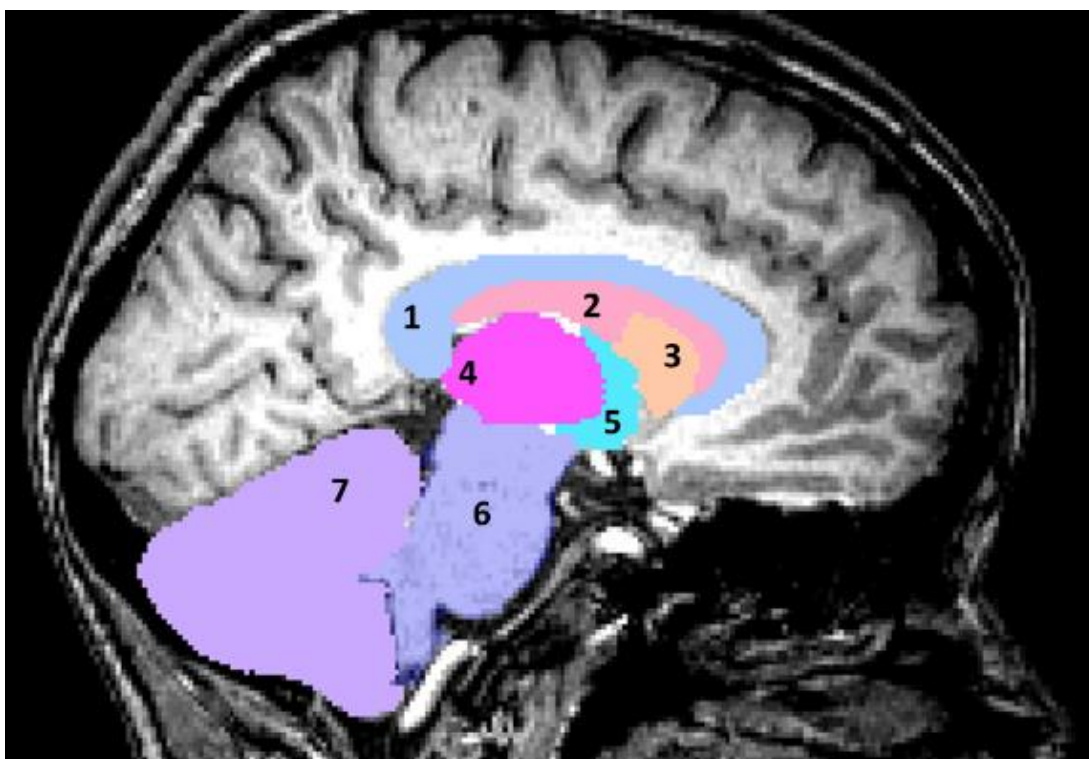


Figure 4.2: Sagittal view of brain internal structures. Each color represents a mask which in turn defines a single structure. 1) Corpus Callosum, 2) Ventricles, 3) Caudate Nucleus, 4) Thalamus, 5) Internal Capsule, 6) Brainstem, 7) Cerebellum.



4.2.2 - Mold Making

Once the 3D models are printed, the model of the brain cortex and the internal structures will help to create two-piece silicon molds or matrixes for casting brain phantoms with a material that was developed with mechanical properties similar to those of brain tissue (Chapter 3). Due to the delicacy of the brain tissue mimicking material, the best choice for mold making was a super-soft silicon rubber (hardness shore 00-10, Ecoflex-series, Smooth-On Inc. Macungie, PA) that will allow full elongation of the matrix to pull apart the lateral walls of the mold when demolding the cast object, otherwise the cast brain model would break and come out in pieces leaving the brain foldings or other thin structures stuck in the mold. The core brain was cast with super-soft silicon rubber (Hardness shore 00-20, Ecoflex-series, Smooth-On Inc.).

The printed model is placed in a box of 10.5 x 9 x 9 cm. (for a 50% size phantom) laid over a small square of clay positioned in the middle of the box, a silicon release agent is sprayed all over the box and the brain model in advance, in order to make removal of the set silicone easier, two tubes are glued to the back of the printed brain model which will work as pour and breather spouts. Next, super-soft silicon rubber is poured into the container filling half of the total volume of the box. The silicon is allowed to set for 4 hrs. then, silicon release is sprayed thoroughly over the new rubber surface and the second half of the box volume is filled with more silicon and allowed to set for other 4 hrs. For the final step the box is disassembled and a two-half mold of super-soft silicon rubber is obtained (Fig 4.4).

Figure 4.4: Brain cortex Negative Mold with 3D printed core brain positioned into place.



4.2.3 - Brain Phantom

Core brain silicone cast needs to be ready before brain cortex casting. The core brain cast will be placed inside the cortex matrix before casting the brain phantom (Fig. 4.4), cerebellum and brainstem will allow accurate positioning of the internal structures in the cast final brain phantom.

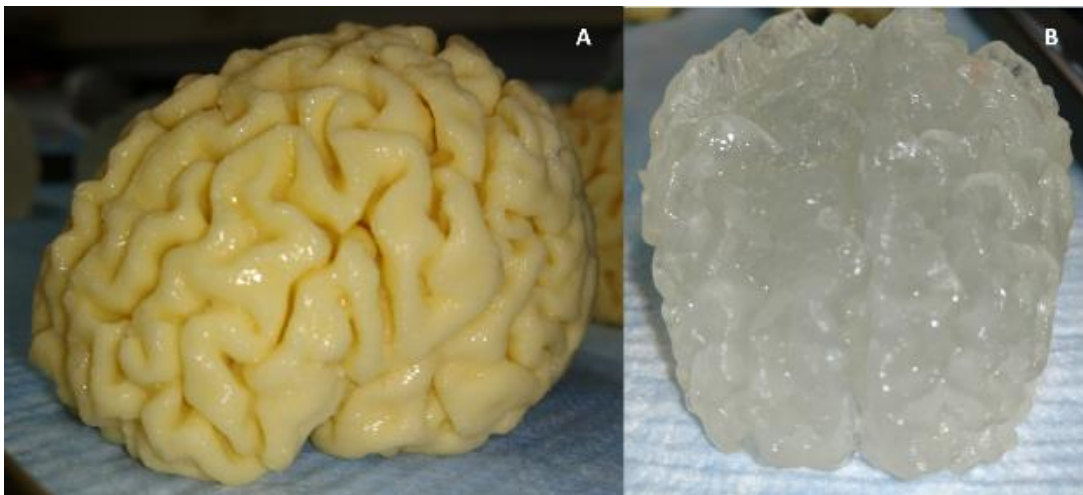
The silicone matrix is sprayed with silicon release thoroughly before putting the two halves together and reinforcing with a surrounding wall of corrugated packing glued with silicon to avoid leaking as well as deformation of the matrix which would alter

phantom volume when pouring the casting material. The matrix is positioned with the openings upwards, the casting (Hydrogel or oil based materials, Chapter 3) material is poured inside and allowed to set for 2-3 hrs. For demolding, the corrugated walls are removed as well as the molds with extreme care to avoid damaging the brain phantoms.

4.3 - Results

Brain phantom prototype scaled by 50% is shown in Fig. 4.5. It was possible to cast the brain model with great accuracy. However hydrogel based brain phantom was difficult to demold even from a soft mold. I was not possible to cast an intact hydrogel brain phantom. The cast objects (emulsion brain cortex and silicon core brain) were measured as well as the 3D printed models (scaled by 50%) and compared with the dimensions of the 3D rendered model in 3-Matic Research 9.0. Dimension measurements in the sagittal, axial and coronal plane were performed. The greatest difference between

Figure 4.5: Cast brain phantoms. A) Oil based material, B) Hydrogel Based Material.



measurements performed in cast, 3D printed and 3D rendered models was 0.7 mm. Measurement J in the cast model resulted 2mm longer than rendered model's dimension due to pour spouts located in that region. Table 4.1 summarizes the measured dimensions (Appendix C defines the measurements performed in this section).

Table 4.1: Dimension measurements performed in cast, 3D printed and Virtual models of brain structures (Appendix C defines each measurement performed).

Internal Structures						
Plane	Measurement	Virtual 3D Object (mm)	Virtual 3D Object Scaled by 50% (mm)	3D Printed Scaled by 50% (mm)	Cast Scaled by 50%(mm)	SD
axial	A	124.05	62.025	62.03	62.6	0.33
axial	B	105.2	52.6	52.4	52.1	0.25
axial	C	62.83	31.415	31.38	31.09	0.18
axial	D	26.69	13.345	13.41	13.16	0.13
Sagittal	E	61.25	30.625	30.84	30.44	0.20
Sagittal	F	80.58	40.29	40.15	40.99	0.45
Sagittal	G	83.2	41.6	41.09	40.96	0.34
Coronal	H	28.73	14.365	14.76	14.87	0.27
Coronal	I	31.96	15.98	15.72	16.16	0.22
Brain Cortex						
Axial	J	175.51	87.755	87.98	89.94	1.20
Axial	K	139.6	69.8	69.85	69.21	0.36
Sagittal	L	171.57	85.785	85.89	86.2	0.22
Sagittal	M	112.93	56.465	56.59	56.7	0.12
Coronal	N	139.18	69.59	69.5	69.38	0.11

Skull

Plane	Measurement	Virtual	Virtual	3D	Cast	SD
		3D Object (mm)	3D Object Scaled by 50% (mm)	Printed Scaled by 50% (mm)	Scaled by 50%(mm)	
Axial	O	128.62	64.31	64.61	-	0.21
Axial	P	163.56	81.78	81.41	-	0.26
Axial	Q	10.38	5.19	5.57	-	0.27
Sagittal	R	90.73	45.365	45.22	-	0.10
Coronal	S	27.12	13.56	13.28	-	0.20
Coronal	T	29.63	14.815	14.51	-	0.22

4.4 - Discussion

Life-sized anatomical replicas by means of 3D printing it's a method that allows visualization of anatomical structures and abnormalities. Physical 3D anatomical models display information that sometimes is not possible to obtain from conventional imaging methods facilitating preoperative surgical planning and allowing rehearsal. There have been reports of studies where the surgeon claimed that the desired surgical outcomes would not had been reached without a 3D physical model as a reference. During surgery, cases that are challenging like a tumor dissection can be achieved with less probability of unexpected findings which can lead to intra-operative complications, as well as time reduction of the surgical procedure, hence, reduction in total procedure costs which certainly represent benefits for the patient [11], [69]–[71]. 3D printed models also provide a mean to train less experienced colleagues in surgical procedures, as well as facilitating clinician-patient communication providing the patient with a better

understanding of their condition as well as communication within the surgical team before and during surgery.

Models that are anatomically accurate were created. However it was not possible to cast an intact hydrogel brain phantom, although mechanical properties of this material showed to be similar to those of brain tissue (Chapter 3), casting with hydrogel was not possible due to its brittleness suggesting being too delicate for surgical planning purposes. Nevertheless, surgical training with hydrogel brain phantoms would be possible because the model would not be handled as it would be in surgical planning since it would be placed in a skull simulating a head. But fabrication of hydrogel brain phantoms would only be possible by means of 3D printing which requires customization of a 3D printer capable of extruding hydrogel material.

The greatest difference between measurements performed in cast, 3D printed and 3D rendered models was 0.7 mm. The degree of accuracy achieved in anatomic printed models depends on the quality of the initial images and post-processing techniques including segmentation and printing. 3D printed physical models based on CT or MRI will be prone to imaging error, thus, improved resolution will subsequently improve 3D printed models.

In terms of digital images, spatial resolution can play an important role during the image segmentation process, the higher the spatial resolution the better representation of the anatomical structures that are going to be threshold. The precision of the

segmented masks, thus, the accuracy of the rendered volume is constrained by the fidelity of the MRI data.

MRI spatial resolution determines the ability to distinguish structures within an image (together with contrast). High spatial resolution techniques will allow to differentiate between two objects that are relatively close together and it is inherently related to the voxel volume. A voxel represents the volume unit defined in a 3-dimensional space. Its dimensions are determined by the pixel and slice thickness. A pixel represents the smallest unit element in a 2D image. It has dimensions given along two axes (x and y) which represents x-y plane spatial resolution and slice thickness represents the measurements in the third axis (z)[72]. Slice thickness will determine how much tissue will be captured within each slice, if the slice thickness is increased, more volume and type of tissue will be included in a single slice and overlapping structures with different signal intensity will subtract detail and produce blurry images (partial volume artifact) while by decreasing slice thickness, details of the anatomical structures will have a better representation[73], [74].

Reducing the slice thickness or pixel size will decrease the size of the voxel resulting in an image with higher spatial resolution which will improve image detail or “sharpness”. It should be noted that anatomical structures have more detail in slices with lower thickness due to the decrease in tissue volume enclosed within a slice, thus, representing greater accuracy when identifying target areas and structures. But signal-to-

noise ratio (SNR), another MRI parameter, is directly proportional to voxel size, smaller voxels produce MR images with lower SNR thus, making the image appear less smooth compared with images with larger voxels [75]. Although, the specifications of the MRI scanner did not affect the accuracy of the brain model, higher quality of resolution made it easier to identify desired areas reducing time of segmentation. However, increasing image resolution in terms of slice thickness also represent an increase of time during the MRI acquisition.

CHAPTER 5

HAPTIC TEST - TISSUE-MIMICKING BRAIN PHANTOMS

5.1 - Introduction

The word “haptic” can be defined as related to or based on the sense of touch. The whole purpose of fabricating a tissue -mimicking material brain phantom is to provide a resident of neurosurgery a model that resembles a human brain, built with a material that “feels” like brain tissue in order to allow the resident to train surgical procedures. As well as it can come in handy to an experienced neurosurgeon who can make use of these brain models for preoperative planning.

In order to assess the tactile/haptic characteristics attributed to the tissue mimicking material brain phantom, haptic tests were carried out by participants who were surveyed about their haptic perception regarding the stiffness or compliance of the brain phantom compared with brain tissue which was evaluated by means of exploratory manual tasks.

5.2 - Materials and Methods

The MRI data of a healthy patient obtained from the Neuroscience Division at the Medical University of South Carolina (MUSC) was used to create tissue-mimicking brain phantoms by means of segmentation, 3D printing and casting (Chapter 4). Brain

phantoms did not contained the silicon core brain since the aim of this study was to compare haptic characteristics between brain tissue and brain substitute materials. Five brain phantoms were fabricated of each tissue mimicking material (Hydrogel based and oil based materials), which through mechanical testing were determined to have similar mechanical properties as brain tissue (Chapter 3). Four brains from six-month old swines were collected from Godley Snell Research Center Clemson University. Pig heads were obtained as a by-product. Heads were collected from the research center immediately after death, placed in ice and transported to the lab where the brains were harvested within 1 hr. post mortem. Phantoms and pig brains were obtained 1 day before the experiment and stored air tightly or in solution respectively at 4°C during the 2 days that lasted the experiments.

The hydrogel and oil brain phantoms were compared with brain tissue by 22 bioengineering students and faculty from the University of Clemson through a haptic test. Clemson University Bioengineering student and staff were recruited for the test through flyers and email announcements. Previous contact with brain tissue was not required since it would be provided to carry out the haptic test. The experiment consisted in performing a series of manual tasks as poking the pig brain and tissue mimicking material phantoms with the finger, poking with a mall probe, cutting with a scalpel, grasping with forceps and slicing with scissors, in order to determine the level of similarity of the “feel” between brain tissue and each of the brain phantoms. Some tools employed to complete

the haptic test, were tools likely to be used during a surgical intervention like the mall probe or forceps which are used to pull apart the brain cortex and grasp desired structures respectively. Although, scalpels or scissors are nor used directly in the brain during surgery due to the delicacy of the same, we considered this tools as keys in terms of haptic perception due to the one main difference between real brain tissue and brain substitute materials based in gelatin: the brittle fracture type that gels experiment when cutting or braking which is no present in brain tissue. Data was collected through a survey (Appendix D) that was filled by the participant after performing each task.

5.3 - Results

In general phantoms were rated as good and very good in terms of similarity with brain tissue. Poking with the finger was rated as very good with a 50% for the emulsion phantom while hydrogel phantom had more votes for a just “good” similarity. In contrast, pocking with a mall probe, emulsion phantom was rated as “good” with a 60% and the hydrogel one only reached a 36%. Cutting with a scalpel was rated similarly for both material phantoms ranging from good to excellent, however, hydrogel had a vote for poor performance and emulsion had relative high rating as “fair” similarity with brain tissue. The feeling when grasping with forces was rated as very good while hydrogel had a tie between good and very good similarity. Finally, cutting slices with the scissors, emulsion phantom was rated as very good with a 50% of votes and the hydrogel with 45% of votes

was rated as good in comparison with brain tissue. Fig. 5.1, 5.2, 5.3, 5.4 and 5.5 summarize the survey results for each task performed during the haptic test.

Figure 5.1: Similarity rating for hydrogel and oil based brain phantoms compared to brain tissue. Tool: Finger.

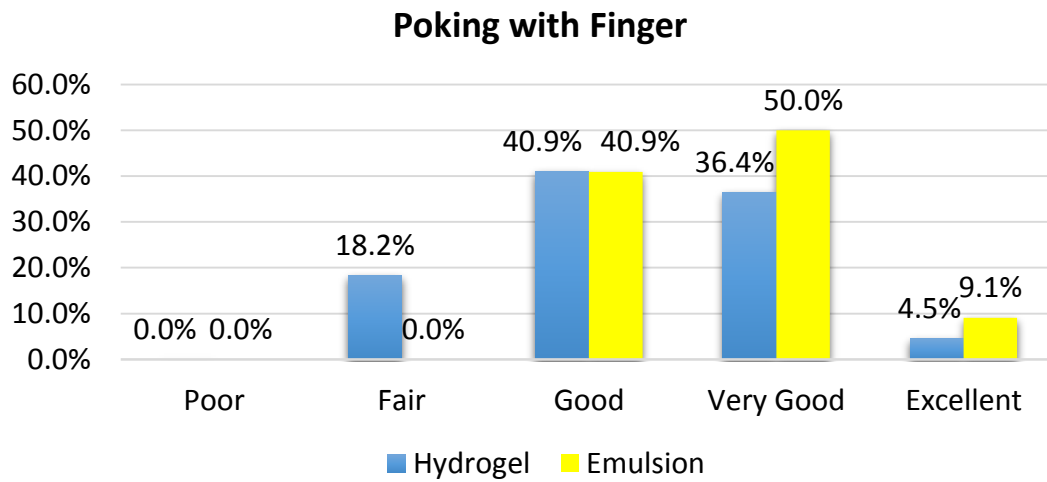


Figure 5.2: Similarity rating for hydrogel and oil based brain phantoms compared to brain tissue. Tool: Mall Probe.

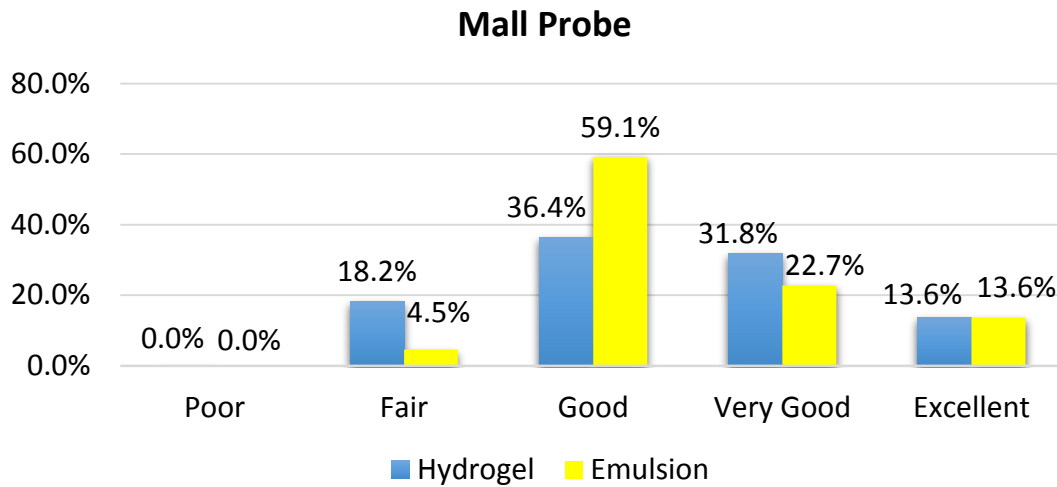


Figure 5.3: Similarity rating for hydrogel and oil based brain phantoms compared to brain tissue. Tool: Scalpel.

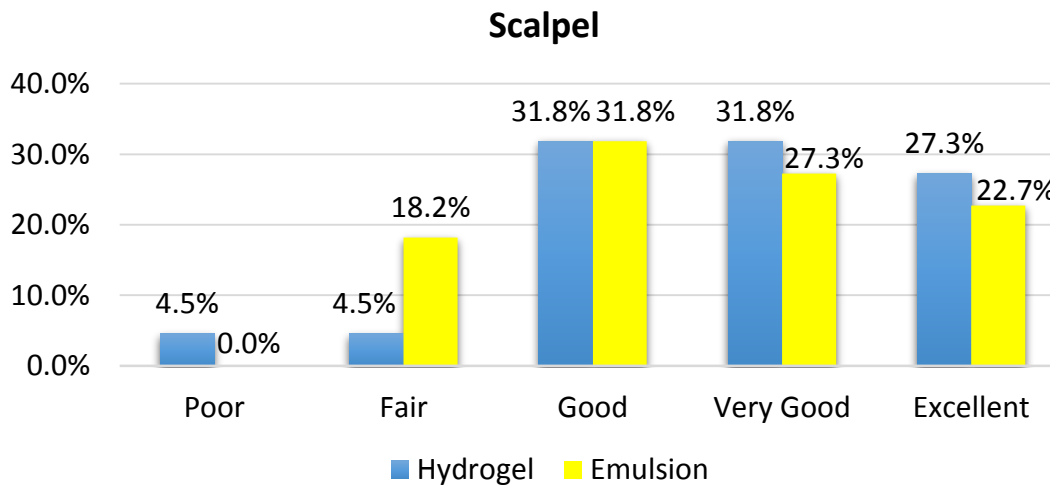


Figure 5.4: Similarity rating for hydrogel and oil based brain phantoms compared to brain tissue. Tool: Forceps.

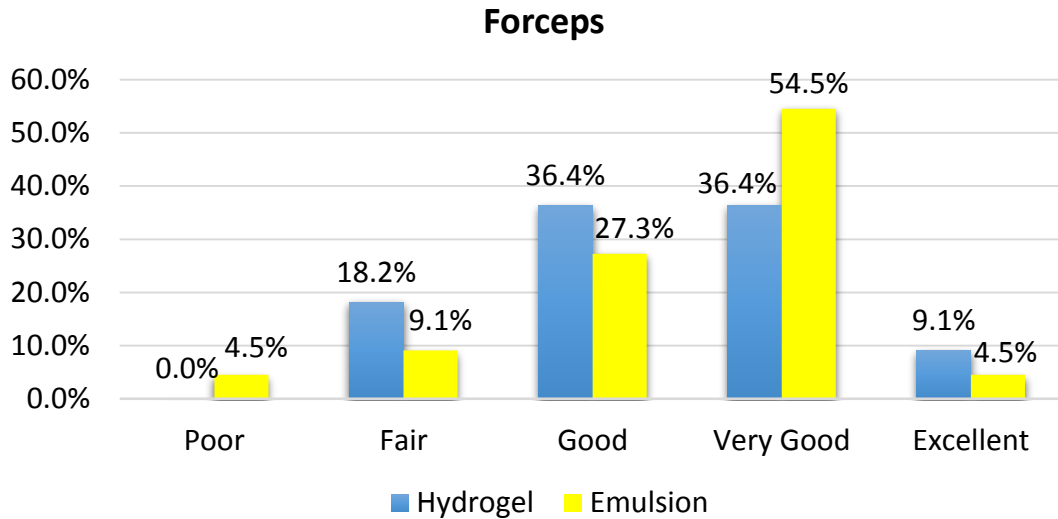
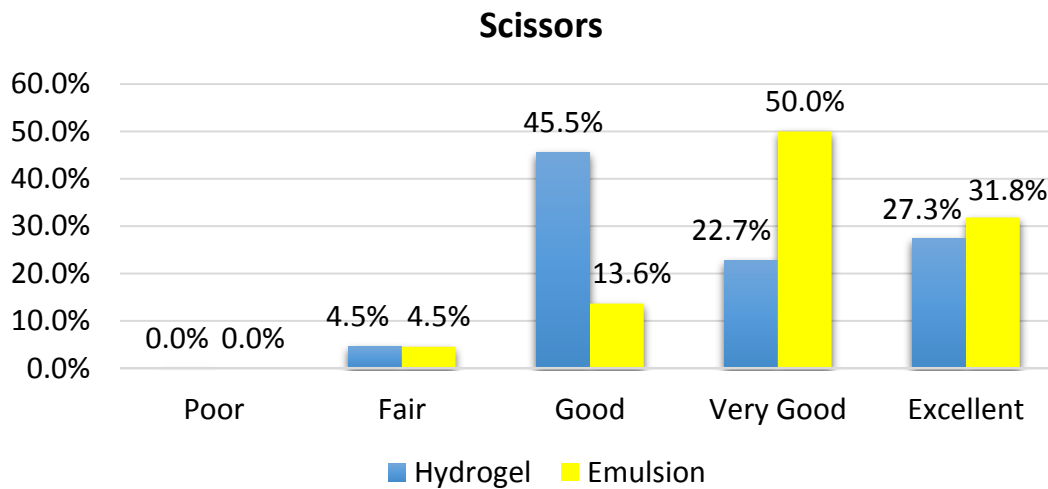


Figure 5.5: Similarity rating for hydrogel and oil based brain phantoms compared to brain tissue. Tool: Scissors.



The overall similarity of hydrogel phantom was rated as good by almost half of the participants and other 40% rated it as very good. Similar results presented the emulsion phantom. (Fig 5.6 and 5.7). Finally, the rating regarding the brain phantom that better resembles brain tissue, slightly over the half of the participants surveyed perceived that the emulsion was more similar to the feel of brain tissue (Fig 5.8).

Major comments provided by the participants were related to a stiffer response of the brain phantoms, this could be attributed to the viscoelastic behavior of brain tissue and tissue-mimicking materials that in section 3.5 was addressed by measuring the relaxation response which was found to be different for all materials on one hand. In the other hand, the mechanical response in this study was measured over strain levels up to 30%, it is possible that participants had applied compressive deformations beyond this limit, however, the brain is not expected to experience high strains during surgery due to the risk of producing TBI. Other comments were related to the level of deformation that brain tissue was able to withstand, hydrogel would experience failure at low strain levels while the emulsion would stand greater strain levels but not without exhibiting any plastic deformation, this was also addressed in section 3.5 where it was determined that hydrogel materials could not withstand compressive deformations greater than 35% of their initial dimension. Another comment referred to the even cuts made in the hydrogel phantom, this was from the beginning one of the drawbacks of working with gelatin, which at the time of braking by any means there will be a brittle fracture behavior resembling a broken glass.

Figure 5.6: Overall similarity between hydrogel phantom and Brain Tissue.

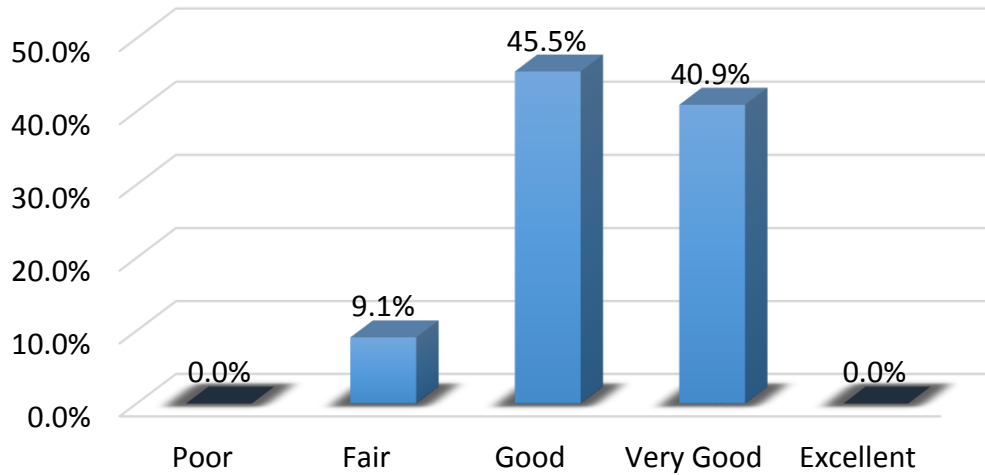


Figure 5.7: Overall similarity between emulsion phantom and Brain Tissue.

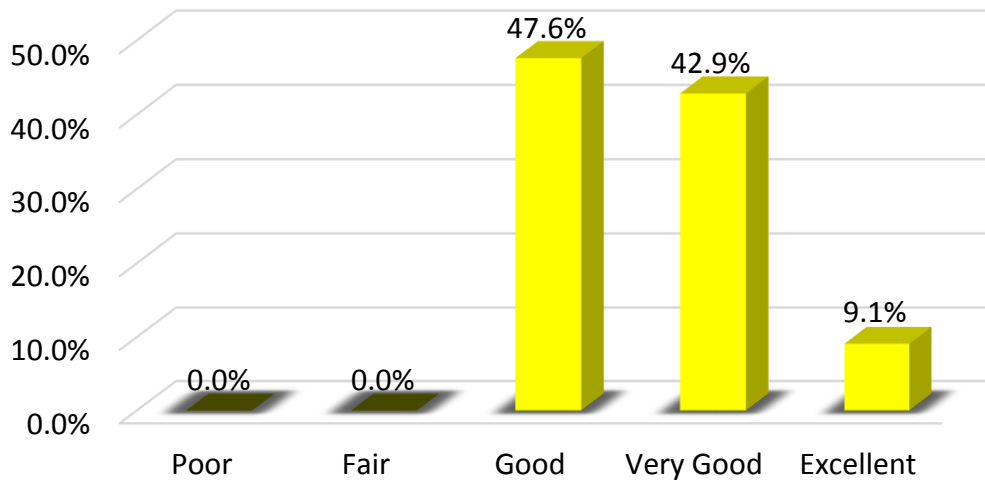
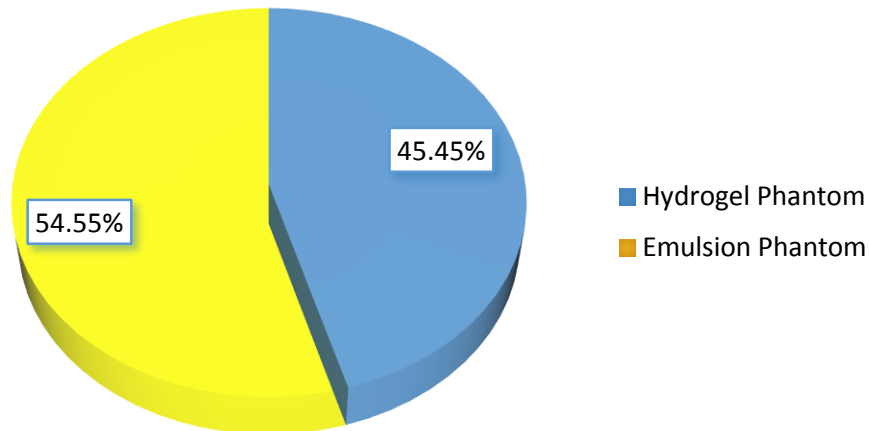


Figure 5.8: Final vote of participants regarding the question which brain phantom resembles better the feel of brain tissue.



5.4 - Discussion

The expanded use in the field of medicine of 3D anatomy models has led to innovation in the fabrication of patient-specific models based on imaging data [2]. There have been reported cases where 3D models fabricated by means of rapid prototyping were used to train the methods for dissecting complex anatomical areas [5], or the application of solid replicas of skull based tumors for patient education, diagnosis and preoperative planning, [66] as well as a simulation based-training for aneurism surgeries [11]. The most innovative models are fabricated with multiple materials varying consistency and density with an inbuilt pathological entity. [10]. These models were

generally constructed either with resins, rigid plastic or rubbery materials, which in any case resemble the feel of soft tissue.

Using hydrogel and oil based materials previously mechanically characterized to ensure a similar mechanical behavior to that of brain tissue, we have been able to fabricate brain phantoms that are anatomically accurate and duplicate actual brain tissue mechanical properties, thus, providing the realism that has been missing in model-aided training and surgical planning.

The haptic fidelity of brain tissue in the tissue-mimicking material phantoms was tested by 22 participants who rated from poor to excellent in a 5-point Likert scale the “feel” of brain phantoms made out of hydrogel and oil based materials.

Both tissue-mimicking materials demonstrated to have similar mechanical properties to brain tissue but there are still big differences regarding other physical properties like texture, adhesiveness, brittleness and density that will affect the perception of how similar something feels related to another thing. Having in mind that the goal is to fabricate a 3D brain model suitable for training or planning surgery we need to take into account that our brain model should meet some requirements including a material structurally stable at very low stiffness, but strong enough to maintain its configuration when fabricated, handled and eventually printed, therefore, a softer material would result counterproductive, as our model wouldn't be suitable for surgical planning purposes.

CHAPTER 6

CONCLUSIONS AND FUTURE WORK

6.1 - Conclusions

6.1.1 - Tissue-mimicking material mechanical characterization

The mechanical properties of porcine brain tissue were investigated at strain rates typical of surgical procedures. Applying unconfined compression test set up it was found that tissue-mimicking materials' elastic modulus and peaks stresses up to 30% of strain are similar to those of brain tissue as well as a markedly strain rate dependency for all three materials.

6.1.2 - 3D modeling

One of the advantages of haptic real models is the ability to obtain an overview of complex anatomical structures from any perspective enhancing the surgeon's accurate understanding of the pathology regarding the size, configuration and 3-dimensional relationship with the surrounding structures making it possible to confirm the right diagnosis of any particular disease. As a result tissue mimicking material phantoms could be found useful for neurosurgery, primarily because they improve the understanding of the anatomical situation. Second, as in all surgical procedures, there is a learning process

before becoming proficient in a given surgical intervention. The teaching of surgical techniques to less experienced neurosurgeons is difficult due to the risk that represents any surgical procedure with non-experienced staff as well as human structures are not available in the quantities necessary to allow extensive practice. The desire for more realistic training environments has led to the development of life-sized brain replicas which can be fabricated in large numbers and for a wide range of uses.

6.1.3 - Haptic Test

This study provided empirical evidence that the tissue-mimicking phantoms resemble the “feel” of brain tissue.

6.1.4 - Summary

The use of brain phantoms that resemble mechanical properties of brain tissue is the additional tactile and visual experience with potential in planning, training and simulation. It is not expected that the use of brain phantoms change the surgical plan but serve as a model to help understand the problem, know the exact position of critical structures and anticipate difficulties substantially improving surgical outcomes as well as enhancing the learning process of future neurosurgeons.

6.2 - Limitations of the present study and future work

6.2.1 - Limitations

During mechanical characterization of brain tissue mixed white matter and gray matter specimens were used, gray matter is found to be isotropic while white matter is found to be anisotropic [40] and in this study the tissue samples were selected without consideration of white matter content and alignment. Although, previous studies on mechanical characterization of brain tissue have reported that at large enough samples, anisotropy does not have an effect on the mechanical response of brain tissue, sample heterogeneity may play an important role in the mechanical characterization of brain tissue. Additionally, the proposed brain phantom is intended to be used as a brain replica for two cases to be considered in neurosurgical procedures:

1. Surgical training haptic brain phantom with realistic sense of touch which would require an average brain with most common mechanical properties. To achieve this goal, mechanical constants would need to be determined which would require tests to be conducted in humans in vivo. Mechanical characterization in this study was conducted in pig brains in vitro.
2. Pre-operative planning for a particular patient, in this case the average brain is not suitable. Patient specific mechanical properties would have to be identified.

This work might be criticized because mechanical tests were performed in order to mimic brain tissue mechanical properties at room temperature which is not the body temperature in which a neurosurgeon would be working during a surgical intervention. In section 3.4 it was determined that mechanical properties are temperature dependent. However, the purpose of developing a tissue mimicking brain phantom that resembles mechanical properties of brain tissue is surgical training or planning, when the time comes, people is not going to wait until the models reach a certain temperature to start working on it. Neither are they going to heat up the model to reach a body temperature so they can start planning a surgery. Nevertheless, in theory, the stiffness of the brain substitute materials can be lowered by using lower concentrations of gelatin in order to fabricate a model that resembles mechanical properties at body temperature with a material with the same characteristics at room temperature, but in practice is improbable because of the high damage sensitivity that this material would exhibit causing it to break up at very low strains which in terms of surgical training would no represent a problem. However, due to the nature of the manufacturing materials, these will still have to be stored at low temperatures to prevent dehydration and degradation on one hand, and on the other, fabrication of brain phantoms following the process discussed in this study would be impossible at least for the hydrogel based material.

Finally, outcomes of a haptic test performed by neurosurgeons may differ from results obtained from regular students. According with a study that compared the ability of practicing veterinarians and veterinary students to identify stiffness values, although

neither group was able to identify more than 2 stiffness levels, results indicated that veterinarians performed significantly better than the veterinarian students suggesting that stiffness perception is a trainable skill. Therefore, haptic stiffness test should be performed with the help of neurosurgeons and experts in surgical simulation, in order to be able to improve the brain substitute materials and provide a more reliable haptic perception on the ability of the brain phantoms to meet the needs for neurosurgery planning and resident's training.

6.2.2 - Future work

Accuracy and realism are essential as well as needs to be met when developing suitable models for the purpose of training and planning surgery. In order to fulfill all the criteria that are necessary to train future neurosurgeons, the models should be qualitatively and quantitatively assessed during simulated surgical procedures by neurosurgeons. Additional Haptic tests including samples with different storing time should be performed in order to determine brain phantom's shelf life.

Simulation models often assume gray and white matter are indistinguishable (Hansen and Larsen, 1998; Miller et al., 2000) and because of the lack of validated tissue properties, the realistic haptic sense of these models may be limited. With the use of Magnetic Resonance Elastography which is a technique that measures the stiffness of soft tissue by imaging the propagation of shear waves using MRI[28] it is possible to measure mechanical properties of white and gray matter and be able to mimic their mechanical

properties separately, as our study only addressed the measurement of mechanical properties of mixed matters.

Additional studies should aim to develop brain phantoms that take pathophysiology into consideration as well as incorporating other polymers that mimic the heterogeneous nature and different mechanical properties of pathological structures.

Future work also should aim to develop specific brain substitute materials more suitable for specific uses. For training purposes, replicating the mechanical properties of brain tissue close to human body temperature (37°C) should be assessed. However, this would make brain substitute material too soft, thus, not suitable for planning surgery, consequently, a stiffer material should be developed to stand greater strains in order to enhance handleability but preserving the haptic fidelity of brain tissue. Additionally, brain models for training purposes should be designed so that they include all of the structures involved in a neurosurgical procedure including skin, skull, Dura matter, brain and pathological structures. This way trainees would learn and practice the whole procedure.

With the advent of 3D printers, brain models could be reproduced with different materials, making possible the fabrication of models with varying tissue properties. 3D printers specifically designed to extrude soft materials allow the creation of models with areas of different stiffness. Currently, 3D printing technology is being used to print soft materials in the fields of biology to print cells, extracellular matrices, and hydrogels[76], while in culinary arts soft material printers have been designed to print foods exceeding

our wildest expectations such as printing chocolate, gummy candies and even a pizza. [77]. Thereby, the fabrication or customization of a device capable of 3D printing the tissue-mimicking materials that were developed in this study, would allow us to fabricate not just brain phantoms but complete head models that include many structures such as skin, and Dura matter. Regarding the brain structures, 3D printing would also open the possibility of eventually add blood vessels to the models making them more realistic and thorough regarding all structures found in a human head.

REFERENCES

- [1] H. M. Richard K. Reznick, "Teaching surgical skills-Changes in the wind," *N. Engl. J. Med.*, vol. 355, no. 25, pp. 2664–2669, 2006.
- [2] F. Rengier, A. Mehndiratta, H. von Tengg-Kobligk, C. M. Zechmann, R. Unterhinninghofen, H.-U. Kauczor, and F. L. Giesel, "3D printing based on imaging data: review of medical applications," *Int. J. Comput. Assist. Radiol. Surg.*, vol. 5, no. 4, pp. 335–341, 2010.
- [3] M. Bridges and D. L. Diamond, "The financial impact of teaching surgical residents in the operating room," *Am. J. Surg.*, vol. 177, no. 1, pp. 28–32, 1999.
- [4] B. Eftekhar, M. Ghodsi, E. Ketabchi, and A. R. Ghazvini, "Play dough as an educational tool for visualization of complicated cerebral aneurysm anatomy.," *BMC Med. Educ.*, vol. 5, no. 1, p. 15, 2005.
- [5] K. Mori, T. Yamamoto, Y. Nakao, and T. Esaki, "Development of artificial cranial base model with soft tissues for practical education: Technical note," *Neurosurgery*, vol. 66, pp. 339–341, 2010.
- [6] V. Waran, D. Pancharatnam, H. Thambinayagam, R. Raman, A. Rathinam, Y. Balakrishnan, T. Tung, and Z. Rahman, "The Utilization of Cranial Models Created Using Rapid Prototyping Techniques in the Development of Models for Navigation Training," *J. Neurol. Surg. Part A Cent. Eur. Neurosurg.*, vol. 75, no. 1, pp. 012–015, 2013.
- [7] V. Waran, V. Narayanan, R. Karuppiah, H. C. Thambynayagam, K. A. Muthusamy, Z. A. A. Rahman, and R. W. Kirollos, "Neurosurgical endoscopic training via a realistic 3-dimensional model with pathology.," *Simul. Healthc.*, vol. 10, no. 1, pp. 43–8, 2015.
- [8] V. Waran, R. Menon, D. Pancharatnam, A. K. Rathinam, Y. K. Balakrishnan, T. S. Tung, R. Raman, N. Prepageran, H. Chandran, and Z. A. A. Rahman, "The creation and verification of cranial models using three-dimensional rapid prototyping technology in field of transnasal sphenoid endoscopy," *Am. J. Rhinol. Allergy*, vol. 26, no. 5, pp. 132–136, 2012.
- [9] R. a Kockro, A. Stadie, C. Charalampaki, and I. Ng, "Surgical Technique Application FOR N EUROSURGICAL P LANNING AND T RAINING," *Neurosurgery*, vol. 61, no. November, pp. 379–391, 2007.

- [10] V. Waran, V. Narayanan, R. Karuppiyah, S. L. F. Owen, and T. Aziz, "Utility of multimaterial 3D printers in creating models with pathological entities to enhance the training experience of neurosurgeons.," *J. Neurosurg.*, vol. 120, no. 2, pp. 489–492, 2014.
- [11] G. Wurm, M. Lehner, B. Tomancok, R. Kleiser, and K. Nussbaumer, "Cerebrovascular biomodeling for aneurysm surgery: simulation-based training by means of rapid prototyping technologies," *Surg Innov*, vol. 18, no. 3, pp. 294–306, 2011.
- [12] M. Oishi, M. Fukuda, N. Yajima, K. Yoshida, M. Takahashi, T. Hiraishi, T. Takao, A. Saito, and Y. Fujii, "Interactive presurgical simulation applying advanced 3D imaging and modeling techniques for skull base and deep tumors.," *J. Neurosurg.*, vol. 119, no. 1, pp. 94–105, 2013.
- [13] L. Z. Shuck and S. H. Advani, "Rheological Response of Human Brain Tissue in Shear," *J. Basic Eng.*, vol. 94, no. 4, pp. 905–911, 1972.
- [14] L. E. Bilston, Z. Liu, and N. Phan-Thien, "Linear viscoelastic properties of bovine brain tissue in shear," *Biorheology*, vol. 34, no. 6, pp. 377–385, 1997.
- [15] K. K. Darvish and J. R. Crandall, "Nonlinear viscoelastic effects in oscillatory shear deformation of brain tissue," *Med. Eng. Phys.*, vol. 23, no. 9, pp. 633–645, 2001.
- [16] M. Hrapko, J. a W. van Dommelen, G. W. M. Peters, and J. S. H. M. Wismans, "The mechanical behaviour of brain tissue: large strain response and constitutive modelling.," *Biorheology*, vol. 43, no. 5, pp. 623–36, 2006.
- [17] K. Miller and K. Chinzei, "Constitutive modelling of brain tissue: experiment and theory.," *J. Biomech.*, vol. 30, no. 11/12, pp. 1115–1121, 1997.
- [18] T. P. Prevost, A. Balakrishnan, S. Suresh, and S. Socrate, "Biomechanics of brain tissue," *Acta Biomater.*, vol. 7, no. 1, pp. 83–95, 2011.
- [19] G. Franceschini, D. Bigoni, P. Regitnig, and G. A. Holzapfel, "Brain tissue deforms similarly to filled elastomers and follows consolidation theory," *J. Mech. Phys. Solids*, vol. 54, no. 12, pp. 2592–2620, 2006.
- [20] A. Tamura, S. Hayashi, K. Nagayama, and T. Matsumoto, "Mechanical Characterization of Brain Tissue in High-Rate Compression," *J. Biomech. Sci. Eng.*, vol. 2, no. 3, pp. 263–274, 2007.
- [21] S. Cheng and L. E. Bilston, "Unconfined compression of white matter," *J. Biomech.*, vol. 40, no. 1, pp. 117–124, 2007.

- [22] M. Hrapko, J. A. W. Van Dommelen, G. W. M. Peters, and J. S. H. M. Wismans, "Characterisation of the mechanical behaviour of brain tissue in compression and shear," *Biorheology*, vol. 45, no. 6, pp. 663–676, 2008.
- [23] K. Miller and K. Chinzei, "Mechanical properties of brain tissue in tension," *J. Biomech.*, vol. 35, no. 4, pp. 483–490, 2002.
- [24] F. Velardi, F. Fraternali, and M. Angelillo, "Anisotropic constitutive equations and experimental tensile behavior of brain tissue," *Biomech. Model. Mechanobiol.*, vol. 5, no. 1, pp. 53–61, 2006.
- [25] A. Tamura, S. Hayashi, K. Nagayama, and T. Matsumoto, "Mechanical Characterization of Brain Tissue in High-Rate Extension," *J. Biomech. Sci. Eng.*, vol. 3, no. 2, pp. 263–274, 2008.
- [26] J. A. W. Van Dommelen, T. P. J. Van der Sande, M. Hrapko, and G. W. M. Peters, "Mechanical properties of brain tissue by indentation: Interregional variation," *J. Mech. Behav. Biomed. Mater.*, vol. 3, no. 2, pp. 158–166, 2010.
- [27] T. P. Prevost, G. Jin, M. A. De Moya, H. B. Alam, S. Suresh, and S. Socrate, "Dynamic mechanical response of brain tissue in indentation in vivo, in situ and in vitro," *Acta Biomater.*, vol. 7, no. 12, pp. 4090–4101, 2011.
- [28] R. Muthupillai, P. J. Rossman, D. J. Lomas, J. F. Greenleaf, S. J. Riederer, and R. L. Ehman, "Magnetic resonance imaging of transverse acoustic strain waves.," *Magn. Reson. Med.*, vol. 36, no. 2, pp. 266–274, 1996.
- [29] P. J. McCracken, A. Manduca, J. Felmlee, and R. L. Ehman, "Mechanical transient-based magnetic resonance elastography," *Magn. Reson. Med.*, vol. 53, no. 3, pp. 628–639, 2005.
- [30] U. Hamhaber, I. Sack, S. Papazoglou, J. Rump, D. Klatt, and J. Braun, "Three-dimensional analysis of shear wave propagation observed by in vivo magnetic resonance elastography of the brain," *Acta Biomater.*, vol. 3, no. 1, pp. 127–137, 2007.
- [31] L. Xu, Y. Lin, J. C. Han, Z. N. Xi, H. Shen, and P. Y. Gao, "Magnetic resonance elastography of brain tumors: preliminary results," *Acta Radiol*, vol. 48, no. 3, pp. 327–330, 2007.
- [32] S. M. Atay, C. D. Kroenke, A. Sabet, and P. V Bayly, "Measurement of the dynamic shear modulus of mouse brain tissue in vivo by magnetic resonance elastography.," *J. Biomech. Eng.*, vol. 130, no. 2, p. 021013, 2008.

- [33] M. A. Green, L. E. Bilston, and R. Sinkus, "In vivo brain viscoelastic properties measured by magnetic resonance elastography," *NMR Biomed.*, vol. 21, pp. 755–764, 2008.
- [34] P. Schiavone, F. Chassat, T. Boudou, E. Promayon, F. Valdivia, and Y. Payan, "In vivo measurement of human brain elasticity using a light aspiration device," *Med. Image Anal.*, vol. 13, no. 4, pp. 673–678, 2009.
- [35] H. Metz, J. McElhaney, and A. K. Ommaya, "A comparison of the elasticity of live, dead, and fixed brain tissue," *J. Biomech.*, vol. 3, no. 4, pp. 453–458, 1970.
- [36] K. Miller, K. Chinzei, G. Orsengo, and P. Bednarz, "Mechanical properties of brain tissue in-vivo: Experiment and computer simulation," *J. Biomech.*, vol. 33, no. 11, pp. 1369–1376, 2000.
- [37] M. I. Miga, K. D. Paulsen, P. J. Hoopes, F. E. Kennedy, a Hartov, and D. W. Roberts, "In vivo modeling of interstitial pressure in the brain under surgical load using finite elements.," *J. Biomech. Eng.*, vol. 122, no. 4, pp. 354–363, 2000.
- [38] A. Gefen and S. S. Margulies, "Are in vivo and in situ brain tissues mechanically similar?," *J. Biomech.*, vol. 37, no. 9, pp. 1339–1352, 2004.
- [39] K. B. Arbogast and S. S. Margulies, "Material characterization of the brainstem from oscillatory shear tests.," *J. Biomech.*, vol. 31, no. 9, pp. 801–807, 1998.
- [40] M. T. Prange and S. S. Margulies, "Regional, directional, and age-dependent properties of the brain undergoing large deformation.," *J. Biomech. Eng.*, vol. 124, no. 2, pp. 244–252, 2002.
- [41] T. Kaster, I. Sack, and A. Samani, "Measurement of the hyperelastic properties of ex vivo brain tissue slices," *J. Biomech.*, vol. 44, no. 6, pp. 1158–1163, 2011.
- [42] B. Fischl and A. M. Dale, "Measuring the thickness of the human cerebral cortex from magnetic resonance images.," *Proc. Natl. Acad. Sci. U. S. A.*, vol. 97, no. 20, pp. 11050–5, 2000.
- [43] K. Miller, "Method of testing very soft biological tissues in compression," *J. Biomech.*, vol. 38, no. 1, pp. 153–158, 2005.
- [44] S. Nicolle, M. Lounis, and R. Willinger, "Shear Properties of Brain Tissue over a Frequency Range Relevant for Automotive Impact Situations: New Experimental Results.," *Stapp Car Crash J.*, vol. 48, pp. 239–58, Nov. 2004.
- [45] K. S. Anseth, C. N. Bowman, and L. Brannon-Peppas, "Mechanical properties of hydrogels and their experimental determination," *Biomaterials*, vol. 17, no. 17, pp. 1647–1657, 1996.

- [46] E. M. Ahmed, "Hydrogel: Preparation, characterization, and applications: A review," *J. Adv. Res.*, vol. 6, no. 2, pp. 105–121, 2015.
- [47] Q. Chen, B. Suki, and K.-N. An, "Dynamic mechanical properties of agarose gels modeled by a fractional derivative model.," *J. Biomech. Eng.*, vol. 126, no. 5, pp. 666–671, 2004.
- [48] A. Karimi and M. Navidbakhsh, "Material properties in unconfined compression of gelatin hydrogel for skin tissue engineering applications," *Biomed. Eng. / Biomed. Tech.*, vol. 59, no. 6, pp. 479–486, 2014.
- [49] Q. Liu, G. Subhash, and D. F. Moore, "Loading velocity dependent permeability in agarose gel under compression," *J. Mech. Behav. Biomed. Mater.*, vol. 4, no. 7, pp. 974–982, 2011.
- [50] J. S. O. Brien and E. L. Sampson, "Lipid composition of the normal human brain :," vol. 6, no. 9, 1965.
- [51] M. R. Pamidi and S. H. Advani, "Nonlinear Constitutive Relations for Human Brain Tissue," *Trans. ASME. J. Biomech.*, vol. 100, no. 3, pp. 44–48, 1978.
- [52] K. B. Sahay, R. Mehrotra, U. Sachdeva, and A. K. Banerji, "Elastomechanical characterization of brain tissues," *J. Biomech.*, vol. 25, no. 3, pp. 319–326, 1992.
- [53] M. Farshad, M. Barbezat, P. Flüeler, F. Schmidlin, P. Graber, and P. Niederer, "Material characterization of the pig kidney in relation with the biomechanical analysis of renal trauma," *J. Biomech.*, vol. 32, no. 4, pp. 417–425, 1999.
- [54] K. Miller, "Constitutive model of brain tissue suitable for finite element analysis of surgical procedures.," *J. Biomech.*, vol. 32, no. 5, pp. 531–537, 1999.
- [55] L. E. Bilston, Z. Liu, and N. Phan-Thien, "Large strain behaviour of brain tissue in shear: some experimental data and differential constitutive model.," *Biorheology*, vol. 38, no. 4, pp. 335–45, 2001.
- [56] B. R. Donnelly and J. Medige, "Shear properties of human brain tissue," *J. Biomech. Eng.*, vol. 119, no. November 1997, pp. 423–432, 1997.
- [57] F. Pervin and W. W. Chen, "Dynamic mechanical response of bovine gray matter and white matter brain tissues under compression," *J. Biomech.*, vol. 42, no. 6, pp. 731–735, 2009.
- [58] A. Garo, M. Hrapko, J. A. W. van Dommelen, and G. W. M. Peters, "Towards a reliable characterisation of the mechanical behaviour of brain tissue: The effects of post-mortem time and sample preparation.," *Biorheology*, vol. 44, no. 1, pp. 51–58, 2007.

- [59] D. W. A. Brands, P. H. M. Bovendeerd, G. W. M. Peters, and J. S. H. M. Wismans, "The large shear strain dynamic behavior of in-vitro porcine brain tissue and a silicone gel model material," *44th Stapp car crash Conf. J.*, vol. 44, no. June 2016, pp. 249–260, 2000.
- [60] K. L. Thibault and S. S. Margulies, "Age-dependent material properties of the porcine cerebrum: Effect on pediatric inertial head injury criteria," *J. Biomech.*, vol. 31, no. 12, pp. 1119–1126, 1998.
- [61] K. Arbogast and S. Margulies, "Regional differences in mechanical properties of the porcine central nervous system," *Proc. 41st Stapp Car Crash Conf.*, pp. 293–300, 1997.
- [62] F. Shen, T. E. Tay, J. Z. Li, S. Nigen, P. V. S. Lee, H. K. Chan, and H. K. Shen, F. and Tay, T.E. and Li, J.Z. and Nigen, S. and Lee, P.V.S. and Chan, "Modified Bilston Nonlinear Viscoelastic Model for Finite Element Head Injury Studies," *J. Biomech. Eng., Trans. ASME*, vol. 128, no. 5, pp. 797–801, 2006.
- [63] M. Hrapko, J. A. W. van Dommelen, G. W. M. Peters, and J. S. H. M. Wismans, "The influence of test conditions on characterization of the mechanical properties of brain tissue.," *J. Biomech. Eng.*, vol. 130, no. 3, p. 031003, Jun. 2008.
- [64] M. Samii and V. M. Gerganov, "Surgery of extra-axial tumors of the cerebral base," *Neurosurgery*, vol. 62, no. 6, pp. 1153–1168, 2008.
- [65] P. S. D'Urso, R. G. Thompson, R. L. Atkinson, M. J. Weidmann, M. J. Redmond, B. I. Hall, S. J. Jeavons, M. D. Benson, and W. J. S. Earwaker, "Cerebrovascular biomodelling: A technical note," *Surg. Neurol.*, vol. 52, no. 5, pp. 490–500, 1999.
- [66] P. . D'Urso, R. . Atkinson, M. . Weidmann, M. . Redmond, B. . Hall, W. J. . Earwaker, R. . Thompson, and D. . Effeney, "Biomodelling of skull base tumours," *J. Clin. Neurosci.*, vol. 6, no. 1, pp. 31–35, 1999.
- [67] P. S. D'Urso, T. M. Barker, W. J. Earwaker, L. J. Bruce, R. L. Atkinson, M. W. Lanigan, J. F. Arvier, and D. J. Effeney, "Stereolithographic biomodelling in cranio-maxillofacial surgery: a prospective trial.," *J. Craniomaxillofac. Surg.*, vol. 27, no. 1, pp. 30–37, 1999.
- [68] P. S. D'Urso, R. L. Atkinson, M. W. Lanigan, W. J. Earwaker, I. J. Bruce, a Holmes, T. M. Barker, D. J. Effeney, and R. G. Thompson, "Stereolithographic (SL) biomodelling in craniofacial surgery.," *Br. J. Plast. Surg.*, vol. 51, no. 7, pp. 522–530, 1998.
- [69] M. T. Izatt, P. L. P. J. Thorpe, R. G. Thompson, P. S. D'Urso, C. J. Adam, J. W. S. Earwaker, R. D. Labrom, and G. N. Askin, "The use of physical biomodelling in complex spinal surgery," *Eur. Spine J.*, vol. 16, no. 9, pp. 1507–1518, 2007.

- [70] M. Poulsen, C. Lindsay, T. Sullivan, and P. D'Urso, "Stereolithographic modelling as an aid to orbital brachytherapy," *Int. J. Radiat. Oncol. Biol. Phys.*, vol. 44, no. 3, pp. 731–735, 1999.
- [71] J. L. Silberstein, M. M. Maddox, P. Dorsey, A. Feibus, R. Thomas, and B. R. Lee, "Physical models of renal malignancies using standard cross-sectional imaging and 3-dimensional printers: A pilot study," *Urology*, vol. 84, no. 2, pp. 268–272, 2014.
- [72] D. R. Varma, "Managing DICOM images: Tips and tricks for the radiologist," *Indian J. Radiol. Imaging*, vol. 22, no. 1, pp. 4–13, 2012.
- [73] Y. P. Du, D. L. Parker, W. L. Davis, and G. Cao, "Reduction of partial-volume artifacts with zero-filled interpolation in three-dimensional MR angiography.," *J. Magn. Reson. imaging*, vol. 4, no. 5, pp. 733–41, 1994.
- [74] E. Bullmore, M. Brammer, G. Rouleau, B. Everitt, A. Simmons, T. Sharma, S. Frangou, R. Murray, and G. Dunn, "Computerized Brain Tissue Classification of Magnetic Resonance Images: A New Approach to the Problem of Partial Volume Artifact," *NeuroImage*, vol. 2, no. 2, pp. 133–147, 1995.
- [75] S. J. Savio, L. C. V Harrison, T. Luukkaala, T. Heinonen, P. Dastidar, S. Soimakallio, and H. J. Eskola, "Effect of slice thickness on brain magnetic resonance image texture analysis.," *Biomed. Eng. Online*, vol. 9, no. 1, p. 60, 2010.
- [76] V. Mironov, T. Boland, T. Trusk, G. Forgacs, and R. R. Markwald, "Organ printing: Computer-aided jet-based 3D tissue engineering," *Trends Biotechnol.*, vol. 21, no. 4, pp. 157–161, 2003.
- [77] C. Lin, "3D Food Printing: A Taste of the Future," *J. Food Sci. Educ.*, vol. 14, no. 3, pp. 86–87, 2015.
- [78] John A Beal, (2016,November 30) "Human brain right dissected lateral view description."
https://en.wikipedia.org/wiki/White_matter#/media/File:Human_brain_right_dissected_lateral_view_description.JPG

APPENDICES

APPENDIX A

Mechanical testing of Hydrogels

A.1 - Gelatin (G) with Chromium (Cr) Mechanical Characterization

Gelatin-Chromium was prepared by adding the respectively concentration of gelatin and chromium to 100 ml. of distilled water previously heated at 50°C. Figures 1 and 2 depict the stress-strain response of each mixture compared to brain tissue mechanical response.

Figure A.1: Stress-Strain response for Gelatin- Chromium samples tested at 1/s strain rate and 45% strain.

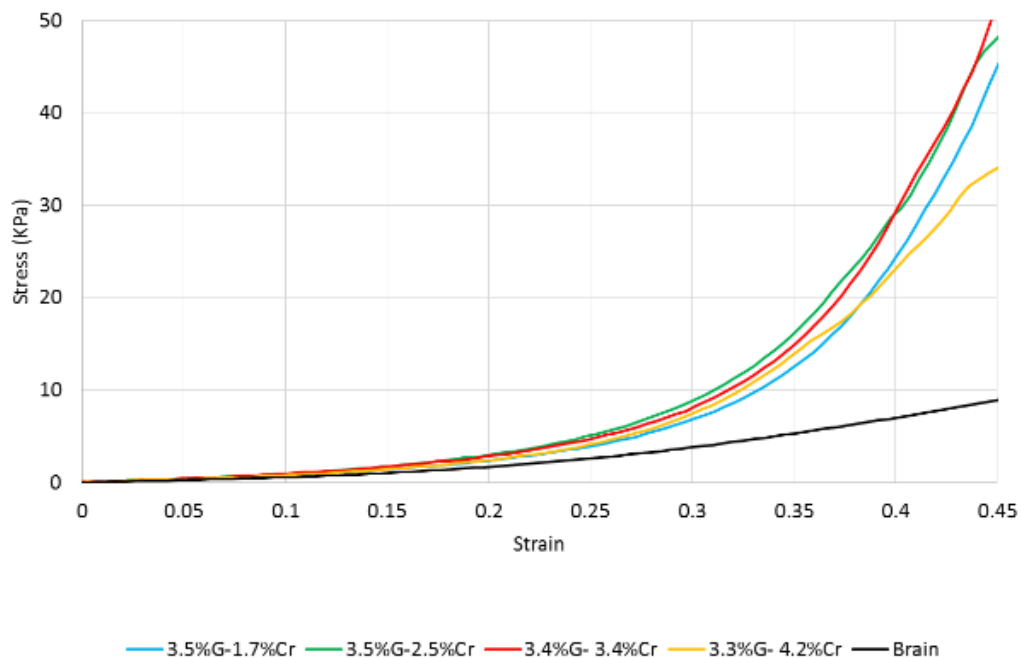
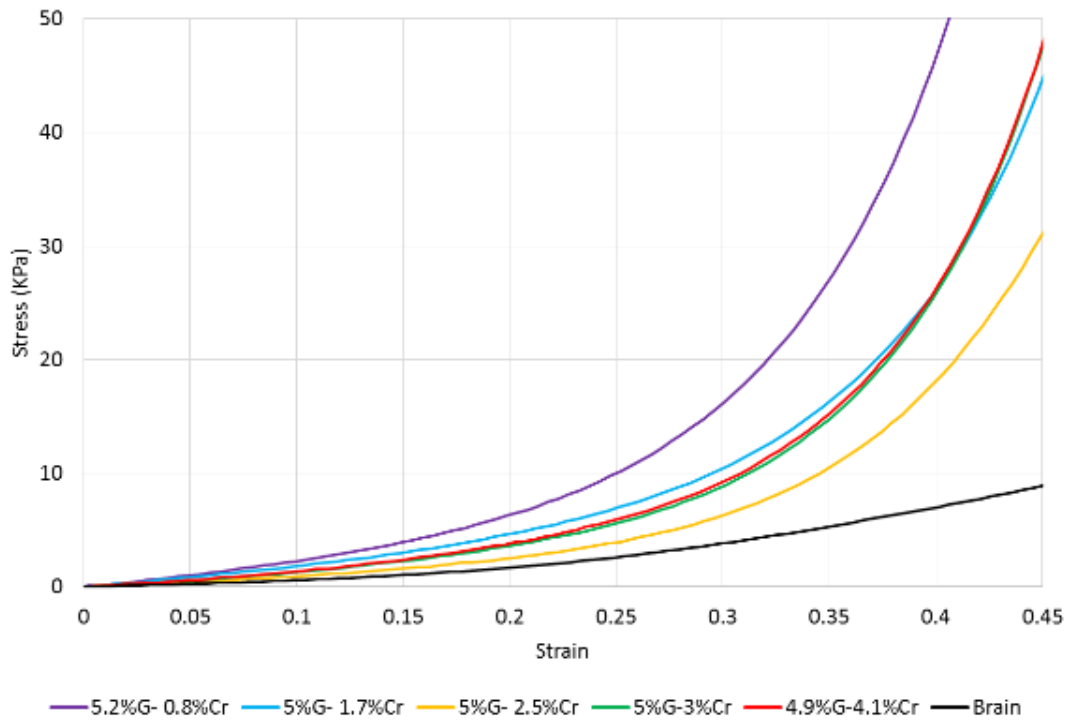


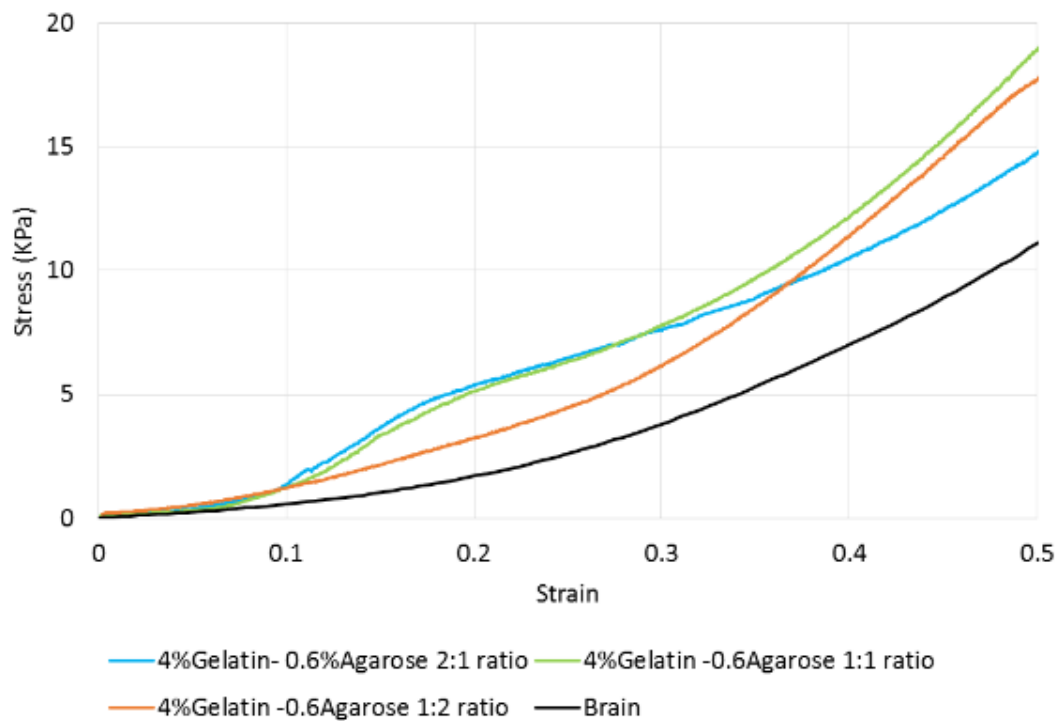
Figure A.2: Stress-Strain response for Gelatin- Chromium samples tested at 1/s strain rate and 45% strain.



A.2 - 4% Gelatin - 0.6% Agarose Mechanical characterization

Gelatin-agarose mixtures were prepared and described in chapter 3. Fig 3 Depicts the stress-strain response of each mixture compared to brain tissue mechanical response.

Figure A.3: Stress-Strain response for Gelatin- Agarose samples tested at 1/s strain rate and 45% strain.



APPENDIX B

STATISTICAL ANALYSIS

B.1 - Anatomical location affect. Anterior vs Mid vs Posterior regions of the brain. (95% Confidence interval).

B.1.1 - Elastic moduli 10% Strain

Anova: Single Factor

SUMMARY

<i>Groups</i>	<i>Count</i>	<i>Sum</i>	<i>Average</i>	<i>Variance</i>
Row 1	16	85.23656	5.327285	2.315544
Row 2	6	34.58398	5.763997	0.39362
Row 3	15	84.67783	5.645189	2.312236

ANOVA

<i>Source of Variation</i>	<i>SS</i>	<i>df</i>	<i>MS</i>	<i>F</i>	<i>P-value</i>	<i>F crit</i>
Between Groups	1.184711	2	0.592356	0.291579	0.748933	3.275898
Within Groups	69.07256	34	2.031546			
Total	70.25727	36				

B.1.2 - Elastic moduli 20% Strain

Anova: Single Factor

SUMMARY

<i>Groups</i>	<i>Count</i>	<i>Sum</i>	<i>Average</i>	<i>Variance</i>
Row 1	16	165.4546	10.34092	6.769247
Row 2	6	73.13521	12.1892	2.249261
Row 3	15	166.4317	11.09545	6.195419

ANOVA

<i>Source of Variation</i>	<i>SS</i>	<i>df</i>	<i>MS</i>	<i>F</i>	<i>P-value</i>	<i>F crit</i>
Between Groups	15.46636	2	7.733179	1.317797	0.281052	3.275898
Within Groups	199.5209	34	5.868261			
Total	214.9872	36				

B.1.3 - Elastic moduli 30% Strain

Anova: Single Factor

SUMMARY

<i>Groups</i>	<i>Count</i>	<i>Sum</i>	<i>Average</i>	<i>Variance</i>
Row 1	16	304.6868	19.04292	8.247037
Row 2	6	148.3446	24.7241	6.889212
Row 3	15	306.8095	20.45396	16.08131

ANOVA

<i>Source of Variation</i>	<i>SS</i>	<i>df</i>	<i>MS</i>	<i>F</i>	<i>P-value</i>	<i>F crit</i>
Between Groups	141.0104	2	70.50521	3.254212	0.057542	3.275898
Within Groups	383.29	34	11.27324			
Total	524.3004	36				

B.1.4 - Elastic moduli 40% Strain

Anova: Single Factor

SUMMARY

<i>Groups</i>	<i>Count</i>	<i>Sum</i>	<i>Average</i>	<i>Variance</i>
Row 1	16	468.3588	29.27242	19.00814
Row 2	6	238.6341	39.77235	27.8426
Row 3	15	493.1674	32.87782	39.87151

ANOVA

<i>Source of Variation</i>	<i>SS</i>	<i>df</i>	<i>MS</i>	<i>F</i>	<i>P-value</i>	<i>F crit</i>
Between Groups	485.9918	2	242.9959	8.408708	0.001079	3.275898
Within Groups	982.5364	34	28.89813			
Total	1468.528	36				

B.1.5 - Elastic Moduli 50% Strain

SUMMARY

<i>Groups</i>	<i>Count</i>	<i>Sum</i>	<i>Average</i>	<i>Variance</i>
Row 1	10	332.7169	33.27169	102.3009
Row 2	6	270.1048	45.01746	220.6417
Row 3	12	507.8739	42.32282	37.65499

ANOVA

<i>Source of Variation</i>	<i>SS</i>	<i>df</i>	<i>MS</i>	<i>F</i>	<i>P-value</i>	<i>F crit</i>
Between Groups	665.405	2	332.7025	3.411464	0.048978	3.38519
Within Groups	2438.121	25	97.52485			
Total	3103.526	27				

B.2 - Post-mortem time effect affect. 24hrs vs 6hrs post-mortem thresholds times. (95% Confidence interval).

B.2.1 - Elastic moduli 10% Strain

F-Test Two-Sample for Variances

	<i>Variable 1</i>	<i>Variable 2</i>
Mean	5.360837	5.526983
Variance	6.913745	1.951591
Observations	9	37
df	8	36
F	3.54262	
P(F<=f) one-tail	0.00403	
F Critical one-tail	2.208518	

t-Test: Two-Sample Assuming Unequal Variances

	<i>Variable 1</i>	<i>Variable 2</i>
Mean	5.360837	5.526983
Variance	6.913745	1.951591
Observations	9	37
Hypothesized Mean Difference	0	
df	9	
t Stat	-0.18337	
P(T<=t) one-tail	0.429285	
t Critical one-tail	1.833113	
P(T<=t) two-tail	0.85857	
t Critical two-tail	2.262157	

B.2.2 - Elastic moduli 20% Strain

F-Test Two-Sample for Variances

	<i>Variable</i> <i>1</i>	<i>Variable</i> <i>2</i>
Mean	11.77025	10.94653
Variance	30.04345	5.971868
Observations	9	37
df	8	36
F	5.030829	
P(F<=f) one-tail	0.000307	
F Critical one-tail	2.208518	

t-Test: Two-Sample Assuming Unequal Variances

	<i>Variable</i> <i>1</i>	<i>Variable</i> <i>2</i>
Mean	11.77025	10.94653
Variance	30.04345	5.971868
Observations	9	37
Hypothesized Mean Difference	0	
df	9	
t Stat	0.440327	
P(T<=t) one-tail	0.335043	
t Critical one-tail	1.833113	
P(T<=t) two-tail	0.670086	
t Critical two-tail	2.262157	

B.2.3 - Elastic Moduli 30% Strain

F-Test Two-Sample for Variances

	<i>Variable</i> <i>1</i>	<i>Variable</i> <i>2</i>
Mean	25.24581	20.50327
Variance	121.2088	14.93864
Observations	9	36
df	8	35
F	8.113775	
P(F<=f) one-tail	3.94E-06	
F Critical one-tail	2.216675	

t-Test: Two-Sample Assuming Unequal Variances

	<i>Variable</i> <i>1</i>	<i>Variable</i> <i>2</i>
Mean	25.24581	20.50327
Variance	121.2088	14.93864
Observations	9	36
Hypothesized Mean Difference	0	
df	8	
t Stat	1.272847	
P(T<=t) one-tail	0.119407	
t Critical one-tail	1.859548	
P(T<=t) two-tail	0.238815	
t Critical two-tail	2.306004	

B.2.4 - Elastic Moduli 40% Strain

F-Test Two-Sample for Variances

	<i>Variable 1</i>	<i>Variable 2</i>
Mean	46.92835	32.43676
Variance	303.4743	40.79245
Observations	9	37
df	8	36
F	7.439472	
P(F<=f) one-tail	8.35E-06	
F Critical one-tail	2.208518	

t-Test: Two-Sample Assuming Unequal Variances

	<i>Variable 1</i>	<i>Variable 2</i>
Mean	46.92835	32.43676
Variance	303.4743	40.79245
Observations	9	37
Hypothesized Mean Difference	0	
df	9	
t Stat	2.455783	
P(T<=t) one-tail	0.018205	
t Critical one-tail	2.821438	
P(T<=t) two-tail	0.03641	
t Critical two-tail	3.249836	

B.2.5 - Elastic Moduli 50% Strain

F-Test Two-Sample for Variances

	<i>Variable</i> <i>1</i>	<i>Variable</i> <i>2</i>
Mean	58.37404	39.6677
Variance	251.3527	114.9454
Observations	8	28
df	7	27
F	2.186713	
P(F<=f) one-tail	0.067879	
F Critical one-tail	2.373208	

t-Test: Two-Sample Assuming Equal Variances

	<i>Variable</i> <i>1</i>	<i>Variable</i> <i>2</i>
Mean	58.37404	39.6677
Variance	251.3527	114.9454
Observations	8	28
Pooled Variance	143.0293	
Hypothesized Mean Difference	0	
df	34	
t Stat	3.901657	
P(T<=t) one-tail	0.000214	
t Critical one-tail	1.690924	
P(T<=t) two-tail	0.000429	
t Critical two-tail	2.032245	

B.3 - Brain tissue and brain substitute materials comparison

B.3.1 - Peak stress of Brain vs Emulsion.

B.3.1.1 - 10% Strain

t-Test: Two-Sample Assuming Equal Variances

	<i>Variable</i> <i>1</i>	<i>Variable</i> <i>2</i>
Mean	0.743167	0.552698
Variance	0.011473	0.019516
Observations	10	37
Pooled Variance	0.017907	
Hypothesized Mean Difference	0	
df	45	
t Stat	3.993569	
P(T<=t) one-tail	0.000119	
t Critical one-tail	1.679427	
P(T<=t) two-tail	0.000238	
t Critical two-tail	2.014103	

B.3.1.2 - 20% Strain

t-Test: Two-Sample Assuming Equal Variances

	<i>Variable</i> <i>1</i>	<i>Variable</i> <i>2</i>
Mean	1.737977	1.50576
Variance	0.067859	0.061424
Observations	10	37
Pooled Variance	0.062711	
Hypothesized Mean Difference	0	
df	45	
t Stat	2.601809	
P(T<=t) one-tail	0.006254	
t Critical one-tail	1.679427	
P(T<=t) two-tail	0.012509	
t Critical two-tail	2.014103	

B.3.1.3 - 30% Strain

t-Test: Two-Sample Assuming Equal Variances

	<i>Variable</i> <i>1</i>	<i>Variable</i> <i>2</i>
Mean	3.504497	3.559384
Variance	0.367844	0.232168
Observations	10	37
Pooled Variance	0.259303	
Hypothesized Mean Difference	0	
df	45	
t Stat	-0.30242	
P(T<=t) one-tail	0.381861	
t Critical one-tail	1.679427	
P(T<=t) two-tail	0.763723	
t Critical two-tail	2.014103	

B.3.2 - Peak stress of Brain vs Hydrogel. (95% Confidence interval).

B.3.2.1 - 10% Strain

t-Test: Two-Sample Assuming Equal Variances

	<i>Variable</i> <i>1</i>	<i>Variable</i> <i>2</i>
Mean	0.488547	0.552698
Variance	0.003188	0.019516
Observations	10	37
Pooled Variance	0.01625	
Hypothesized Mean Difference	0	
df	45	
t Stat	-1.41198	
P(T<=t) one-tail	0.082417	
t Critical one-tail	1.679427	
P(T<=t) two-tail	0.164833	
t Critical two-tail	2.014103	

B.3.2.2 - 20% Strain

t-Test: Two-Sample Assuming Equal Variances

	<i>Variable</i> <i>1</i>	<i>Variable</i> <i>2</i>
Mean	1.300233	1.50576
Variance	0.020181	0.061424
Observations	10	37
Pooled Variance	0.053175	
Hypothesized Mean Difference	0	
df	45	
t Stat	-2.50073	
P(T<=t) one-tail	0.008051	
t Critical one-tail	1.679427	
P(T<=t) two-tail	0.016103	
t Critical two-tail	2.014103	

B.3.2.3 - 30% Strain

t-Test: Two-Sample Assuming Equal Variances

	<i>Variable</i> <i>1</i>	<i>Variable</i> <i>2</i>
Mean	3.192363	3.559384
Variance	0.140334	0.232168
Observations	10	37
Pooled Variance	0.213802	
Hypothesized Mean Difference	0	
df	45	
t Stat	-2.22709	
P(T<=t) one-tail	0.015494	
t Critical one-tail	1.679427	
P(T<=t) two-tail	0.030988	
t Critical two-tail	2.014103	

B.3.3 - Elastic moduli of Brain vs Emulsion. (95% Confidence interval).

B.3.3.1 - 10% Strain

t-Test: Two-Sample Assuming Equal Variances

	<i>Variable</i> <i>1</i>	<i>Variable</i> <i>2</i>
Mean	6.247723	5.526983
Variance	0.329757	1.951591
Observations	10	37
Pooled Variance	1.627224	
Hypothesized Mean Difference	0	
df	45	
t Stat	1.585284	
P(T<=t) one-tail	0.059953	
t Critical one-tail	1.679427	
P(T<=t) two-tail	0.119905	
t Critical two-tail	2.014103	

B.3.3.2 - 20% Strain

t-Test: Two-Sample Assuming Equal Variances

	<i>Variable</i> <i>1</i>	<i>Variable</i> <i>2</i>
Mean	9.948097	10.94653
Variance	2.43499	5.971868
Observations	10	37
Pooled Variance	5.264492	
Hypothesized Mean Difference	0	
df	45	
t Stat	-1.22093	
P(T<=t) one-tail	0.114235	
t Critical one-tail	1.679427	
P(T<=t) two-tail	0.22847	
t Critical two-tail	2.014103	

B.3.3.3 - 30% Strain

t-Test: Two-Sample Assuming Equal Variances

	<i>Variable</i> <i>1</i>	<i>Variable</i> <i>2</i>
Mean	17.6652	20.53624
Variance	12.28556	14.5639
Observations	10	37
Pooled Variance	14.10823	
Hypothesized Mean Difference	0	
df	45	
t Stat	-2.14464	
P(T<=t) one-tail	0.018709	
t Critical one-tail	1.679427	
P(T<=t) two-tail	0.037417	
t Critical two-tail	2.014103	

B.3.4 - Elastic moduli of Brain vs Hydrogel. (95% Confidence interval).

B.3.4.1 - 10% Strain

t-Test: Two-Sample Assuming Equal Variances

	<i>Variable</i> <i>1</i>	<i>Variable</i> <i>2</i>
Mean	4.885466	5.526983
Variance	0.31878	1.951591
Observations	10	37
Pooled Variance	1.625029	
Hypothesized Mean Difference	0	
df	45	
t Stat	-1.41198	
P(T<=t) one-tail	0.082417	
t Critical one-tail	1.679427	
P(T<=t) two-tail	0.164833	
t Critical two-tail	2.014103	

B.3.4.2 - 20% Strain

t-Test: Two-Sample Assuming Equal Variances

	<i>Variable</i> <i>1</i>	<i>Variable</i> <i>2</i>
Mean	9.295768	10.94653
Variance	1.204662	5.971868
Observations	10	37
Pooled Variance	5.018427	
Hypothesized Mean Difference	0	
df	45	
t Stat	-2.06753	
P(T<=t) one-tail	0.022232	
t Critical one-tail	1.679427	
P(T<=t) two-tail	0.044463	
t Critical two-tail	2.014103	

B.3.4.3 - 30% Strain

t-Test: Two-Sample Assuming Equal Variances

	<i>Variable</i> <i>1</i>	<i>Variable</i> <i>2</i>
Mean	16.38014	20.53624
Variance	4.885374	14.5639
Observations	10	37
Pooled Variance	12.6282	
Hypothesized Mean Difference	0	
df	45	
t Stat	-3.28146	
P(T<=t) one-tail	0.001	
t Critical one-tail	1.679427	
P(T<=t) two-tail	0.002	
t Critical two-tail	2.014103	

B.4 - Relaxation test

Time constants and their coefficients statistical analysis. Tukey- Kramer Analysis (95% Confidence interval).

H_0 : Material A = Material B

H_1 : Material A \neq Material B

B= Brain tissue, E= Emulsion, GC=Gelatin with Chromium, GA= Gelatin with Agarose

B.4.1 - G_1

Anova: Single Factor

SUMMARY

<i>Groups</i>	<i>Count</i>	<i>Sum</i>	<i>Average</i>	<i>Variance</i>
Column 1	5	2.6698	0.53396	0.0006
Column 2	5	1.5627	0.31254	0.001111
Column 3	4	1.5196	0.3799	0.001367
Column 4	5	1.2508	0.25016	0.000271
Column 5	5	1.825	0.365	0.000453

ANOVA

<i>Source of Variation</i>	<i>SS</i>	<i>df</i>	<i>MS</i>	<i>F</i>	<i>P-value</i>	<i>F crit</i>
Between Groups	0.223135	4	0.055784	76.57248	1.9E-11	2.895107
Within Groups	0.013842	19	0.000729			
Total	0.236976	23				

W_{ij}		Comparison	$Y_i - Y_j$	Reject H_0 ?
0.064337	B	E50%	0.22142	Y
0.068239	B	GC	0.15406	Y
0.064337	B	E35%	0.25016	Y
0.064337	B	GA	0.16896	Y
0.068239	E50%	GC	0.06736	N
0.064337	E50%	E35%	0.06238	N
0.064337	E50%	GA	0.05246	N
0.068239	GC	E35%	0.12974	Y
0.068239	GC	GA	0.0149	N
0.064337	E35%	GA	0.11484	Y

B.4.2 - τ_1

Anova: Single Factor

SUMMARY

Groups	Count	Sum	Average	Variance
Column 1	5	0.600458	0.120092	0.000178
Column 2	5	1.174731	0.234946	0.000123
Column 3	4	1.233165	0.308291	0.001032
Column 4	5	1.400758	0.280152	0.000513
Column 5	5	0.552567	0.110513	5.49E-05

ANOVA

Source of Variation	SS	df	MS	F	P-value	F crit
Between Groups	0.156012	4	0.039003	112.7981	5.84E-13	2.895107
Within Groups	0.00657	19	0.000346			
Total	0.162582	23				

W_{ij}		Comparison	$Y_i - Y_j$	Reject H_0 ?
0.044324	B	E50%	0.114855	Y
0.047013	B	GC	0.1882	Y
0.044324	B	E35%	0.280152	Y
0.044324	B	GA	0.009578	N
0.047013	E50%	GC	0.073345	Y
0.044324	E50%	E35%	0.044205	N
0.044324	E50%	GA	0.124433	Y
0.047013	GC	E35%	0.02814	N
0.047013	GC	GA	0.197778	Y
0.044324	E35%	GA	0.169638	Y

B.4.3 - G_2

Anova: Single Factor

SUMMARY

Groups	Count	Sum	Average	Variance
Column 1	5	0.9173	0.18346	3.48E-05
Column 2	5	0.4463	0.08926	0.000162
Column 3	4	0.6548	0.1637	0.002023
Column 4	5	0.40634	0.081268	0.000373
Column 5	5	0.8434	0.16868	0.000192

ANOVA

Source of Variation	SS	df	MS	F	P-value	F crit
Between Groups	0.045572	4	0.011393	23.74167	3.62E-07	2.895107
Within Groups	0.009118	19	0.00048			
Total	0.054689	23				

W_{ij}		Comparison	Yi-Yj	Reject Ho?
0.052216	B	E50%	0.0942	Y
0.055384	B	GC	0.01976	N
0.052216	B	E35%	0.081268	Y
0.052216	B	GA	0.01478	N
0.055384	E50%	GC	0.07444	Y
0.052216	E50%	E35%	0.007992	N
0.052216	E50%	GA	0.07942	Y
0.055384	GC	E35%	0.082432	Y
0.055384	GC	GA	0.00498	N
0.052216	E35%	GA	0.087412	Y

B.4.4 - τ_2

Anova: Single Factor

SUMMARY

Groups	Count	Sum	Average	Variance
Column 1	5	10.15684	2.031369	0.046829
Column 2	5	20.39386	4.078773	1.042421
Column 3	4	9.762288	2.440572	0.841202
Column 4	5	14.39937	2.879874	1.257253
Column 5	5	5.110804	1.022161	0.016071

ANOVA

Source of Variation	SS	df	MS	F	P-value	F crit
Between Groups	25.21508	4	6.30377	10.00273	0.000157	2.895107
Within Groups	11.9739	19	0.630205			
Total	37.18898	23				

W_{ij}		Comparison	Yi-Yj	Reject Ho?
1.89227	B	E50%	2.047404	Y
2.007056	B	GC	0.409203	N
1.89227	B	E35%	2.879874	Y
1.89227	B	GA	1.009208	N
2.007056	E50%	GC	1.638201	N
1.89227	E50%	E35%	1.198898	N
1.89227	E50%	GA	3.056612	Y
2.007056	GC	E35%	0.439302	N
2.007056	GC	GA	1.418411	N
1.89227	E35%	GA	1.857713	N

B.4.5 - G_3

Anova: Single Factor

SUMMARY

Groups	Count	Sum	Average	Variance
Column 1	5	0.49487	0.098974	9.52E-05
Column 2	5	0.5454	0.10908	3.1E-05
Column 3	4	0.221765	0.055441	6.39E-05
Column 4	5	0.43605	0.08721	0.000135
Column 5	5	0.22275	0.04455	2.7E-05

ANOVA

Source of Variation	SS	df	MS	F	P-value	F crit
Between Groups	0.014984	4	0.003746	52.86812	4.91E-10	2.895107
Within Groups	0.001346	19	7.09E-05			
Total	0.016331	23				

W_{ij}		Comparison	Yi-Yj	Reject Ho?
0.020065	B	E50%	0.010106	N
0.021282	B	GC	0.043533	Y
0.020065	B	E35%	0.08721	Y
0.020065	B	GA	0.054424	Y
0.021282	E50%	GC	0.053639	Y
0.021965	E50%	E35%	0.02187	N
0.020065	E50%	GA	0.06453	Y
0.021282	GC	E35%	0.031769	Y
0.021282	GC	GA	0.010891	N
0.020065	E35%	GA	0.04266	Y

B.4.6 - τ_3

Anova: Single Factor

SUMMARY

Groups	Count	Sum	Average	Variance
Column 1	5	107.8515	21.5703	0.561717
Column 2	5	187.6856	37.53712	6.516138
Column 3	4	101.1659	25.29147	39.17022
Column 4	5	219.9019	43.98038	10.26964
Column 5	5	171.7886	34.35771	19.60035

ANOVA

Source of Variation	SS	df	MS	F	P-value	F crit
Between Groups	1605.322	4	401.3304	28.74188	8E-08	2.895107
Within Groups	265.302	19	13.96326			
Total	1870.624	23				

W_{ij}	Comparison		Yi-Yj	Reject Ho?
8.907087	B	E50%	15.96682108	Y
9.447392	B	GC	3.721178025	N
8.907087	B	E35%	43.98037703	Y
8.907087	B	GA	12.78741675	Y
9.447392	E50%	GC	12.24564305	Y
8.907087	E50%	E35%	6.443259846	N
8.907087	E50%	GA	3.179404327	N
9.447392	GC	E35%	18.6889029	Y
9.447392	GC	GA	9.066238728	N
8.907087	E35%	GA	9.622664172	Y

B.4.7 - G_4

Anova: Single Factor

SUMMARY

Groups	Count	Sum	Average	Variance
Column 1	5	0.41063	0.082126	8.41E-05
Column 2	5	0.8774	0.17548	0.000189
Column 3	4	0.5418	0.13545	0.000224
Column 4	5	1.1743	0.23486	0.00018
Column 5	5	0.6685	0.1337	0.000105

ANOVA

Source of Variation	SS	df	MS	F	P-value	F crit
Between Groups	0.064242	4	0.016061	105.0541	1.11E-12	2.895107
Within Groups	0.002905	19	0.000153			
Total	0.067147	23				

W_{ij}		Comparison	Yi-Yj	Reject Ho?
0.029472	B	E50%	0.093354	Y
0.03126	B	GC	0.053324	Y
0.029472	B	E35%	0.23486	Y
0.029472	B	GA	0.051574	Y
0.03126	E50%	GC	0.04003	Y
0.029472	E50%	E35%	0.01938	N
0.029472	E50%	GA	0.04178	Y
0.03126	GC	E35%	0.09941	Y
0.03126	GC	GA	0.00175	N
0.029472	E35%	GA	0.10116	Y

B.4.8 - τ_4

Anova: Single Factor

SUMMARY

Groups	Count	Sum	Average	Variance
Column 1	5	1201.773	240.3547	125.0304
Column 2	5	1652.077	330.4153	565.4559
Column 3	4	2028.059	507.0147	5030.543
Column 4	5	2123.482	424.6965	1366.936
Column 5	5	2128.323	425.6645	2246.596

ANOVA

Source of Variation	SS	df	MS	F	P-value	F crit
Between Groups	194735.6	4	48683.89	28.63076	8.25E-08	2.895107
Within Groups	32307.7	19	1700.405			
Total	227043.3	23				

W_{ij}		Comparison	Yi-Yj	Reject Ho?
98.29206	B	E50%	90.06064	N
104.2545	B	GC	266.6601	Y
98.29206	B	E35%	424.6965	Y
98.29206	B	GA	185.3099	Y
104.2545	E50%	GC	176.5994	Y
98.29206	E50%	E35%	94.28117	N
98.29206	E50%	GA	95.24923	N
104.2545	GC	E35%	82.31828	N
104.2545	GC	GA	81.35021	N
98.29206	E35%	GA	0.968067	N

B.4.9 - G_5

Anova: Single Factor

SUMMARY

Groups	Count	Sum	Average	Variance
Column 1	5	0.91803	0.183606	9.58E-05
Column 2	5	2.4456	0.48912	0.001799
Column 3	4	1.603835	0.400959	0.004127
Column 4	5	2.83831	0.567662	0.000603
Column 5	5	2.10885	0.42177	0.000313

ANOVA

Source of Variation	SS	df	MS	F	P-value	F crit
Between Groups	0.412645	4	0.103161	82.97461	9.3E-12	2.895107
Within Groups	0.023622	19	0.001243			
Total	0.436268	23				

W_{ij}	Comparison		Yi-Yj	Reject Ho?
0.084048	B	E50%	0.305514	Y
0.089146	B	GC	0.217353	Y
0.084048	B	E35%	0.567662	Y
0.084048	B	GA	0.238164	Y
0.089146	E50%	GC	0.088161	N
0.084048	E50%	E35%	0.078542	N
0.084048	E50%	GA	0.06735	N
0.089146	GC	E35%	0.166703	Y
0.089146	GC	GA	0.020811	N
0.084048	E35%	GA	0.145892	Y

B.5 - Degradation Test (Mechanical characterization)

Mechanical Response of emulsion and hydrogel over time. ANOVA and Fisher's Least Significant Difference analysis (95% Confidence interval).

$H_0: T_a = \text{Material } T_b:$

$H_1: T_a \neq \text{Material } T_b:$

T1= 1 day, T2= 8 days, T3= 15 days, T4= 22 days, T5= 29 days.

B.5.1 - Frozen Emulsion

B.5.1.1 - Peak Stress at 10% Strain

Anova: Single Factor

SUMMARY

<i>Groups</i>	<i>Count</i>	<i>Sum</i>	<i>Average</i>	<i>Variance</i>
Row 1	10	4.623202	0.46232	0.006718
Row 2	10	3.947382	0.394738	0.005174
Row 3	10	2.724372	0.272437	0.006599
Row 4	10	3.808494	0.380849	0.006961
Row 5	10	4.924649	0.492465	0.022287

ANOVA

<i>Source of Variation</i>	<i>SS</i>	<i>df</i>	<i>MS</i>	<i>F</i>	<i>P-value</i>	<i>F crit</i>
Between Groups	0.290986818	4	0.072747	7.619187	8.92E-05	2.578739
Within Groups	0.429652362	45	0.009548			
Total	0.72063918	49				

LSD	Comparison	Yi-Yj	LDS	Reject Ho?	
0.088009	T1	T2	0.067582	0.088009	N
	T1	T3	0.180154	0.088009	Y
	T1	T4	0.081471	0.088009	N
	T1	T5	0.030145	0.088009	N
	T2	T3	0.112572	0.088009	Y
	T2	T4	0.013889	0.088009	N
	T2	T5	0.097727	0.088009	Y
	T3	T4	0.098683	0.088009	Y
	T3	T5	0.210299	0.088009	Y
	T4	T5	0.111616	0.088009	Y

B.5.1.2 - Peak stress at 20% Strain

Anova: Single Factor

SUMMARY

<i>Groups</i>	<i>Count</i>	<i>Sum</i>	<i>Average</i>	<i>Variance</i>
Row 1	10	10.65371	1.065371	0.030515
Row 2	10	8.975789	0.897579	0.022165
Row 3	10	6.131259	0.613126	0.031934
Row 4	10	8.605238	0.860524	0.037762
Row 5	10	10.88081	1.088081	0.086958

ANOVA

Source of Variation	SS	df	MS	F	P-value	F crit
Between Groups	1.464613705	4	0.366153	8.745624	2.6E-05	2.578739
Within Groups	1.884016907	45	0.041867			
Total	3.348630612	49				

LSD	Comparison	Yi-Yj	LDS	Reject Ho?
0.184294	T1 T2	0.167792	0.184294	N
	T1 T3	0.431753	0.184294	Y
	T1 T4	0.204848	0.184294	Y
	T1 T5	0.02271	0.184294	N
	T2 T3	0.26396	0.184294	Y
	T2 T4	0.037055	0.184294	N
	T2 T5	0.190502	0.184294	Y
	T3 T4	0.226905	0.184294	Y
	T3 T5	0.454463	0.184294	Y
	T4 T5	0.227557	0.184294	Y

B.5.1.3 - Peak Stress at 30% Strain

Anova: Single Factor

SUMMARY

Groups	Count	Sum	Average	Variance
Row 1	10	21.70853	2.170853	0.118012
Row 2	10	17.79761	1.779761	0.076172
Row 3	10	11.99531	1.199531	0.114519
Row 4	10	17.04524	1.704524	0.145121
Row 5	10	22.00902	2.200902	0.291594

ANOVA

<i>Source of Variation</i>	<i>SS</i>	<i>df</i>	<i>MS</i>	<i>F</i>	<i>P-value</i>	<i>F crit</i>
Between Groups	6.677251589	4	1.669313	11.19717	2.17E-06	2.578739
Within Groups	6.708757883	45	0.149084			
Total	13.38600947	49				

LSD	Comparison	Yi-Yj	LDS	Reject Ho?
0.347768	T1 T2	0.391093	0.347768	Y
	T1 T3	0.934074	0.347768	Y
	T1 T4	0.466329	0.347768	Y
	T1 T5	0.030048	0.347768	N
	T2 T3	0.542981	0.347768	Y
	T2 T4	0.075236	0.347768	N
	T2 T5	0.421141	0.347768	Y
	T3 T4	0.467745	0.347768	Y
	T3 T5	0.964122	0.347768	Y
	T4 T5	0.496377	0.347768	Y

B.5.1.4 - Elastic Moduli at 10% Strain

Anova: Single Factor

SUMMARY

<i>Groups</i>	<i>Count</i>	<i>Sum</i>	<i>Average</i>	<i>Variance</i>
Row 1	10	46.23202	4.623202	0.671842
Row 2	10	39.47382	3.947382	0.517389
Row 3	10	27.24372	2.724372	0.659887
Row 4	10	38.08494	3.808494	0.696127
Row 5	10	49.24649	4.924649	2.22867

ANOVA

<i>Source of Variation</i>	<i>SS</i>	<i>df</i>	<i>MS</i>	<i>F</i>	<i>P-value</i>	<i>F crit</i>
Between Groups	29.09868	4	7.27467	7.619187	8.92E-05	2.578739
Within Groups	42.96524	45	0.954783			
Total	72.06392	49				

LSD	Comparison	Yi-Yj	LDS	Reject Ho?
0.880089	T1 T2	0.67582	0.880089	N
	T1 T3	1.801541	0.880089	Y
	T1 T4	0.814708	0.880089	N
	T1 T5	0.301447	0.880089	N
	T2 T3	1.125721	0.880089	Y
	T2 T4	0.138889	0.880089	N
	T2 T5	0.977266	0.880089	Y
	T3 T4	0.986832	0.880089	Y
	T3 T5	2.102987	0.880089	Y
	T4 T5	1.116155	0.880089	Y

B.5.1.5 - Elastic Moduli at 20% Strain

Anova: Single Factor

SUMMARY

<i>Groups</i>	<i>Count</i>	<i>Sum</i>	<i>Average</i>	<i>Variance</i>
Row 1	10	60.30511	6.030511	0.882249
Row 2	10	50.28407	5.028407	0.606529
Row 3	10	34.06887	3.406887	0.954884
Row 4	10	47.96744	4.796744	1.237296
Row 5	10	59.56163	5.956163	2.288933

ANOVA

<i>Source of Variation</i>	<i>SS</i>	<i>df</i>	<i>MS</i>	<i>F</i>	<i>P-value</i>	<i>F crit</i>
Between Groups	45.46764	4	11.36691	9.520196	1.15E-05	2.578739
Within Groups	53.72904	45	1.193979			
Total	99.19668	49				

LSD	Comparison	Yi-Yj	LDS	Reject Ho?
0.984176	T1	T2	1.002105	0.984176 Y
	T1	T3	2.515987	0.984176 Y
	T1	T4	1.233767	0.984176 Y
	T1	T5	0.074348	0.984176 N
	T2	T3	1.513882	0.984176 Y
	T2	T4	0.231662	0.984176 N
	T2	T5	0.927757	0.984176 N
	T3	T4	1.28222	0.984176 Y
	T3	T5	2.441638	0.984176 Y
	T4	T5	1.159419	0.984176 Y

B.5.1.6 - Elastic Moduli at 30% Strain

Anova: Single Factor

SUMMARY

<i>Groups</i>	<i>Count</i>	<i>Sum</i>	<i>Average</i>	<i>Variance</i>
Row 1	10	110.5482	11.05482	2.880707
Row 2	10	88.21818	8.821818	1.638171
Row 3	10	58.6405	5.86405	2.568464
Row 4	10	84.40005	8.440005	3.520229
Row 5	10	111.282	11.1282	6.089374

ANOVA

<i>Source of Variation</i>	<i>SS</i>	<i>df</i>	<i>MS</i>	<i>F</i>	<i>P-value</i>	<i>F crit</i>
Between Groups	189.1199	4	47.27996	14.15827	1.48E-07	2.578739
Within Groups	150.2725	45	3.339389			
Total	339.3924	49				

LSD	Comparison	Yi-Yj	LDS	Reject Ho?
1.645917	T1	T2	2.233003	1.645917 Y
	T1	T3	5.023216	0.088009 Y
	T1	T4	2.614816	0.088009 Y
	T1	T5	0.073382	0.088009 N
	T2	T3	2.790212	0.088009 Y
	T2	T4	0.381813	0.088009 Y
	T2	T5	2.306385	0.088009 Y
	T3	T4	2.408399	0.088009 Y
	T3	T5	5.096598	0.088009 Y
	T4	T5	2.688198	0.088009 Y

B.5.2 - Non-Frozen Emulsion

B.5.2.1 - Peak Stress at 10% Strain

Anova: Single Factor

SUMMARY

Groups	Count	Sum	Average	Variance
Row 1	9	4.156903	0.461878	0.011885
Row 2	10	6.693581	0.669358	0.016443
Row 3	11	6.226432	0.566039	0.024776
Row 4	11	7.354447	0.668586	0.04986
Row 5	11	6.87283	0.624803	0.022208

ANOVA

Source of Variation	SS	df	MS	F	P-value	F crit
Between Groups	0.290794	4	0.072698	2.820325	0.035364	2.56954
Within Groups	1.211501	47	0.025777			
Total	1.502294	51				

LSD	Comparison	Yi-Yj	LDS	Reject Ho?
0.148421	T1 T2	0.20748	0.148421	Y
0.145191	T1 T3	0.104161	0.145191	N
0.145191	T1 T4	0.206708	0.145191	Y
0.145191	T1 T5	0.162925	0.145191	Y
0.141141	T2 T3	0.103319	0.141141	N
0.141141	T2 T4	0.000772	0.141141	N
0.141141	T2 T5	0.044555	0.141141	N
0.13774	T3 T4	0.102547	0.13774	N
0.13774	T3 T5	0.058763	0.13774	N
0.13774	T4 T5	0.043783	0.13774	N

B.5.2.2 - Peak stress at 20% Strain

Anova: Single Factor

SUMMARY

<i>Groups</i>	<i>Count</i>	<i>Sum</i>	<i>Average</i>	<i>Variance</i>
Row 1	9	9.472084	1.052454	0.072263
Row 2	11	14.07569	1.279609	0.137231
Row 3	11	14.89632	1.354211	0.159097
Row 4	11	17.15959	1.559963	0.24461
Row 5	11	16.03942	1.458129	0.114914

ANOVA

<i>Source of Variation</i>	<i>SS</i>	<i>df</i>	<i>MS</i>	<i>F</i>	<i>P-value</i>	<i>F crit</i>
Between Groups	1.46488	4	0.36622	2.463145	0.057615	2.565241
Within Groups	7.136632	48	0.14868			
Total	8.601511	52				

LSD	Comparison	Yi-Yj	LDS	Reject Ho?
0.148421	T1 T2	0.227155	0.148421	Y
0.145191	T1 T3	0.301757	0.145191	Y
0.145191	T1 T4	0.507509	0.145191	Y
0.145191	T1 T5	0.405675	0.145191	Y
0.141141	T2 T3	0.074603	0.141141	N
0.141141	T2 T4	0.280355	0.141141	Y
0.141141	T2 T5	0.17852	0.141141	Y
0.13774	T3 T4	0.205752	0.13774	Y
0.13774	T3 T5	0.103918	0.13774	N
0.13774	T4 T5	0.101834	0.13774	N

B.5.2.3 - Peak Stress at 30% Strain

Anova: Single Factor

SUMMARY

<i>Groups</i>	<i>Count</i>	<i>Sum</i>	<i>Average</i>	<i>Variance</i>
Row 1	9	19.08772	2.120858	0.33024
Row 2	10	29.03433	2.903433	0.252991
Row 3	11	28.08105	2.552822	0.534773
Row 4	11	35.88749	3.262499	0.940846
Row 5	11	32.81605	2.983278	0.46732

ANOVA

<i>Source of Variation</i>	<i>SS</i>	<i>df</i>	<i>MS</i>	<i>F</i>	<i>P-value</i>	<i>F crit</i>
Between Groups	7.64337	4	1.910843	3.688547	0.010818	2.56954
Within Groups	24.34824	47	0.518048			
Total	31.99161	51				

LSD	Comparison	Yi-Yj	LDS	Reject Ho?
0.148421	T1 T2	0.782575	0.148421	Y
0.145191	T1 T3	0.431965	0.145191	Y
0.145191	T1 T4	1.141642	0.145191	Y
0.145191	T1 T5	0.86242	0.145191	Y
0.141141	T2 T3	0.350611	0.141141	Y
0.141141	T2 T4	0.359066	0.141141	Y
0.141141	T2 T5	0.079845	0.141141	N
0.13774	T3 T4	0.709677	0.13774	Y
0.13774	T3 T5	0.430455	0.13774	Y
0.13774	T4 T5	0.279222	0.13774	Y

B.5.2.4 - Elastic Moduli at 10% Strain

Anova: Single Factor

SUMMARY

<i>Groups</i>	<i>Count</i>	<i>Sum</i>	<i>Average</i>	<i>Variance</i>
Row 1	9	41.56903	4.618781	1.188472
Row 2	10	66.93581	6.693581	1.644276
Row 3	11	62.26432	5.660393	2.477582
Row 4	11	73.54447	6.685861	4.985977
Row 5	11	68.7283	6.248028	2.22082

ANOVA

<i>Source of Variation</i>	<i>SS</i>	<i>df</i>	<i>MS</i>	<i>F</i>	<i>P-value</i>	<i>F crit</i>
Between Groups	29.07937	4	7.269842	2.820325	0.035364	2.56954
Within Groups	121.1501	47	2.577661			
Total	150.2294	51				

LSD	Comparison	Yi-Yj	LDS	Reject Ho?
0.148421	T1 T2	2.074799	0.148421	Y
0.145191	T1 T3	1.041612	0.145191	Y
0.145191	T1 T4	2.06708	0.145191	Y
0.145191	T1 T5	1.629247	0.145191	Y
0.141141	T2 T3	1.033187	0.141141	Y
0.141141	T2 T4	0.00772	0.141141	N
0.141141	T2 T5	0.445553	0.141141	Y
0.13774	T3 T4	1.025468	0.13774	Y
0.13774	T3 T5	0.587635	0.13774	Y
0.13774	T4 T5	0.437833	0.13774	Y

B.5.2.5 - Elastic Moduli at 20% Strain

Anova: Single Factor

SUMMARY

<i>Groups</i>	<i>Count</i>	<i>Sum</i>	<i>Average</i>	<i>Variance</i>
Row 1	9	53.15181	5.905757	2.56084
Row 2	10	81.61865	8.161865	2.177667
Row 3	11	78.49261	7.135692	4.572388
Row 4	11	98.05148	8.913771	7.402357
Row 5	11	91.66587	8.333261	3.652901

ANOVA

<i>Source of Variation</i>	<i>SS</i>	<i>df</i>	<i>MS</i>	<i>F</i>	<i>P-value</i>	<i>F crit</i>
Between Groups	55.09864	4	13.77466	3.297015	0.018392	2.56954
Within Groups	196.3622	47	4.177919			
Total	251.4608	51				

LSD	Comparison	Yi-Yj	LDS	Reject Ho?
0.148421	T1 T2	2.256108	0.148421	Y
0.145191	T1 T3	1.229935	0.145191	Y
0.145191	T1 T4	3.008014	0.145191	Y
0.145191	T1 T5	2.427504	0.145191	Y
0.141141	T2 T3	1.026173	0.141141	Y
0.141141	T2 T4	0.751905	0.141141	Y
0.141141	T2 T5	0.171396	0.141141	Y
0.13774	T3 T4	1.778078	0.13774	Y
0.13774	T3 T5	1.197569	0.13774	Y
0.13774	T4 T5	0.58051	0.13774	Y

B.5.2.6 - Elastic Moduli at 30% Strain

Anova: Single Factor

SUMMARY

<i>Groups</i>	<i>Count</i>	<i>Sum</i>	<i>Average</i>	<i>Variance</i>
Row 1	9	96.15634	10.68404	9.403858
Row 2	10	141.7888	14.17888	5.348966
Row 3	11	140.0535	12.73214	13.13268
Row 4	11	187.279	17.02536	22.78025
Row 5	11	167.7664	15.25149	12.33433

ANOVA

<i>Source of Variation</i>	<i>SS</i>	<i>df</i>	<i>MS</i>	<i>F</i>	<i>P-value</i>	<i>F crit</i>
Between Groups	234.3826	4	58.59565	4.545716	0.003471	2.56954
Within Groups	605.8441	47	12.8903			
Total	840.2267	51				

LSD	Comparison	Yi-Yj	LDS	Reject Ho?
0.148421	T1 T2	3.494846	0.148421	Y
0.145191	T1 T3	2.048101	0.145191	Y
0.145191	T1 T4	6.341322	0.145191	Y
0.145191	T1 T5	4.567449	0.145191	Y
0.141141	T2 T3	1.446746	0.141141	Y
0.141141	T2 T4	2.846476	0.141141	Y
0.141141	T2 T5	1.072603	0.141141	Y
0.13774	T3 T4	4.293221	0.13774	Y
0.13774	T3 T5	2.519349	0.13774	Y
0.13774	T4 T5	1.773873	0.13774	Y

B.5.3 - Frozen Hydrogel

B.5.3.1 - Peak Stress at 10% Strain

Anova: Single Factor

SUMMARY

	<i>Groups</i>	<i>Count</i>	<i>Sum</i>	<i>Average</i>	<i>Variance</i>
Row 1		5	1.855334	0.371067	0.001763
Row 2		6	2.509933	0.418322	0.007386
Row 3		8	2.298422	0.287303	0.002627
Row 4		7	2.936288	0.41947	0.000991
Row 5		4	1.798275	0.449569	0.001285

ANOVA

<i>Source of Variation</i>	<i>SS</i>	<i>df</i>	<i>MS</i>	<i>F</i>	<i>P-value</i>	<i>F crit</i>
Between Groups	0.108217	4	0.027054	9.371898	9.04E-05	2.75871
Within Groups	0.072169	25	0.002887			
Total	0.180386	29				

LSD	Comparison	Yi-Yj	LDS	Reject Ho?
0.06702	T1 T2	0.047255	0.06702	N
0.063098	T1 T3	0.083764	0.063098	Y
0.064808	T1 T4	0.048403	0.064808	N
0.074247	T1 T5	0.078502	0.074247	Y
0.059774	T2 T3	0.131019	0.059774	Y
0.061577	T2 T4	0.001148	0.061577	N
0.071444	T2 T5	0.031247	0.071444	N
0.057283	T3 T4	0.132167	0.057283	Y
0.067778	T3 T5	0.162266	0.067778	Y
0.069373	T4 T5	0.030099	0.069373	N

B.5.3.2 - Peak stress at 20% Strain

Anova: Single Factor

SUMMARY

<i>Groups</i>	<i>Count</i>	<i>Sum</i>	<i>Average</i>	<i>Variance</i>
Row 1	5	3.902253	0.780451	0.00559
Row 2	6	5.60476	0.934127	0.066721
Row 3	8	5.094074	0.636759	0.010636
Row 4	7	7.092753	1.01325	0.006151
Row 5	4	3.720995	0.930249	0.012604

ANOVA

<i>Source of Variation</i>	<i>SS</i>	<i>df</i>	<i>MS</i>	<i>F</i>	<i>P-value</i>	<i>F crit</i>
Between Groups	0.642495	4	0.160624	7.949541	0.000281	2.75871
Within Groups	0.505135	25	0.020205			
Total	1.14763	29				

LSD	Comparison	Yi-Yj	LDS	Reject Ho?
0.06702	T1	T2	0.153676	0.06702 Y
0.063098	T1	T3	0.143691	0.063098 Y
0.064808	T1	T4	0.2328	0.064808 Y
0.074247	T1	T5	0.149798	0.074247 Y
0.059774	T2	T3	0.297367	0.059774 Y
0.061577	T2	T4	0.079124	0.061577 Y
0.071444	T2	T5	0.003878	0.071444 N
0.057283	T3	T4	0.376491	0.057283 Y
0.067778	T3	T5	0.29349	0.067778 Y
0.069373	T4	T5	0.083002	0.069373 Y

B.5.3.3 - Peak Stress at 30% Strain

Anova: Single Factor

SUMMARY

<i>Groups</i>	<i>Count</i>	<i>Sum</i>	<i>Average</i>	<i>Variance</i>
Row 1	5	7.337697	1.467539	0.021307
Row 2	6	11.61864	1.936441	0.661632
Row 3	8	9.5413	1.192662	0.061098
Row 4	7	14.00803	2.001147	0.014852
Row 5	4	6.470626	1.617657	0.083048

ANOVA

<i>Source of Variation</i>	<i>SS</i>	<i>df</i>	<i>MS</i>	<i>F</i>	<i>P-value</i>	<i>F crit</i>
Between Groups	3.190181	4	0.797545	4.793716	0.005218	2.75871
Within Groups	4.159327	25	0.166373			
Total	7.349508	29				

LSD	Comparison	Yi-Yj	LDS	Reject Ho?
0.06702	T1 T2	0.468901	0.06702	Y
0.063098	T1 T3	0.274877	0.063098	Y
0.064808	T1 T4	0.533608	0.064808	Y
0.074247	T1 T5	0.150117	0.074247	Y
0.059774	T2 T3	0.743778	0.059774	Y
0.061577	T2 T4	0.064706	0.061577	Y
0.071444	T2 T5	0.318784	0.071444	Y
0.057283	T3 T4	0.808484	0.057283	Y
0.067778	T3 T5	0.424994	0.067778	Y
0.069373	T4 T5	0.38349	0.069373	Y

B.5.3.4 - Elastic Moduli at 10% Strain

Anova: Single Factor

SUMMARY

<i>Groups</i>	<i>Count</i>	<i>Sum</i>	<i>Average</i>	<i>Variance</i>
Row 1	5	18.55334	3.710668	0.17631
Row 2	6	25.09933	4.183222	0.73857
Row 3	8	22.98422	2.873027	0.26267
Row 4	7	29.36288	4.194697	0.099073
Row 5	4	17.98275	4.495688	0.128545

ANOVA

<i>Source of Variation</i>	<i>SS</i>	<i>df</i>	<i>MS</i>	<i>F</i>	<i>P-value</i>	<i>F crit</i>
Between Groups	10.8217	4	2.705426	9.371898	9.04E-05	2.75871
Within Groups	7.216858	25	0.288674			
Total	18.03856	29				

<i>LSD</i>	<i>Comparison</i>	<i>Yi-Yj</i>	<i>LDS</i>	<i>Reject Ho?</i>
0.06702	T1	T2	0.472553	0.06702 Y
0.063098	T1	T3	0.837641	0.063098 Y
0.064808	T1	T4	0.484029	0.064808 Y
0.074247	T1	T5	0.78502	0.074247 Y
0.059774	T2	T3	1.310195	0.059774 Y
0.061577	T2	T4	0.011476	0.061577 N
0.071444	T2	T5	0.312466	0.071444 Y
0.057283	T3	T4	1.32167	0.057283 Y
0.067778	T3	T5	1.622661	0.067778 Y
0.069373	T4	T5	0.300991	0.069373 Y

B.5.3.5 - Elastic Moduli at 20% Strain

Anova: Single Factor

SUMMARY

<i>Groups</i>	<i>Count</i>	<i>Sum</i>	<i>Average</i>	<i>Variance</i>
Row 1	5	20.46918	4.093837	0.153762
Row 2	6	30.94827	5.158045	3.042965
Row 3	8	27.95653	3.494566	0.304512
Row 4	7	41.56465	5.937807	0.243558
Row 5	4	19.2272	4.806801	1.030908

ANOVA

<i>Source of Variation</i>	<i>SS</i>	<i>df</i>	<i>MS</i>	<i>F</i>	<i>P-value</i>	<i>F crit</i>
Between Groups	25.46817	4	6.367043	7.069614	0.000596	2.75871
Within Groups	22.51552	25	0.900621			
Total	47.98369	29				

LSD	Comparison	Yi-Yj	LDS	Reject Ho?
0.06702	T1	T2	1.064208	0.06702 Y
0.063098	T1	T3	0.599271	0.063098 Y
0.064808	T1	T4	1.84397	0.064808 Y
0.074247	T1	T5	0.712964	0.074247 Y
0.059774	T2	T3	1.663479	0.059774 Y
0.061577	T2	T4	0.779762	0.061577 Y
0.071444	T2	T5	0.351244	0.071444 Y
0.057283	T3	T4	2.443241	0.057283 Y
0.067778	T3	T5	1.312235	0.067778 Y
0.069373	T4	T5	1.131007	0.069373 Y

B.5.3.6 - Elastic Moduli at 30% Strain

Anova: Single Factor

SUMMARY

<i>Groups</i>	<i>Count</i>	<i>Sum</i>	<i>Average</i>	<i>Variance</i>
Row 1	5	34.35444	6.870888	0.581421
Row 2	6	60.13883	10.02314	31.23344
Row 3	8	44.47225	5.559032	2.319484
Row 4	7	69.15275	9.878965	0.31062
Row 5	4	27.49631	6.874076	3.221844

ANOVA

<i>Source of Variation</i>	<i>SS</i>	<i>df</i>	<i>MS</i>	<i>F</i>	<i>P-value</i>	<i>F crit</i>
Between Groups	107.7429	4	26.93574	3.615369	0.018569	2.75871
Within Groups	186.2585	25	7.450342			
Total	294.0015	29				

LSD	Comparison	Yi-Yj	LDS	Reject Ho?
0.06702	T1 T2	3.152251	0.06702	Y
0.063098	T1 T3	1.311856	0.063098	Y
0.064808	T1 T4	3.008077	0.064808	Y
0.074247	T1 T5	0.003189	0.074247	N
0.059774	T2 T3	4.464108	0.059774	Y
0.061577	T2 T4	0.144175	0.061577	Y
0.071444	T2 T5	3.149063	0.071444	Y
0.057283	T3 T4	4.319933	0.057283	Y
0.067778	T3 T5	1.315045	0.067778	Y
0.069373	T4 T5	3.004888	0.069373	Y

B.5.4 - Non-Frozen Hydrogel

B.5.4.1 - Peak Stress at 10% Strain

Anova: Single Factor

SUMMARY

Groups	Count	Sum	Average	Variance
Row 1	10	4.907744	0.490774	0.001398
Row 2	10	2.496182	0.249618	0.000837
Row 3	10	5.804412	0.580441	0.002312
Row 4	10	6.450853	0.645085	0.003698
Row 5	10	5.139498	0.51395	0.002371

ANOVA

Source of Variation	SS	df	MS	F	P-value	F crit
Between Groups	0.904102	4	0.226026	106.4647	2.44E-22	2.578739
Within Groups	0.095535	45	0.002123			
Total	0.999638	49				

LSD	Comparison	Yi-Yj	LDS	Reject Ho?
0.0415	T1 T2	0.241156	0.0415	Y
	T1 T3	0.089667	0.0415	Y
	T1 T4	0.154311	0.0415	Y
	T1 T5	0.023175	0.0415	N
	T2 T3	0.330823	0.0415	Y
	T2 T4	0.395467	0.0415	Y
	T2 T5	0.264332	0.0415	Y
	T3 T4	0.064644	0.0415	Y
	T3 T5	0.066491	0.0415	Y
	T4 T5	0.131135	0.0415	Y

B.5.4.2 - Peak stress at 20% Strain

Anova: Single Factor

SUMMARY

<i>Groups</i>	<i>Count</i>	<i>Sum</i>	<i>Average</i>	<i>Variance</i>
Row 1	10	12.18388	1.218388	0.00997
Row 2	10	6.133538	0.613354	0.008587
Row 3	10	14.38174	1.438174	0.018133
Row 4	10	16.5033	1.65033	0.03367
Row 5	10	12.98906	1.298906	0.019526

ANOVA

<i>Source of Variation</i>	<i>SS</i>	<i>df</i>	<i>MS</i>	<i>F</i>	<i>P-value</i>	<i>F crit</i>
Between Groups	6.04193	4	1.510483	84.02176	2.77E-20	2.578739
Within Groups	0.808977	45	0.017977			
Total	6.850908	49				

LSD	Comparison	Yi-Yj	LDS	Reject Ho?
0.120764	T1 T2	0.605034	0.120764	Y
	T1 T3	0.219786	0.120764	Y
	T1 T4	0.431942	0.120764	Y
	T1 T5	0.080518	0.120764	N
	T2 T3	0.824821	0.120764	Y
	T2 T4	1.036976	0.120764	Y
	T2 T5	0.685552	0.120764	Y
	T3 T4	0.212156	0.120764	Y
	T3 T5	0.139268	0.120764	Y
	T4 T5	0.351424	0.120764	Y

B.5.4.3 - Peak Stress at 30% Strain

Anova: Single Factor

SUMMARY

<i>Groups</i>	<i>Count</i>	<i>Sum</i>	<i>Average</i>	<i>Variance</i>
Row 1	10	26.19898	2.619898	0.044202
Row 2	10	12.69334	1.269334	0.050325
Row 3	10	30.39255	3.039255	0.112883
Row 4	10	36.43264	3.643264	0.247668
Row 5	10	28.06292	2.806292	0.130582

ANOVA

<i>Source of Variation</i>	<i>SS</i>	<i>df</i>	<i>MS</i>	<i>F</i>	<i>P-value</i>	<i>F crit</i>
Between Groups	30.66386	4	7.665964	65.44723	3.54E-18	2.578739
Within Groups	5.270939	45	0.117132			
Total	35.9348	49				

LSD	Comparison	Yi-Yj	LDS	Reject Ho?
0.308256	T1 T2	1.350564	0.308256	Y
	T1 T3	0.419357	0.308256	Y
	T1 T4	1.023366	0.308256	Y
	T1 T5	0.186394	0.308256	N
	T2 T3	1.769921	0.308256	Y
	T2 T4	2.37393	0.308256	Y
	T2 T5	1.536958	0.308256	Y
	T3 T4	0.604009	0.308256	Y
	T3 T5	0.232963	0.308256	N
	T4 T5	0.836972	0.308256	Y

B.5.4.4 - Elastic Moduli at 10% Strain

Anova: Single Factor

SUMMARY

<i>Groups</i>	<i>Count</i>	<i>Sum</i>	<i>Average</i>	<i>Variance</i>
Row 1	10	49.07744	4.907744	0.139817
Row 2	10	24.96182	2.496182	0.083656
Row 3	10	58.04412	5.804412	0.231202
Row 4	10	64.50853	6.450853	0.369769
Row 5	10	51.39498	5.139498	0.237061

ANOVA

<i>Source of Variation</i>	<i>SS</i>	<i>df</i>	<i>MS</i>	<i>F</i>	<i>P-value</i>	<i>F crit</i>
Between Groups	90.41022	4	22.60256	106.4647	2.44E-22	2.578739
Within Groups	9.553544	45	0.212301			
Total	99.96377	49				

LSD	Comparison	Yi-Yj	LDS	Reject Ho?
0.415002	T1 T2	2.411561	0.415002	Y
	T1 T3	0.896669	0.415002	Y
	T1 T4	1.543109	0.415002	Y
	T1 T5	0.231755	0.415002	N
	T2 T3	3.30823	0.415002	Y
	T2 T4	3.95467	0.415002	Y
	T2 T5	2.643316	0.415002	Y
	T3 T4	0.64644	0.415002	Y
	T3 T5	0.664914	0.415002	Y
	T4 T5	1.311354	0.415002	Y

B.5.4.5 - Elastic Moduli at 20% Strain

Anova: Single Factor

SUMMARY

Groups	Count	Sum	Average	Variance
Row 1	10	72.76139	7.276139	0.418047
Row 2	10	36.37356	3.637356	0.434003
Row 3	10	85.77331	8.577331	0.772091
Row 4	10	100.5245	10.05245	1.52431
Row 5	10	78.49565	7.849565	0.925541

ANOVA

Source of Variation	SS	df	MS	F	P-value	F crit
Between Groups	227.6567	4	56.91418	69.85062	1.02E-18	2.578739
Within Groups	36.66593	45	0.814798			
Total	264.3226	49				

LSD	Comparison	Yi-Yj	LDS	Reject Ho?
0.813017	T1 T2	3.638783	0.813017	Y
	T1 T3	1.301192	0.813017	Y
	T1 T4	2.776311	0.813017	Y
	T1 T5	0.573426	0.813017	N
	T2 T3	4.939975	0.813017	Y
	T2 T4	6.415093	0.813017	Y
	T2 T5	4.212208	0.813017	Y
	T3 T4	1.475119	0.813017	Y
	T3 T5	0.727766	0.813017	N
	T4 T5	2.202885	0.813017	Y

B.5.4.6 - Elastic Moduli at 30% Strain

Anova: Single Factor

SUMMARY

<i>Groups</i>	<i>Count</i>	<i>Sum</i>	<i>Average</i>	<i>Variance</i>
Row 1	10	140.151	14.0151	1.309065
Row 2	10	65.59804	6.559804	1.782432
Row 3	10	160.1081	16.01081	4.190391
Row 4	10	199.2934	19.92934	10.21783
Row 5	10	150.7385	15.07385	5.082321

ANOVA

<i>Source of Variation</i>	<i>SS</i>	<i>df</i>	<i>MS</i>	<i>F</i>	<i>P-value</i>	<i>F crit</i>
Between Groups	952.0542	4	238.0135	52.69973	2.04E-16	2.578739
Within Groups	203.2384	45	4.516409			
Total	1155.293	49				

LSD	Comparison	Yi-Yj	LDS	Reject Ho?
1.914128	T1 T2	7.455294	1.914128	Y
	T1 T3	1.995712	0.0415	Y
	T1 T4	5.914242	0.0415	Y
	T1 T5	1.058757	0.0415	Y
	T2 T3	9.451006	0.0415	Y
	T2 T4	13.36954	0.0415	Y
	T2 T5	8.514051	0.0415	Y
	T3 T4	3.918531	0.0415	Y
	T3 T5	0.936954	0.0415	Y
	T4 T5	4.855485	0.0415	Y

B.6 - Degradation Test – Emulsion Weight loss

Anova: Single Factor

SUMMARY

<i>Groups</i>	<i>Count</i>	<i>Sum</i>	<i>Average</i>	<i>Variance</i>
Column 1	7	17.80193	2.543133	0.375049
Column 2	7	11.87295	1.696135	0.358309
Column 3	7	13.93952	1.99136	0.441678
Column 4	7	13.133	1.876142	0.329983
Column 5	7	13.47223	1.924604	0.111605

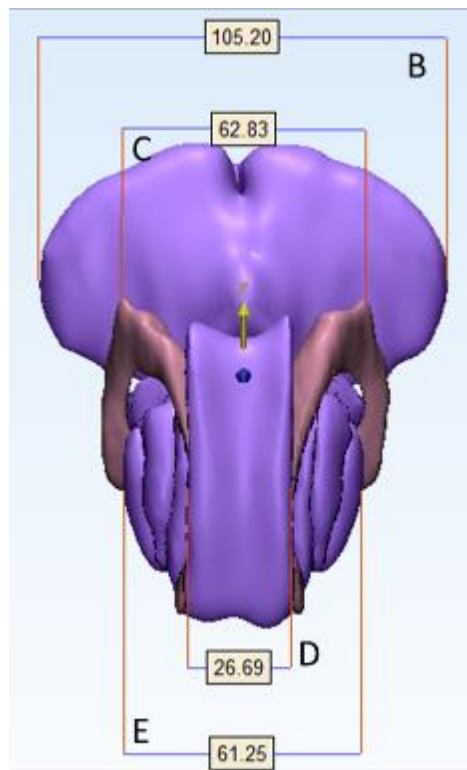
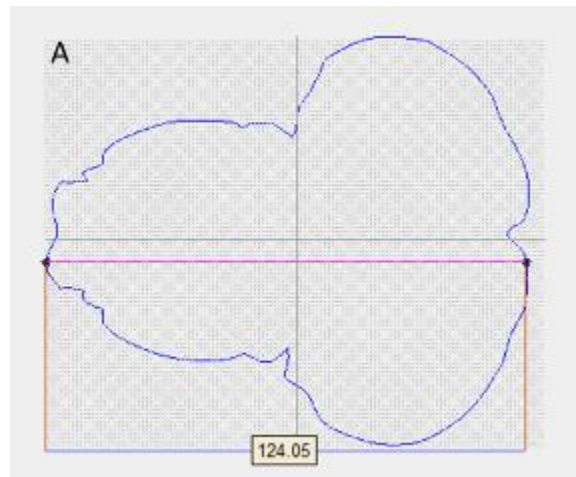
ANOVA

<i>Source of Variation</i>	<i>SS</i>	<i>df</i>	<i>MS</i>	<i>F</i>	<i>P-value</i>	<i>F crit</i>
Between Groups	2.857616	4	0.714404	2.209554	0.091772	2.689628
Within Groups	9.699746	30	0.323325			
Total	12.55736	34				

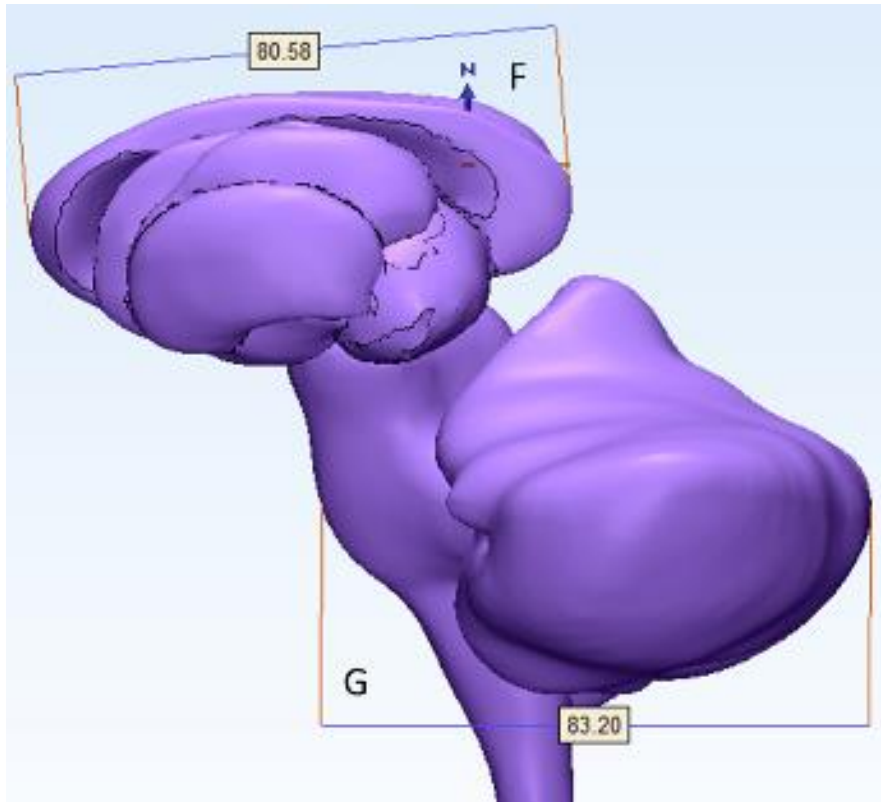
APPENDIX C

DEFINITION OF MEASUREMENTS FOR 3D MODELS

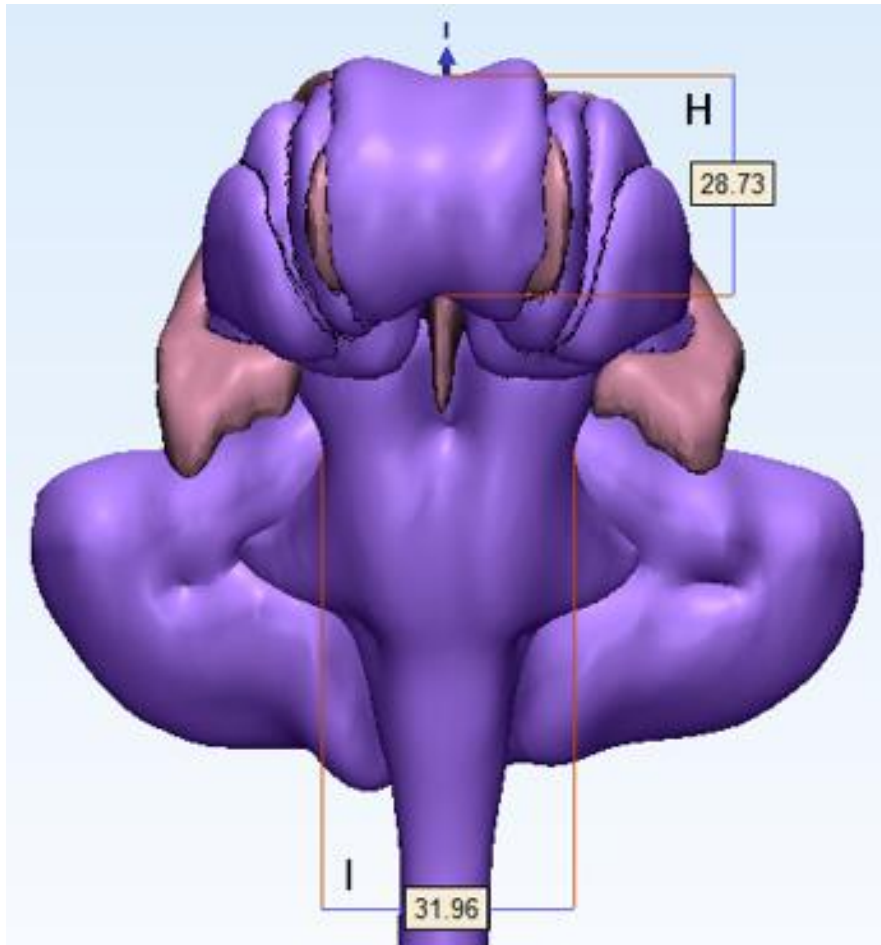
C.1 - Internal Structures Axial Plane Measurements A, B, C, D and E.



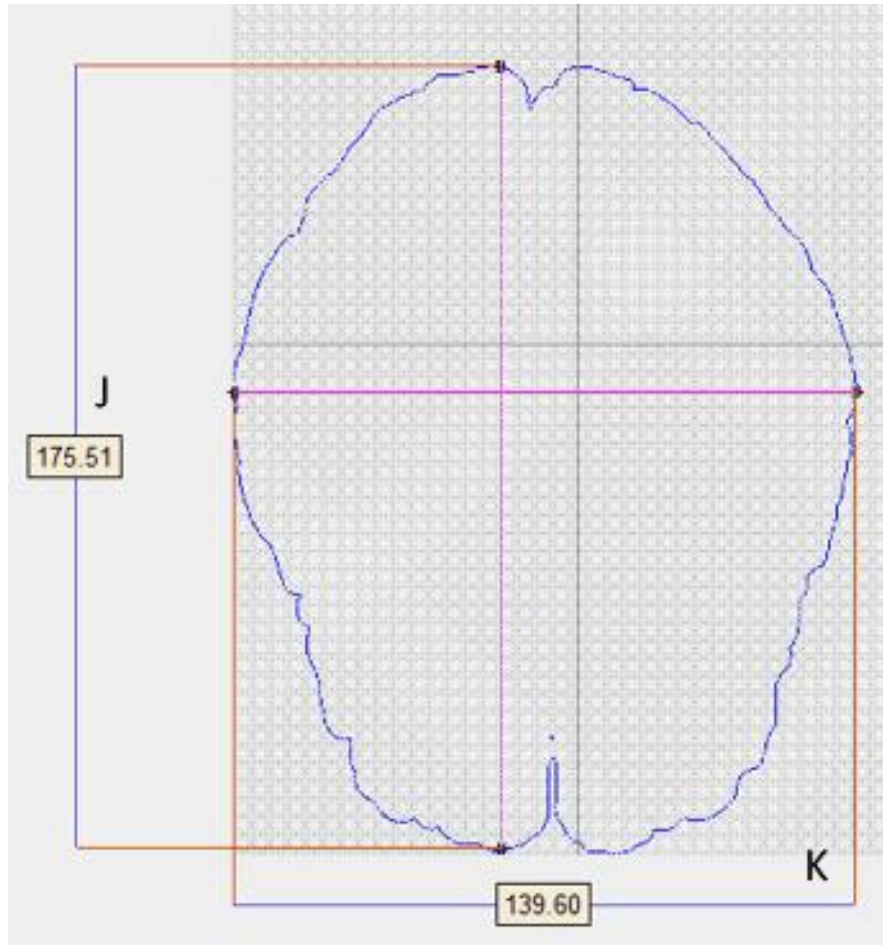
C.2 - Internal Structures Sagittal Plane Measurements F and G.



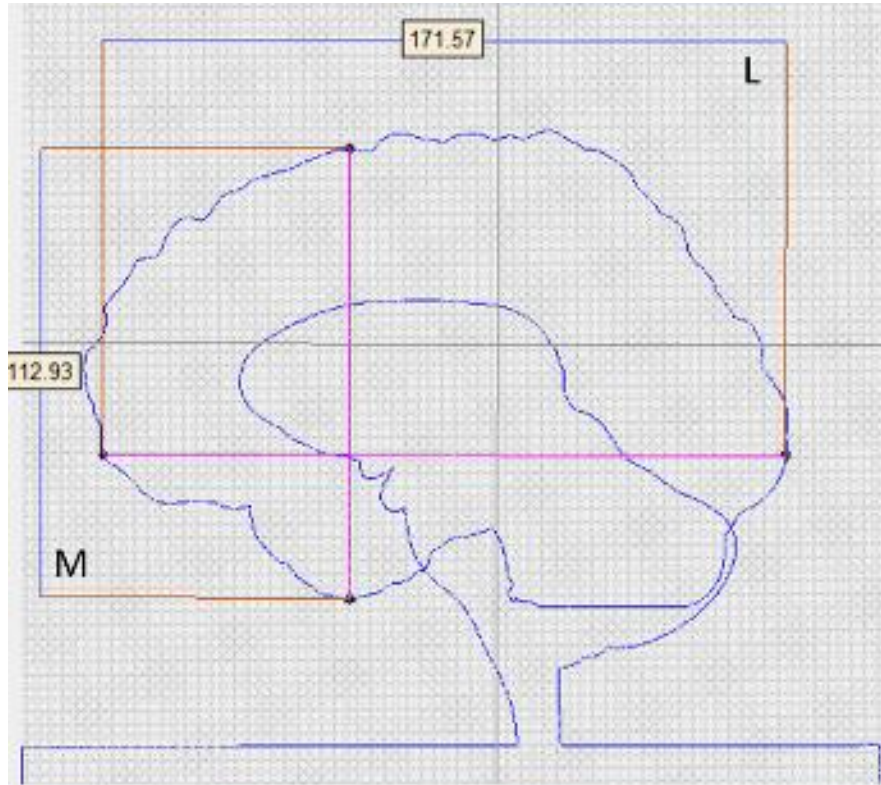
C.3 - Internal Structures Coronal Plane Measurements H and I.



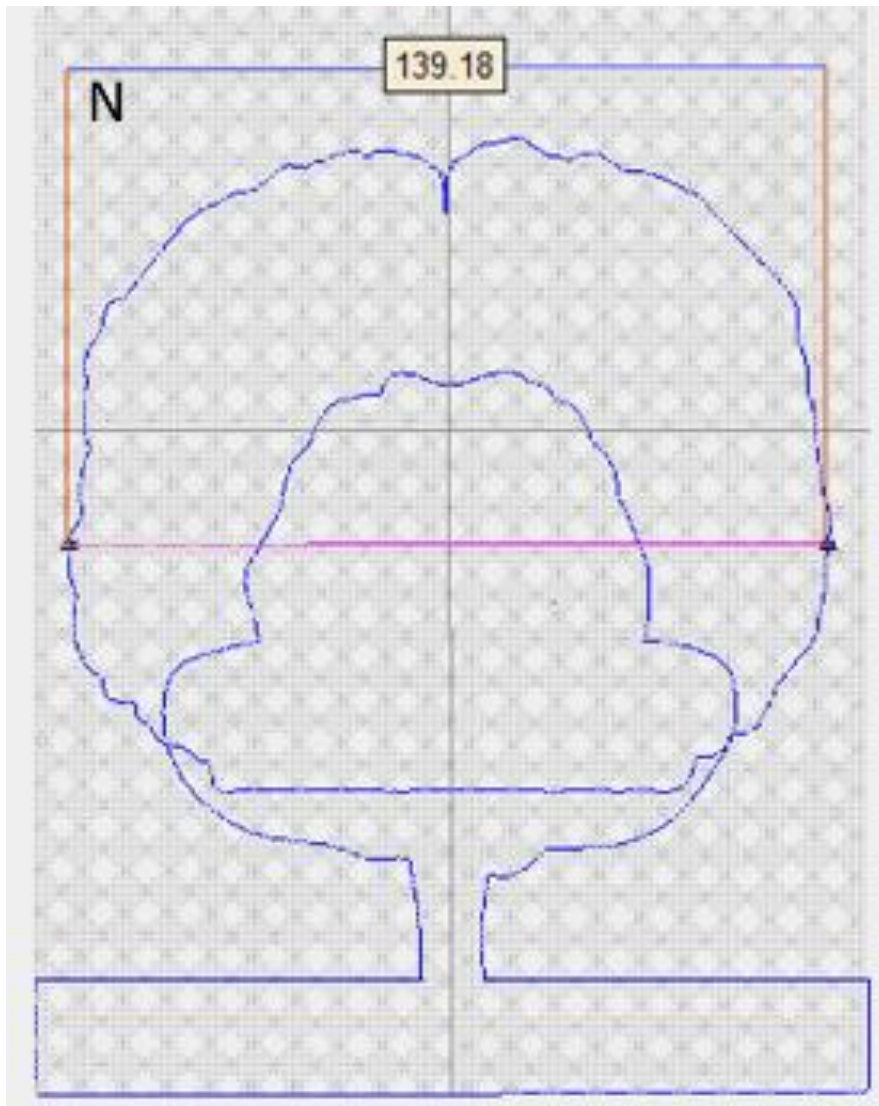
C.4 - Brain Cortex Axial Plane Measurements J and K.



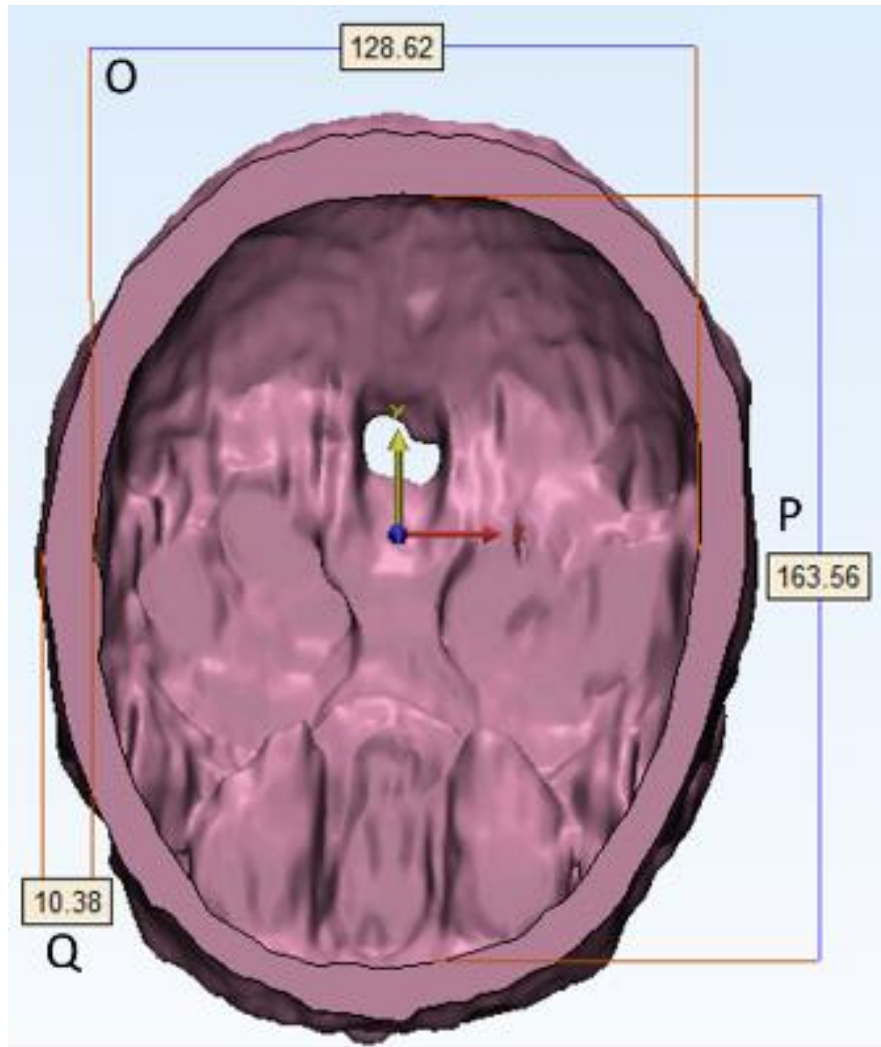
C.5 - Brain Cortex Sagittal Plane Measurements L and M.



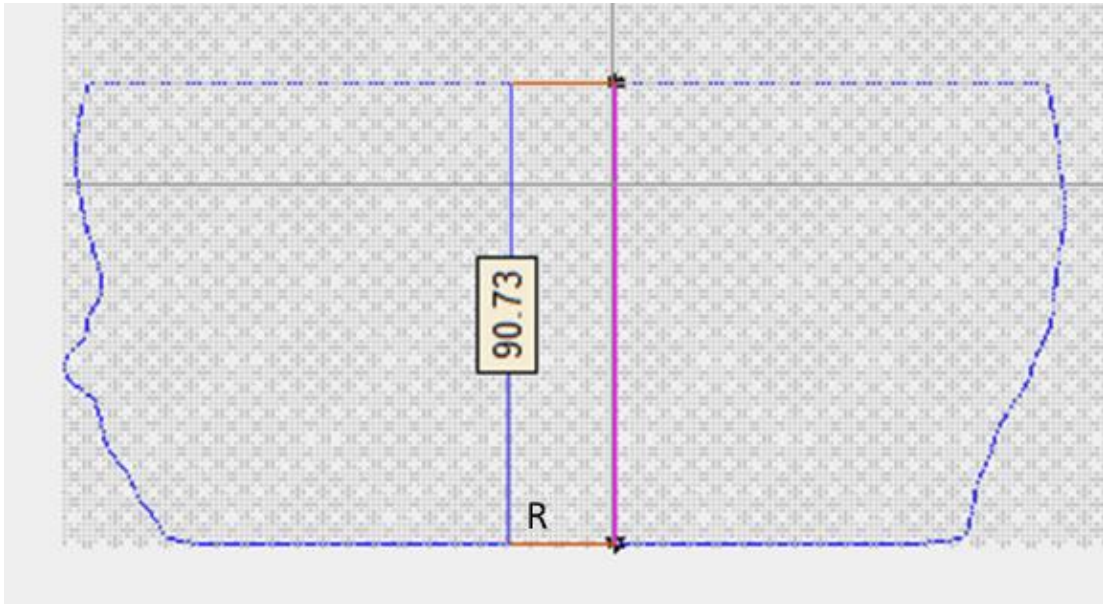
C.6 - Brain Cortex Coronal Plane Measurements N.



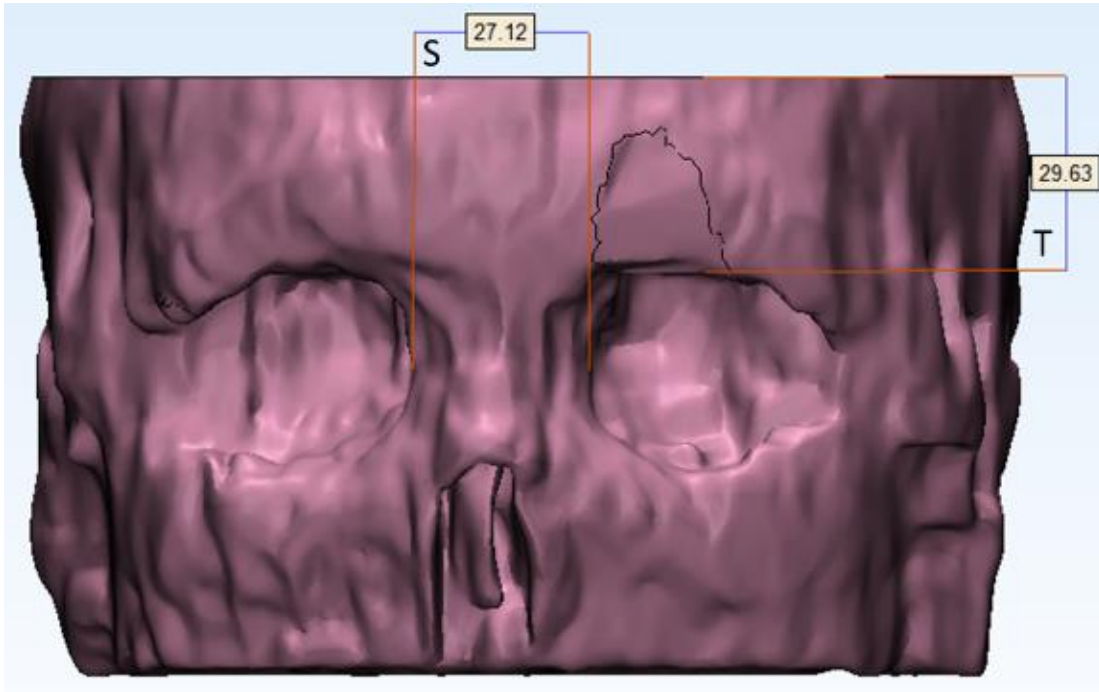
C.7 - Skull Axial Plane Measurements O, P and Q.



C.8 - Skull Sagittal Plane Measurements R.



C.9 - Skull Coronal Plane Measurements S and T.



APPENDIX D

SURVEY

Thank you for agreeing to take part in this important survey measuring the difference between brain tissue and a hydrogel based brain model and an oil based brain model. The objective is to figure out whether the brain models “feel” like real brain tissue. Be assured that all answers you provide will be kept in the strictest confidentiality. Please follow the instructions to perform each given task and complete the survey.

Instructions:


I- Put on protective gear: Lab coat, gloves and eyeglasses.





II- Perform each task as follows: For each task take the tool needed, perform the task, put the tool back in its place and then proceed to answer the corresponding question.

*Caution: Concentrate on what you are doing specially when using the scalpel: Hold the scalpel from the handle, hold it firmly so that it does not slip and keep your fingers away from the blade. Pay attention to the task underway.

1- Have you ever been in contact with brain tissue? Yes
 No
 If yes, what kind of animal brain? _____

Please rate the following questions according to the similarity in handleability, material property, and overall “feeling” that you feel there is between the brain tissue the hydrogel based brain (colorless) and the oil brain (yellow), scale of 1 – 5: (1) poor , (2) fair, (3) good, (4) very good and (5) excellent.

		Poor		Good		Excellent
2- Using your fingers, poke the brain tissue and then the colorless brain. Rate the level of similarity between the brain tissue and the colorless brain.		1	2	3	4	5
3- Using your fingers poke the brain tissue and then the yellow brain. Rate the level of similarity between the brain tissue and the yellow brain.		1	2	3	4	5

4- Use the mall probe to poke the brain tissue and then the colorless brain. Rate the level of similarity between the brain tissue and the colorless brain.		1	2	3	4	5
5- Use the mall probe to poke the brain tissue and then the yellow brain. Rate the level of similarity between the brain tissue and the yellow brain.		1	2	3	4	5
6- Take the scalpel and cut (about 10mm thick slice) the brain tissue and then the colorless brain. Rate the level of similarity between the brain tissue and the colorless brain.		1	2	3	4	5
7- Take the scalpel and cut (about 10mm thick slice) the brain tissue and then the yellow brain. Rate the level of similarity between the brain tissue and the yellow brain.		1	2	3	4	5
8- Pick with the Forceps the slice of brain tissue you just cut with the scalpel and squeeze it gently and then do the same with the colorless brain. Rate the level of similarity between the brain tissue and the colorless brain.		1	2	3	4	5
9- Pick with the Forceps the piece of brain tissue you just cut with the scalpel and squeeze it gently and then do the same with the yellow brain. Rate the level of similarity between the brain tissue and the yellow brain.		1	2	3	4	5
10- Using the scissors chop the slice of brain tissue you cut with the scalpel and then do the same with the colorless brain. Rate the level of similarity between the brain tissue and the colorless brain.		1	2	3	4	5
11- Using the scissors chop the slice of brain tissue you cut with the scalpel and then do the same with the yellow brain. Rate the level of similarity between the brain tissue and the yellow brain.		1	2	3	4	5
12- Overall similarity between the colorless and brain tissue		1	2	3	4	5
13- Overall similarity between the Yellow brain and brain tissue		1	2	3	4	5

14. - Which brain do you think is the most similar to brain tissue?

Yellow Colorless

15. Do you have any other comments or suggestions in how to improve the “feel” of the brain models?

General Information

Gender_____

Age_____

- Yellow brain = Emulsion brain phantom, Colorless Brain= Hydrogel brain phantom